INFORMATION TO USERS

This manuscript has been reproduced from the microfilm master. UMI films the

text directly from the original or copy submitted. Thus, some thesis and

dissertation copies are in typewriter face, while others may be from any type of

computer printer.

The quality of this reproduction is dependent upon the quality of the copy

submitted. Broken or indistinct print, colored or poor quality illustrations and

photographs, print bleedthrough, substandard margins, and improper alignment

can adversely affect reproduction.

In the unlikely event that the author did not send UMI a complete manuscript and

there are missing pages, these will be noted. Also, if unauthorized copyright

material had to be removed, a note will indicate the deletion.

Oversize materials (e.g., maps, drawings, charts) are reproduced by sectioning

the original, beginning at the upper left-hand comer and continuing from left to

right in equal sections with small overlaps.

Photographs included in the original manuscript have been reproduced

xerographically in this copy. Higher quality 6" x 9" black and white photographic

prints are available for any photographs or illustrations appearing in this copy for

an additional charge. Contact UMI directly to order.

Bell & Howell Information and Learning 300 North Zeeb Road, Ann Arbor, MI 48106-1346 USA

U\_800-521-0600

# Bi- and Tripolar Phospholipid Interfaces: Characterization and Interaction with Proteins

by

#### Tara Heitner

A thesis submitted to the Faculty of Graduate Studies and Research in partial fulfillment of the requirements for the degree of

Doctor of Philosophy

Department of Chemistry

McGill University

Montreal, Quebec

Canada

©Tara Heitner November 1997



National Library of Canada

Acquisitions and Bibliographic Services

395 Wellington Street Ottawa ON K1A 0N4 Canada Bibliothèque nationale du Canada

Acquisitions et services bibliographiques

395, rue Wellington Ottawa ON K1A 0N4 Canada

Your file Votre rétérence

Our file Notre référence

The author has granted a nonexclusive licence allowing the National Library of Canada to reproduce, loan, distribute or sell copies of this thesis in microform, paper or electronic formats.

The author retains ownership of the copyright in this thesis. Neither the thesis nor substantial extracts from it may be printed or otherwise reproduced without the author's permission.

L'auteur a accordé une licence non exclusive permettant à la Bibliothèque nationale du Canada de reproduire, prêter, distribuer ou vendre des copies de cette thèse sous la forme de microfiche/film, de reproduction sur papier ou sur format électronique.

L'auteur conserve la propriété du droit d'auteur qui protège cette thèse. Ni la thèse ni des extraits substantiels de celle-ci ne doivent être imprimés ou autrement reproduits sans son autorisation.

0-612-44451-1



To my family

#### **ABSTRACT**

An understanding of the molecular structure-function relationships of diacyl phospholipids is demanded in fields of study such as drug delivery, therapeutics, metabolism and physiology. Of particular interest are the properties of lipid derivatives where one or both acyl chains contain a polar moiety. Phospholipid analogs of distearolyphosphatidylcholine (DSPC) bearing polar groups (SO<sub>2</sub>, SO, S and CO) in the acyl chain(s) were synthesized and characterized using differential scanning calorimetry (DSC) and the Langmuir film-balance technique (LFB). Through the development of a detailed structure-function relationship map we have endeavored to understand the effect of the functional group on lipid conformation, phase, morphology and stability. Many of the measured properties prove to be sensitive to the chemical nature of the specific functional group and its position in the acyl chain, and whether one (mono) or both (bis) acyl chains are derivatized. For example, phospholipids with an SO<sub>2</sub> group in each chain form aggregates with greater thermal stability than the reference material DSPC. When mixed with DSPC, phase separation occurs over a broad composition range (10% -90%). If the SO<sub>2</sub> group is placed in only one chain, or if one measures the properties of the bis-SO derivative the lipid aggregates are found to possess lower thermal stability than DSPC and mix more readily with the unfunctionalised lipid. The enhanced thermal stability is attributed to cooperative dipole-dipole interactions which enhance chain-chain cohesive interactions. In the LFB experiment both surface pressure and surface potential isotherms provide a description of the properties of functionalised lipids at the air-water interface. A functional group position-dependent phase transition mechanism is revealed for phospholipids bearing SO<sub>2</sub> and SO groups in their acyl chains. The mechanism changes from being order-disorder to reorientational with placement of the polar groups at positions further away from the headgroup. The monolayer critical temperature (T<sub>c</sub>) is used as a

diagnostic of the mechanism; T<sub>c</sub> corresponds to the bilayer phase transition temperature (T<sub>m</sub>) in the former case, but not in the latter. Surface dipole experiments permit direct observation of the conformation of the functionalised lipid chain due to the presence of the polar groups in the chain. The conformation of the lipid in the expanded film ultimately controls the type of transition followed. Where bipolar lipids adopt a prone position in the expanded film, mono-polar lipids adopt a vertical position. A methodology which normalizes the temperature-dependent isotherms of structurally-related materials for the purpose of their direct comparison is also presented. Normalization reveals that a destabilized condensed film occurs as the position of the SO<sub>2</sub> group moves further from the lipid headgroup.

The LFB technique is used to determine the interaction of the enzyme protein tyrosine phosphatase (PTPase, SHP-1) with lipid monolayers. The LFB technique in conjunction with fluorescence resonance energy transfer experiments (FRET) were used to directly monitor the interaction of protein with lipid interfaces. FRET experiments measure the protein-lipid surface association, whereas penetration of the lipid monolayer by SHP-1 can be monitored directly by the LFB. Studies on the effect of headgroup structure, lipid surface density, and SHP-1 subphase concentration supports a self consistent model in which cohesive protein-lipid interactions control a first order penetration mechanism. The rate of penetration ( $k_{obs}$ ) is dependent on the lipid surface charge density while the extent of penetration is governed by hydrophobic interactions.

#### RÉSUMÉ

L'étude des relations entre la structure et les fonctions de phospholipides diacylés est primordiale pour mieux comprendre la libération contrôlée de médicaments, la thérapeutique, les métabolismes de et la physiologie. Il est particulièrement intéressant d'étudier les propriétés de dérivés lipidiques ayant une entité polaire à l'une ou aux deux des chaînes acylées. Des analogues du phospholipide DSPC (distearoylphosphatidylcholine) contenant différents groupes polaires (SO<sub>2</sub>, SO, S ou CO) ont été synthétisés puis caractérisés par calorimétrie différentielle et par la balance Langmuir. L'étude détaillée de la relation entre la structure et les fonctions de ces différents phospholipides nous a permis de mieux définir l'effet du groupe fonctionel sur la conformation du lipide, la nature de la phase, la morphologie et la stabilité des agrégats. Les mesures de ces propriétés sont sensibles à la nature chimique du groupe fonctionel en question, ainsi qu'à sa position le long de la chaîne acylée et varient selon le nombre de chaînes dérivées. Par example, des phospholipides ayant un goupe SO<sub>2</sub> sur chaque chaîne forment des agrégats ayant une stabilité thermique supérieure à celle du phospholipide de référence DSPC. Lorsque les lipides fonctionalisés sont par ailleurs mélangés à la DSPC, la séparation de phase est observée dans un grand domaine de composition (10%-90%). Si le groupe SO<sub>2</sub> est présent sur une seule chaîne, ou si on mesure les propriétés du dérivé bis-SO, les agrégats lipidiques sont thermiquement moins stables que la pure DSPC et se mélangent plus facilement au lipide non fonctionalisé. Cette augmentation de la stabilité thermique est attribuée à la présence d'intéractions coopératives dipôle-dipôle, ce qui a pour effet d'augmenter les intéractions de cohésion. La pression de surface et les isothermes obtenus avec la balance Langmuir renseignent sur les propriétés des lipides fonctionalisés à l'interface air-eau. Les phospholipides contenant les groupes SO<sub>2</sub> ou SO dans leurs chaînes acylées montrent un mécanisme de transition de phase qui dépend de la position du groupe

fonctionel. Le mécanisme évolue d'une transition de type ordre-désordre vers une transition de réorientation lorsque les groupes polaires sont situés à des positions de plus en plus éloignées de la tête polaire. La température critique de la monocouche (T<sub>C</sub>) est utilisée comme diagnostique pour déterminer le type de mécanisme; T<sub>C</sub> correspondant à la température de transition de phase (T<sub>m</sub>) dans le premier cas. Les mesures de potentiels de surface permettent d'observer directement la conformation des chaînes lipidiques fonctionalisées grâce à la présence du groupe polaire. La conformation des chaînes du film expansé contrôle à toute fin pratique le type de transition qui s'en suit. Dans le film expansé, les lipides bipolaires se couchent horizontalement, alors que les lipides monopolaires se placent de façon verticale. Afin de mieux comparer les propriétés des lipides entre elles, une méthodologie consistant à normaliser les isothermes pris à différentes températures a été développée. Les résultats après normalisation montrent une destabilisation accrue du film condensé à mesure que le groupe SO<sub>2</sub> s'éloigne de la tête polaire.

La technique Langmuir a aussi été utilisée afin de déterminer l'intéraction entre la protéine enzymatique tyrosine phosphatase (PTPase, SHP-1) et les monocouches lipidiques. La technique de la balance Langmuir combinée à la fluorescence de transfert d'énergie par résonnance (fluorescence resonnance energy transfer, FRET) ont été utilisées pour suivre l'intéraction de la protéine avec les interfaces lipidiques. Les expériences par FRET permettent de mesurer l'association électrostatique en surface, alors que la cinétique de pénétration de la SHP-1 à l'intérieur de la monocouche lipidique peut être mesurée en utilisant la balance Langmuir. Les études de l'effet de la structure de la tête polaire, de la densité du lipide à la surface, et de la concentration de la SHP-1 dans la sous-phase supportent un modèle selon lequel les intéractions de cohésion protéine-lipide contrôlent le mécanisme de pénétration qui est de premier ordre. La vitesse de pénétration (kobs) dépend de la densité de charge de surface du lipide, alors que l'importance de la pénétration est gouvernée par les intéractions hydrophobes.

#### **FOREWORD**

In accordance with guideline 7 of the "Guidelines concerning Thesis Preparation" (Faculty of Graduate Studies and Research), the following text is cited:

"The candidate has the option, subject to the approval of the Department, of including as part of the thesis the text, or duplicated published text (see below), of an original paper, or papers. In this case the thesis must still conform to all other requirements explained in Guidelines Concerning Thesis Preparation. Additional Material (procedural and design data as well as descriptions of equipment) must be provided in sufficient detail (e.g. in appendices) to allow a clear and precise judgment to be made of the importance and originality of the research reported. The thesis should be more than a mere collection of manuscripts published or to be published. It must include a general abstract, a full introduction and literature review and a final overall conclusion. Connecting texts which provide logical bridges between different manuscripts are usually desirable in the interests of cohesion.

It is acceptable for these to include as chapters authentic copies of papers already published, provided these are duplicated clearly on regulation thesis stationary and bound as an integral part of the thesis. Photographs or other materials which do not duplicate well must be included in their original form. In such instances, connecting texts are mandatory and supplementary explanatory material is almost always necessary.

The inclusion of manuscripts co-authored by the candidate and others is acceptable but the candidate is required to make an explicit statement on who contributes to such work and to what extent, and supervisors must always attest to the accuracy of the claims, e.g. before the Oral Committee. Since the task of the Examiners is made more difficult in these cases, it is in the candidate's interest to make the responsibilities of authors perfectly clear. Candidates following this option must inform the Department before it submits the thesis for review."

This dissertation was written in the form of four papers. The papers each comprise one chapter in the main body of the thesis (Chapters 2 to 5), with a general introduction to this work in the first chapter and a conclusion in the sixth. These papers will be submitted for publication in November-December 1997. A list of their titles is given below:

Chapter 2: Role of Interchain Dipole-Dipole Interactions in the Stabilization of Phospholipid Aggregates. (to be submitted to *Biophysics Journal*)

Chapter 3: Bipolar phospholipid monolayers: Temperature dependence of the phase transition. (submitted to *Langmuir*)

Chapter 4: Surface dipole and pressure isotherms of sulfone-functionalised phospholipids reveal an orientational phase transition mechanism. (submitted to *Langmuir*)

Chapter 5: The interaction of protein tyrosine phosphatase SHP-1 with phospholipids: A monolayer and fluorescence resonance energy transfer study. (submitted to the *Journal of Biological Chemistry*)

All of these papers include my research director, Prof. R.B. Lennox, as co-author since the research was done under his supervision and in acknowledgment of his input and guidance. Chapters 2, 3, and 4 include Dr. Gilles Berthiaume as a co-author in acknowledgment of his work in synthesizing the majority of the lipids used in these studies. Dana Tanenbaum was a summer student who first measured the melting temperatures of many of the lipids investigated in Chapter 2. Ling Wei initially studied the monolayer properties of the SO<sub>2</sub> and SO functionalised phospholipids in Chapter 3. Dr. Marko Pregel is included as a co-author in Chapter 5 for his work in the preparation and purification of SHP-1 used in the monolayer and fluorescence studies under the direction of Dr. A.C. Storer who is also included as a co-author. Other than these contributions, all of the research and analysis presented in this dissertation was initiated and performed by myself.

#### **ACKNOWLEDGMENTS**

I would like to extend my gratitude to my research supervisor, Prof. Bruce Lennox, for his assistance and guidance during my doctoral training. He provided a rich learning environment in which I had the pleasure of working with numerous talented scientists including, Dr. Louis Cuccia, Dr. Antonella Badia, Dr. Zhigang Qi, Dr. Frank Chubb, Dr. Michelle Meszaros, Fuyuang Ma, Joy Klass, Pollyanna Peters, Emmanuelle Boubour, Linette Demers, Caroline Bourg and Gabrielle Farkas. Many thanks to Dr. Marko Pregel for his collaboration and input on the SHP-1 project. I would especially like to mention Dr. Louis Cuccia for his encouragement, support and inspiration (and also for his patience!). My sincere thanks goes to Dr. Juliet Cox, the newest member of our lab, for the hours spent correcting my thesis and for her friendship. I cannot forget the benevolence that others in the department have extended to me, especially Shanti Singh, who always took the time to help out or to answer my questions, Prof. David Ronis for his insightful ideas and discussions and Prof. Linda Reven for her encouragement and support. Thank you to Emmanuelle Boubour for her excellent translation of my dissertation abstract.

I am grateful to the McConnell Major Fellowship Fund and to the Quebec Black Medical Association for their financial support during my doctoral research.

I owe a great deal of thanks to the many friends I made here at McGill. In arbitrary order these include Laura Deakin, Tina Kouri, Tanya Kanigan, Mary-Jane Young, Charlie Abrams, Mark Wall, Andrew Brown, Jason Chisham, Norbert Schuler, Rick Hodge and Claudine Koss. These individuals are among those who have added to the incredible experience that has been the last five years and who have provided me with many wonderful memories.

Lastly I thank my family, that incredible support network. My mother and father for their emotional and financial support. My brother, Sule, for being an incredible musician. My sister, Dawn, and her husband, Ross, for always being ready to help out and for having Erin. To Erin for baby therapy. To Rover and Kody for puppy therapy. To my grandmothers, Granny and Bubbie and to all my Aunts and Uncles who have encouraged me from the beginning.

#### LIST OF SYMBOLS AND ABBREVIATIONS

 $\begin{array}{ccc} A_{c} & & \text{critical area} \\ A_{t} & & \text{transition area} \\ A_{cond} & & \text{condensed area} \\ A_{on} & & \text{onset area} \end{array}$ 

 $\Delta A_t$  change in area during the transition

 $\begin{array}{lll} \Delta A_{total} & \text{area change in surface expansion LFB experiment} \\ \text{bis(nSO_2)-C_{17}-PC} & \text{bis(n-heptadecylsulfone)-phosphatidylcholine} \\ \text{bis(nS)-C_{17}-PC} & \text{bis(n-heptadecylsulfone)-phosphatidylcholine} \\ \text{bis(n-heptadecylsulfide)-phosphatidylcholine} \end{array}$ 

BSA bovine serum albumin

1C<sub>18</sub>,2(nSO<sub>2</sub>)C<sub>17</sub>-PC 1-stearoyl,2-(n-heptadecylsulfone)-phosphatidylcholine 1-stearoyl,2-(n-heptadecylsulfoxide)-phosphatidylcholine 1-stearoyl,2-(n-heptadecylsulfide)-phosphatidylcholine 1-stearoyl,2-(n-heptadecylsulfide)-phosphatidylcholine 1-stearoyl,2-(n-heptadecylketone)-phosphatidylcholine

D diffusion constant (cm²/s)
DSC differential scanning calorimetry
DMPC dimyristoylphosphatidylcholine (C14)
DPPC dipalmitoylphosphatidylcholine (C16)
DSPC distearoylphosphatidylcholine (C18)

DTT dithiothreitol

EDTA ethylenediaminetetraacetic acid epidermal growth factor

E dielectric constant mole fraction

F<sub>max</sub> saturation fluorescence level

FAB-MS fast atomic bombardment mass spectrometry

%F F/F<sub>0</sub> x 100

Fo baseline fluorescence steady-state fluorescence

FRET fluorescence resonance energy transfer dansyl-DHPE dansyl N-5-dimethylaminonaphthalene salt

FWHM full width at half maximum

FT-IR Fourier transform infrared spectroscopy

Γ surface concentration (mol/cm2)

 $\Delta H$  enthalpy of transition

 $\Delta H_{inc}$  enthalpy of transition per methylene group

HEPES (N-[2-hydroxyethyl]piperazine-N'-[2-ethanesulfonic acid])

KDassoc dissociation constant for the associated protein-lipid complex

KDpenetration dissociation constant for the penetrated protein-lipid complex

k<sub>obs</sub> observed first-order rate constant

 $L_{\alpha}$  penetration rate constant liquid crystalline phase

L<sub>β'</sub> gel phase

L<sub>t</sub> surface concentration of lipid LFB Langmuir film-balance technique

 $\mu_{app}$  apparent surface dipole  $\mu_{app}^{max}$  maximum surface dipole

 $\mu_{app}^{cond}$  surface dipole of the condensed monolayer

change in surface dipole during the phase transition  $\Delta \mu_{app}$ 

critical surface pressure (mN/m)  $\pi_{\mathsf{C}}$ transition surface pressure (mN/m)  $\pi_t$ 

π surface pressure (mN/m) change in surface pressure  $\Delta \pi$ steady state surface pressure  $\pi_{\text{SS}}$ 

 $P_{\beta^{\prime}}$ ripple phase PΆ phosphatidic acid PC phosphatidylcholine PG phosphatidylglycerol phosphatidylethanolamine PE PS phosphatidylserine

**PTPase** protein tyrosine phosphatase **NMR** nuclear magnetic resonance

Q T<sub>m</sub> TLC quantum efficiency

main bilayer phase transition temperature

thin layer chromatography  $\Delta S$ entropy of transition

 $\Delta S_{inc}$ entropy of transition per methylene group

 $T_c$ critical temperature

rate of molecular area change with surface pressure

**XPS** X-ray photoelectron spectroscopy

## LIST OF FIGURES

Figure 1.1	Glycerol backbone structure of the two main categories of phospholipids.	1-1
Figure 1.2	Headgroup structure of some natural phospholipids.	1-2
Figure 1.3	Examples of the chemical diversity of the lipid fatty acid chain.	1-3
Figure 1.4	Representative examples of bipolar lipids.	1-5
Figure 1.5	Schematic representation of polymorphic aggregates and corresponding molecular shapes of component lipids.	1-7
Figure 2.1	Distearoylphosphatidylcholine (DSPC) and phospholipid analogs used in the present study.	2-6
Figure 2.2	Binary mixtures of bis( $11SO_2$ )C <sub>17</sub> -PC with DSPC at values of $f$ .	2-15
Figure 2.3	Binary mixtures of bipolar lipid $1C_{18}$ , $2(9SO_2)C_{17}$ -PC and DSPC at different values of $f$ .	2-17
Figure 2.4	Proton-decoupled <sup>31</sup> P solid-state NMR of hydrated SO <sub>2</sub> -functionalised lipids.	2-22
Figure 2.5	Schematic of alignment of (a) sulfone (b) sulfoxy groups (c) and mono-substituted lipids	2-24
Figure 3.1	Schematic representation of (a) a bilayer lipid vesicle and (b) the order-disorder phase transition of lipid bilayers.	3-4
Figure 3.2	Schematic representation of the two-dimensional phase diagram of a phospholipid monolayer.	3-5
Figure 3.3	Generalized conformational changes which occur during compression of phospholipid monolayers.	3-7
Figure 3.4	Temperature dependence of phospholipid isotherms (a) $1C_{18}$ ,2(5SO <sub>2</sub> )C <sub>17</sub> -PC (b) $1C_{18}$ ,2(7SO <sub>2</sub> )C <sub>17</sub> -PC (c) $1C_{18}$ ,2(9SO <sub>2</sub> )C <sub>17</sub> -PC (d) $1C_{18}$ ,2(11SO <sub>2</sub> )C <sub>17</sub> -PC on a water subphase.	3-15
Figure 3.5	(a) Isotherms of lipid standards run at $T_r = (T_m - 15^{\circ}C)$ (b) Normalized isotherms of lipid standards run at $T_r = (T_m - 15^{\circ}C)$ on a water subphase.	3-16

Figure 3.6	Normalized isotherms of DSPC (34°C), $1C_{18}$ , $2(5SO_2)C_{17}$ -PC (18°C), $1C_{18}$ , $2(7SO_2)C_{17}$ -PC (17°C) and $C_{18}$ , $2(9SO_2)C_{17}$ -PC (28°C) ( $T_c$ - $T$ = 20°C) on a water subphase.	3-17
Figure 3.7	Isotherm normalization (a) DMPC, DPPC, DSPC, $1C_{18},2(nSO_2)C_{17}$ -PC, $n=5,7,9,11$ . As the temperature is increased the transition surface pressure increases until $\pi_t = \pi_c$ and $\pi_t/\pi_c \rightarrow 1$ . The area of the transition goes to zero as $T_c$ is approached and $T_c$ - $T \rightarrow 0$ .	3-19
Figure 3.8	Schematic representation of bilayer and monolayer phase transitions	3-28
Figure 4.1	Contribution of component molecular dipoles of a phospholipid to the observed apparent dipole $\mu_{app}$ .	4-5
Figure 4.2	Isotherms of (a)DPPC and (b)DSPC monolayers at an air/water interface at 25°C. Surface pressure and surface potential were recorded simultaneously. Surface dipole values were calculated from the measured surface potential using Equation 4.1.	4-12
Figure 4.3	Isotherms of (a) bis(11SO)C <sub>17</sub> -PC and (b) bis(11SO <sub>2</sub> )C <sub>17</sub> -PC monolayers at an air/water interface at 25°C.	4-13
Figure 4.4	Isotherms of (a) bis(5SO)C <sub>17</sub> -PC and (b) bis(5SO <sub>2</sub> )C <sub>17</sub> -PC monolayers at an air/water interface at 25°C.	4-14
Figure 4.5	Possible conformations of lipids which could be adopted at the air/water interface in the expanded lipid film.	4-15
Figure 4.6	Isotherms of (a)1C <sub>18</sub> ,2(7SO <sub>2</sub> )C <sub>17</sub> -PC and (b)1C <sub>18</sub> ,2(11SO <sub>2</sub> )C <sub>17</sub> -PC monolayers at an air/water interface at 25°C.	4-19
Figure 4.7	Isotherms of bis(7SO <sub>2</sub> )C <sub>17</sub> -PC monolayers at an air/water interface at (a) 25°C and (b) 33°C. Surface pressure and surface potential were recorded simultaneously. Surface dipole values were calculated from the measured surface potential using Equation 4.1.	4-21
Figure 4.8.	Proposed model to account for the differences between the surface dipole isotherms of functionalised and unfunctionalised phospholipids.	4-21
Figure 5.1	Fluorescence transfer between tryptophan residues and dansyl-DHPE lipid probe at egg-PA and egg-PC vesicles containing 1% lipid probe.	5-12

Figure 5.2	Proposed model depicting the interaction mechanism of SHP-1 with lipid assemblies.	5-13
Figure 5.3	(a) representative results of surface pressure $(\pi)$ as a function of the final bulk substrate concentration of SHP-1 with stirring at an egg-PA / buffer interface spread to an initial film pressure of 20 mN/m . 0.9 nM, 1.8 nM, 3.6 nM, 7.1 nM, 17.8 nM. (b) observed rate constants obtained from a first order fit of the data shown in (a)	5-14
Figure 5.4	(a) Representative kinetics obtained in the constant surface area mode of SHP-1 (3.58 nM bulk concentration) at the lipid/buffer interface where monolayers were spread to an initial surface pressure ( $\pi_i$ ) of 20 mN/m.(b) kinetics obtained in the surface expansion mode at 20 mN/m 35°C and [SHP-1] <sub>subphase</sub> of 3.44 nM. egg-PA, egg-PG, egg-PS, egg-PE and egg-PC.	5-17
Figure 5.5	(a) interaction of SHP-1 (3.6 nM bulk concentration) at the egg-PA/buffer interface where films were spread to initial surface pressures of 15 mN/m, 20 mN/m, 25 mN/m and 30 mN/m (O) (b) effect of initial surface pressure on the extent of protein penetration into films of egg-PA at the lipid/buffer interface. $\Delta \pi$ values were taken from curves shown in (a).	5-20
Figure 5.6	Penetration kinetics of SHP-1 into egg-PA monolayers at 20 mN/m, 25°C in the surface expansion mode at subphase concentrations of 0.88 nM, 1.92 nM, 2.68 nM.	5-22
Figure 5.7	Comparison of SHP-1 penetration kinetics obtained in the constant surface area mode with that obtained in the surface expansion mode at a protein subphase concentration of 0.88 nM.	5-22
Figure 5.8	Assessment of the role of diffusion in penetration kinetics obtained in (a) the constant surface area mode: 0.9 nM, 1.8 nM, 3.6 nM, 7.1 nM, 17.8 nM and (b) the surface expansion mode: 0.88 nM, 1.92 nM, 2.68 nM.	5-24
Figure 5.9	Schematic representation of adsorption kinetics and the corresponding adsorption isotherm for (a) [protein] <sub>subphase</sub> $\approx K_d$ and (b) [protein] <sub>subphase</sub> $\approx K_d$ . SHP-1 penetration kinetics observed by the LFB technique in the constant surface area mode are represented by situation (b). a,b,c,d and e correspond to arbitrary protein subphase concentrations in increasing order. The response corresponds to $\pi$ in the LFB experiments and to F/F <sub>0</sub> x100 in the FRET experiment.	5-27
Figure 6.1	Schematic representation of SHP-1 truncated protein analogs obtained by tryptic and peptic digests of the full-length enzyme.	6-6

Figure AI.1	Temperature dependence of monolayers isotherms of DMPC, DPPC and DSPC.	AI-iii
Figure AI.2	Graphs from which the critical parameters ( $T_c$ , $\pi_c$ , $A_c$ ) listed in Table 3.1 are taken.	AI-iv, v
Figure AI.3	Critical temperatures derived from the 2D Clausius- Clapeyron equation	AI-vi

# LIST OF TABLES

Table 2.1	Thermophysical data for the bis(nSO <sub>2</sub> )C <sub>17</sub> -PC lipid series.	2-10
Table 2.2	Thermophysical information of the 1C <sub>18</sub> ,2(nSO <sub>2</sub> )C <sub>17</sub> -PC lipid series	2-11
Table 2.3	Main transition temperatures of mono-functionalised phospholipids, 1C18,2(nX)C17-PC.	2-25
Table 2.4	Main Transition Temperatures of Bis-Substituted Phospholipids, bis(nX)C17-PC.	2-25
Table 2.3	Main transition temperatures of branched chain and unsaturated lipids.	2-26
Table 2.6	Physical constants of functional groups	2-26
Table 3.1	Critical parameters obtained from the temperature dependence of the phase transition.	3-14
Table 3.2	Transition area and surface pressures of SO <sub>2</sub> functionalised lipid monolayers in two temperature ranges. The isothermal compressibility data is listed.	3-20
Table 3.3	Literature values describing the phase transition of functionalised fatty acids.	3-21
Table 4.1	Variation in the apparent surface dipole $(\mu_{app})$ during the monolayer phase transition.	4-11
Table 5.1	kobs obtained from a least squares first order kinetic fit.	5-15
Table 5.2	Dependence of observed rate of penetration on the lipid headgroup chemical structure at [SHP-1] <sub>subphase</sub> (3.44 nM).	5-18
Table 5.3	Penetration rate constants and saturation levels $(\pi_{ss})$ of SHP-1 into egg-PA monolayers at different initial surface pressures.	5-20
Table AI.1	Measured features of the monolayer phase transition taken from the temperature dependence of the phase transition	AI-i

### TABLE OF CONTENTS

Abstract	iii
Résumé	v
Foreword	vii
Acknowledgments	xiii
List of Symbols and Abbreviations	xiv
List of Figures	xvi
List of Tables	xx
Table of Contents	xxi
Chapter One	
General Introduction	1-1
Chapter Two	
Role of Interchain Dipole-Dipole Interactions in the Stabilizat Phospholipid Aggregates	ion of
Abstract	2-1
Introduction	2-2
Materials and Methods	2-5
Results and Discussion	2-8
Conclusions	2-27
References	
Chapter Three	
Temperature dependence of the monolayer phase transitions of isothe mono-polar and bipolar phospholipids.	rms of
Abstract	3-1
Introduction	
	3-10

Results	3-11
Discussion	3-22
Conclusions	3-29
References	3-31
Chapter Four	
Surface dipole and pressure isotherms of sulfone-functio phospholipids reveal an orientational phase transition mechanism.	nalised
Abstract	4-1
Introduction	4-3
Materials and Methods	4-7
Results and Discussion	4-8
Conclusion	4-23
References	4-24
Chapter Five  The interaction of protein tyrosine phosphatase SHP-1 with phospho A monolayer and fluorescence resonance energy transfer study.	lipids:
Abstract	
	5-1
Introduction	
Introduction	5-2
	5-2 5-6
Materials and Methods	5-2 5-6 5-11
Materials and Methods.  Results  Discussion	5-2 5-6 5-11
Materials and Methods  Results  Discussion	5-2 5-6 5-11 5-25 5-32
Materials and Methods  Results  Discussion  Conclusion	5-2 5-6 5-11 5-25 5-32
Materials and Methods  Results  Discussion  Conclusion  References	5-2 5-6 5-11 5-25 5-32 5-34
Materials and Methods  Results  Discussion  Conclusion  References  Chapter 6	5-2 5-6 5-11 5-25 5-32 5-34
Materials and Methods.  Results  Discussion  Conclusion  References  Chapter 6  General Conclusion	5-2 5-6 5-11 5-25 5-32 5-34
Materials and Methods.  Results  Discussion  Conclusion  References  Chapter 6  General Conclusion  Contribution to original knowledge.	5-2 5-6 5-11 5-25 5-32 5-34 6-1 6-4 6-5

#### Chapter 1

#### 1.1. General Introduction

One remarkable aspect of membrane chemistry is the enormous diversity of the component phospholipids. Lipids are divided into different classes based on their arrangement of the glycerol backbone, headgroup structure, and acyl-chain composition. Two main categories of lipids as defined by their backbone structure are the phosphodiglycerides and sphingolipids (Figure 1.1). The phosphoglycerides are the most commonly found membrane lipids and of these, lipids possessing the phosphocholine headgroup are the most common (Figure 1.2). Other common lipid headgroup structures include phosphatidylglycerol, phosphatidylserine, phosphatidylethanolamine, phosphatidic acid and phosphatidylinositol (Figure 1.2). Variation of the lipid acyl chain structure provides further elements of structural diversity for lipids. Examples of various acyl chain structures found in nature are shown in Figure 1.3.

Figure 1.1. Glycerol backbone structure of the two main categories of phospholipids

Figure 1.2. Head group structure of some natural phospholipids

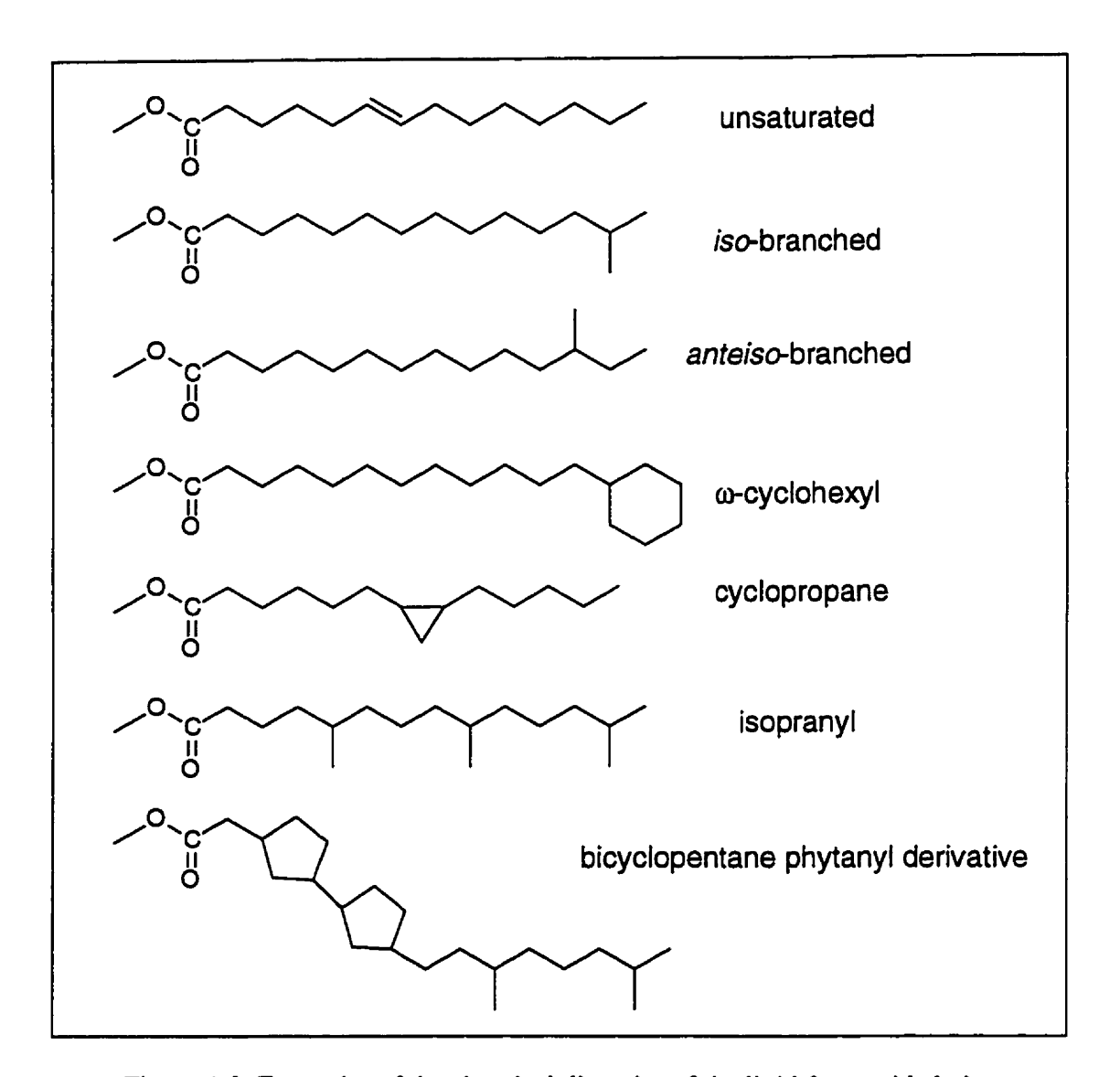


Figure 1.3. Examples of the chemical diversity of the lipid fatty acid chain.

Bipolar phospholipids or bolaforms are lipids which possess two hydrophilic groups which act as separate entities. Examples of naturally occurring bipolar lipids include archaebacterial phospholipids and lipid hydroperoxides. These lipids represent two types of bipolar lipids: the former possessing two headgroups and the latter possessing a polar group in the acyl chain. Of the two types of lipids the latter is of particular interest to the present discussion. They both, however, illustrate quite effectively how bipolarity can in one case lead to greater liposome stability and in the other lead to membrane disruption. In the case of archaebacterial phospholipids, the bolaforms have two polar headgroups

connected by either one or two long aliphatic chains (i.e. C40) (Figure 1.4 (c)).

Archaebacteria thrive under conditions of very high temperature, pH, saturated salt solution or anaerobiosis.<sup>2</sup> The term 'extremophile' is often applied to these bacteria. The survival of these organisms is due in part to the enhanced physical and chemoenzymatic stability of their cell membranes. Several studies have been carried out to identify the molecular origin of the membrane stability. Thermal analysis<sup>2-4</sup> and the structural analysis of monolayer isotherms of these unusual lipids<sup>4, 5</sup> have both been used to identify why a bolalipid exerts such a stabilizing effect. Rationalizations include to depressed abilities of these membranes to aggregate and fuse, the ability to shrink and expand, their ability to resist enzymatic degradation, and the fact that they present a large diffusion barrier to ionic materials<sup>2</sup>.

In the case of hydroperoxy lipids, a polar -OOH group is found within the acyl chain. This functional group arises from oxidative stress in biological organisms (Figure 1.4 (b)). Lipid hydroperoxides represent one example of a physiologically important bipolar lipid. Exposure of the membrane to an oxidant can lead to radical propagation reactions that result in accumulation of oxidized phospholipids in the cell membrane.<sup>6</sup> These lipids effect changes including changes in permeability, altered fluidity gradients and modified lipid-protein interactions. The hydrolysis of PC's by PLA2 is found to be increased at oxidized lipid membranes. This effect has been attributed to a favorable conformational change in the lipid headgroup region which facilitates access to the sn-2 ester bond, thereby ensuring their preferential hydrolysis<sup>7,8</sup> and has been implicated in the first step of a repair mechanism of the cell against oxidative damage. 9-12 Although there is extensive literature describing lipid peroxidation very little is known about how the lipid hydroperoxides affect membrane function. Lipid hydroperoxides are very difficult to study because of their reactivity. The synthesis and study of stable lipid analogs of lipid hydroperoxides such as those shown in Figure 1.4 (d) and (e) may be useful for studying the properties of these molecules.

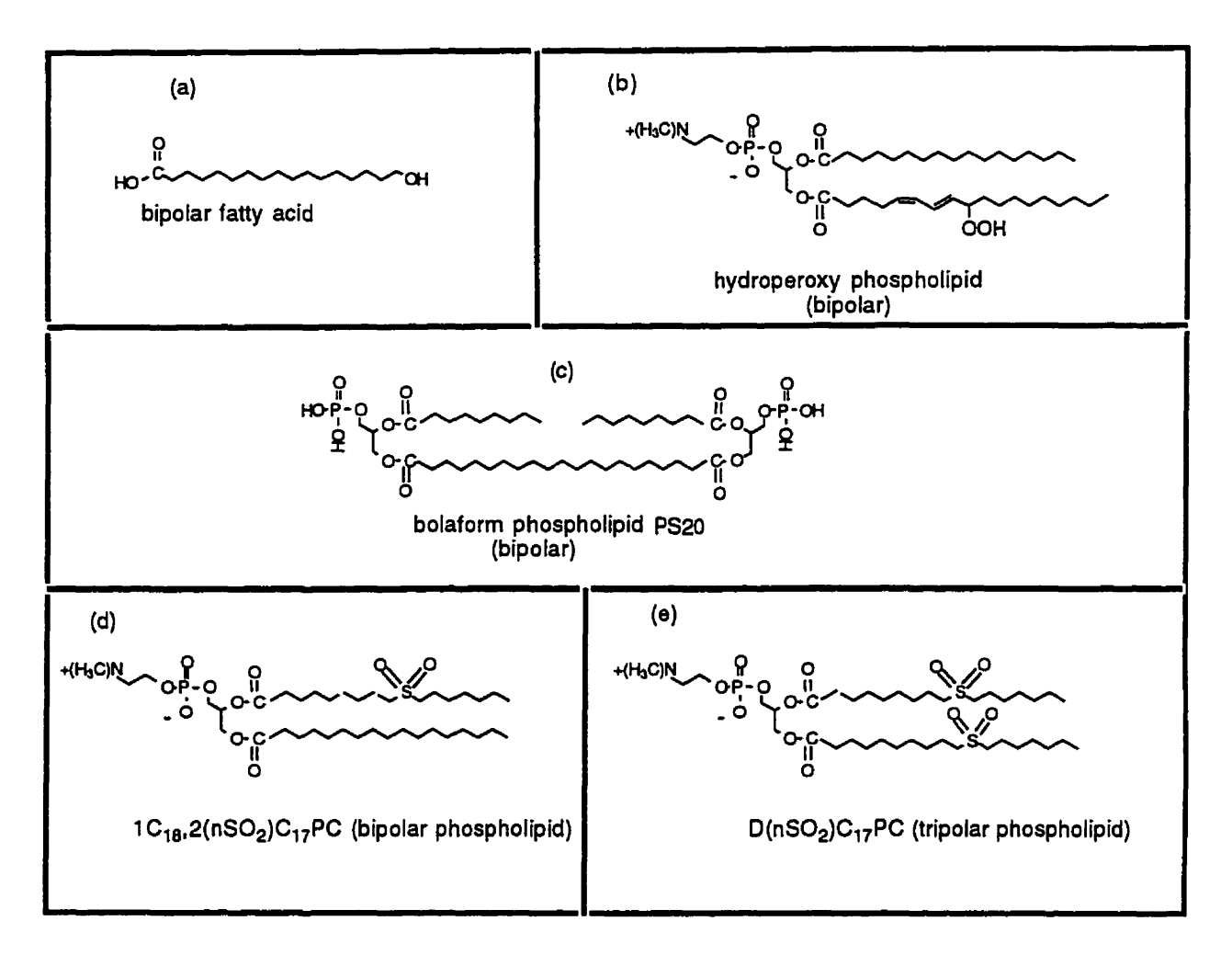


Figure 1.4. Representative examples of bipolar lipids.

The physical properties of phospholipids bearing polar functional groups is the topic of the present dissertation. Studies of the physical properties of lipids possessing polar groups in their acyl chains include phospholipids bearing keto, <sup>13, 14</sup> and ether groups, <sup>15, 16</sup> fatty acids bearing mid-chain sulfoxy groups, <sup>17, 18</sup> and terminal ester <sup>19</sup> and hydroxy groups <sup>20</sup> (Figure 1.4 (f)). Lipids bearing SO<sub>2</sub>, SO, S and CO groups in one or both acyl chains have been synthesized and characterized by differential scanning calorimetry (DSC) and the Langmuir film-balance technique (LFB). Some representative examples of these types of bipolar phospholipids are shown in Figure 1.4 (d) and (e).

#### Chapter 1 - General Introduction

What is generally sought in the characterization of lipid assemblies is information concerning the lipid conformation, the morphology of the assembly, the phases which can be accessed, and the stability of the assemblies. Lipid chain conformation is a complicated issue since there is always a distribution of various lipid conformations. Experiments such as NMR<sup>21-23</sup> and IR<sup>23, 24</sup> yield information concerning average chain order from which conformational assignments can be made. Information concerning the phase, stability and mixing of lipid aggregates can be obtained from measurement of the T<sub>m</sub>. This measurement has the advantage that it can be readily made with great precision and the results yield information concerning the thermodynamics of the transition.<sup>25, 26</sup> The Langmuir filmbalance technique (LFB) also yields information concerning phase and stability. When conducted in parallel with surface potential measurements, fluorescence microscopy, surface IR and neutron scattering the LFB experiment can yield detailed information concerning phase and lipid conformation in the monolayer state.<sup>27</sup>

Depending on their physical structure, hydrated phospholipids are found in many different morphologies. Structures with long range periodicity in one, two, or three dimensions can be formed and are dependent upon lipid conformation and solvent conditions. Structure and are dependent upon lipid conformation and solvent conditions. Is Israelachvili has shown that the structure of a self-assembled lipid aggregate can be predicted from the evaluation of the shape of the lipid molecule itself (Figure 1.5). Morphology and stability of self-assemblies of pure phospholipids depends largely on the ratio of the polar headgroup volume to the volume of the hydrophobic tails. Diacyl phospholipids self assemble into various morphologies including isotropic, cubic, and inverted nonlamellar, and hexagonal phases but the lamellar morphology is the most common. Lipids possessing bulky groups near the headgroup will adopt non-lamellar morphologies as do lipids bearing ω-cyclohexyl groups. The physical properties of membranes (fluidity, phase transition, permeability, phase, morphology) can regulate membrane and protein function.

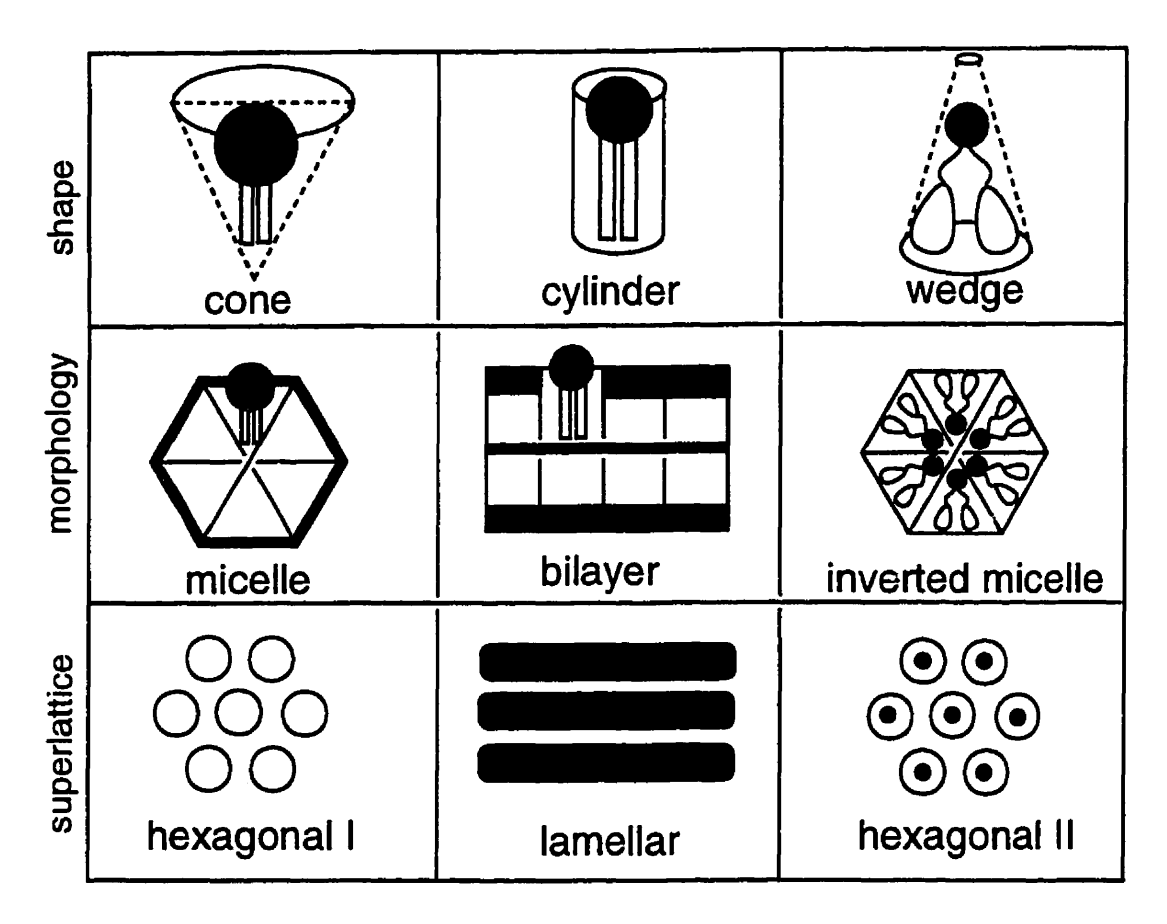


Figure 1.5. Schematic representation of polymorphic aggregates and corresponding molecular shapes of component lipids (adapted from Israelachvili<sup>29</sup>).

There are many reasons to study unconventional or synthetic phospholipids. Lipids with modified structures can lead to insights into the functional role of different types of lipids and fatty acids within the membrane. Phospholipids serve an important role in conserving membrane function and there are many examples where integral membrane protein function is modulated by membrane lipids.<sup>35-37</sup> The presence of acyl chains with varying degrees of unsaturation induces morphological changes in cell membranes.<sup>32</sup>

Another motivation for the study of lipid analogs is in the use of liposomes in drug delivery. Liposomal drug carriers in vivo are of limited use because the liposomes are unstable under physiologic conditions.<sup>38</sup> Liposomes formed from neutral lipids are more

stable than those comprised than anionic lipids.<sup>39</sup> Liposomes can be useful as delivery agents as they can trap hydrophilic agents within the interior of the liposome or hydrophobic agents within the vesicle bilayer. They are potentially biocompatible, are readily controlled, and may enhance the therapeutic efficiency of a drug by protecting the drug from enzymatic degradation, increasing the availability in tissues and by permitting a controlled release.<sup>40</sup> It is therefore of interest to study the effect of the placement of polar groups in the phospholipid acyl chain on membrane physical properties such as phase, morphology and stability for fundamental purposes, and for potential applications.

#### 1.2. Outline of thesis

Chapter 2 presents a systematic investigation of the stability of bipolar (monofunctionalised) and tripolar (bis-functionalised) phospholipids and the miscibility of these lipids with unfunctionalised diacyl phospholipids. Differential scanning calorimetry (DSC) is used to determine the main phase transition temperature (T<sub>m</sub>) of lipid vesicles. Variation of the position of the polar functional groups in the acyl chain leads to changes in the properties of the resulting lipid aggregates.

In Chapter 3 the Langmuir film-balance technique (LFB) is used to study the monolayer phase behaviour of these bipolar (mono-functionalised) and tripolar (bisfunctionalised). Conceptual difficulties arose upon attempting to extract valid structural information from the monolayer isotherms using literature methodologies. Among the most important of these difficulties was how to reconcile monolayer phase differences between structurally related phospholipids in the analysis of monolayer isotherms. Although both the DSC experiment and the monolayer experiment are extensively used to characterize the interfacial behavior of phospholipids it is uncommon to find a correlation between the two techniques. This problem arises because the temperature at which measurements are made greatly affects the phase of the aggregate in the monolayer isotherm. To account for this

#### Chapter 1 - General Introduction

difference in phase behaviour the concept of a reduced temperature normalization process is discussed.

In Chapter 4 the surface potential of the mono- and bis-functionalised phospholipid monolayer is sensitive to the orientation of the dipole at the interface ( $\mu$ ). The surface potential-area (A) curves provide new insight into the molecular details of the transitions observed in the  $\pi$ -A isotherms.

Chapter 5 diverges from discussion of how modification of lipid structure leads to modification of lipid properties. The kinetics of the protein tyrosine phosphatase (PTPase) binding to phospholipid monolayers using the Langmuir film-balance technique is presented. The issue of an enhancement at anionic lipid interfaces is addressed. Through analysis of the effects of headgroup, surface density and protein subphase concentration a self-consistent model for the interaction emerges. The differences between the kinetics obtained in the constant surface area mode and those obtained in the surface expansion mode are also discussed.

#### 1.3. References

- (1) Gennis, R. B. <u>Biomembranes: Molecular Structure and Function</u>. Springer-Verlag: London 1989.
- (2) Yamauchi, K., Kinoshita, M. Prog. Polym. Sci., 1993, 18, 763-804.
- (3) Gliozzi, A., Paoli, G., Pisani, D., Gliozzi, F., De Rosa, M., Gambacorta, A. Biochim. Biophys. Acta, 1986, 861, 420-428.
- (4) Kim, J., Thompson, D.H.; Langmuir, 1992, 8, 637-644.
- (5) Dote, J. L., Barger, W.R., Behroozi, F., Chang, E.L.; Lo, S.L., Montague, C.E., Nagumo, M. *Langmuir*, **1990**, 6, 1017-1023.
- (6) Rice-Evans, C., Burdon, R. Prog. Lipid Res., 1993, 32, 71-110.
- (7) van den Berg, J. J. M., Op den Kamp, J.A.F., Lubin, B.H., Kuypers, F.A. *Biochemistry*, **1993**, 32, 4926-4967.
- (8) Wratten, M. L., van Ginkel, G., van't Veld, A.A., Bekker, A., van Faassen, E.E., Sevanian, A. *Biochemistry*, **1992**, 31, 10901-10907.
- (9) Fujita, S., Suzuki, K. J.A.O.C.S., 1990, 67, 1008-1015.
- (10) van Kuijk, F. J. G. M., Sevanian, A., Handelman, G.J., Dratz, E.A. T.I.B.S., 1987, 12, 31-34.
- (11) Salgo, M. G., Corongiu, F.P., Sevanian, A. Arch. Biochem. Biophys., 1993, 304, 123-132.
- (12) Sevanian, A., Muakkassah-Kelly, S.F., Montestruque, S. Arch. Biochem. Biophys., 1983, 223, 441-452.
- (13) Menger, F. M., Wood, M.G., Richardson, Jr. S., Zhou Q.; Elrington A.R., Sherrod M.J. J. Am. Chem. Soc., 1988, 110, 6797-6803.
- (14) Menger, F. M., Wood M.G. Jr., Zhou Q.Z., Hopkins, H.P. J. Am. Chem. Soc., 1988, 110, 6804-6810.
- (15) Pidgeon, C., Markovitch, R.J., Liu, M.D., Holzer, T.J., Novak, R.M., Keyer, K. A. J.Biol. Chem., 1993, 268, 7773-7778.
- (16) Pidgeon, C., Qiu, X. Biochemistry, 1994, 33, 960-972.
- (17) Georges, C., Lewis, J.T., Llewellyn, J.P., Salvago, S., Taylor, D.M., Stirling, J.M., Vogel, V. J. Chem. Soc. Faraday Trans., 1988, 84, 1531-1542.
- (18) Oliveira, O. N., Taylor, D.M., Lewis, T.J., Salvagno, S., Stirling, C.J.M. Journal of the Chemical Society, Faraday Transactions, 1989, 85, 1009-1018.
- (19) Vogel, V., Mobius, D. Thin Solid Films, 1985, 132, 205-219.
- (20) Cadenhead, D. A., Muller-Landau, F., Kellner, B.M.J. J. Coll. Interf. Sci., 1978, 66, 597-601.

#### Chapter 1 - General Introduction

- (21) Xu, Z., Cafiso, D.S. Biophys. J., 1986, 49, 779-783.
- (22) de Haan, J. W., de Weerd, R.J.E.M., van de Ven, L.J.M., den Otter, F.A.H., Buck, H.M. J. Phys. Chem., 1985, 89, 5518-5521.
- (23) Lewis, R. N. A. H., McElhaney, R.N., Monck, M.A., Cullis, P.R. *Biophys. J.*, 1994, 67, 197-207.
- (24) Casal, H. L., McElhaney, R.N. Biochemistry, 1990, 29, 5423-5427.
- (25) McElhaney, R. N. Chem. Phys. Lipids., 1982, 30, 229-259.
- (26) Silvius, J. R. Chem. Phys. Lipids, 1991, 57, 241-252.
- (27) Kuhn, H., Mobius, D., Ed. Monolayer Assemblies (Second Ed. ed.). 1993.
- (28) Seddon, J. M., Cevc, G. In <u>Phospholipids Handbook</u> G. Cevc, Ed.; Marcel Dekker, Inc.: New York 1993 (pp. 403-454).
- (29) Israechvili, J. N. Intermolecular and Surface Forces (2 ed.). Academic Press: San Diego 1992.
- (30) Lindblom, G., Rilfors, L. Biochimica at Biophysica Acta, 1989, 988, 221-256.
- (31) Lewis, R. N. A. H., McElhaney, R.N., Harper, P.E., Turner, D.C., Gruner, S.M. Biophys. J, 1994, 66, 1088-1103.
- (32) Epand, R. M., Epand, R.F., Ahmed, N., Chen, R. Chem. Phys. Lipids, 1991, 57, 75-80.
- (33) Silvius, J. R., Lyons, M., Yeagle, P.L., O'Leary, T.J. Biochemistry, 1985, 24, 5388-5395.
- (34) Lewis, R. N. A. H., McElhaney, R.N. Biochemistry, 1985, 24, 4903-4911.
- (35) Verger, R., Pattus, F. Chem. Phys. Lipids, 1982, 30, 189-227.
- (36) Weiner, H., Wang, Y. Biochemistry, 1994, 33, 12860-12867.
- (37) Cornell, D. G., Dluhy, R.A. Biochemistry, 1989, 28, 2789-2797.
- (38) Scherphof, G., Damen, J., Hoekstra, D. In <u>Liposomes: From Physical Structure to Therapeutic Applications</u> C. G. Knight, Ed.; Elsevier/North-Holland Biomedical Press: New York 1981 (pp. 299-322).
- (39) Hernandez-Caselles, T., Villalain, J., Gomez-Fernandez, J.C. Mol. Cell. Biol., 1993, 120, 119-126.
- (40) Namba, Y. In <u>Phospholipids Handbook</u> C. G., Ed.; Marcel Dekker, Inc.: New York 1993 (pp. 879-894).

#### Chapter 2

# Role of Interchain Dipole-Dipole Interactions in the Stabilization of Phospholipid Aggregates

(co-authors: Gilles Berthiaume, Dana Tanenbaum and R.B.Lennox)

#### Abstract

Analogs of the phospholipid distearoylphosphatidylcholine (DSPC) possessing the polar sulfone (SO<sub>2</sub>) group in the acyl chains have been synthesized and are shown to demonstrate interesting thermal properties including stability enhancement and extreme phase separation when mixed with DSPC. Thermal behaviour was studied by differential scanning calorimetry (DSC). The extent of the stability enhancement is a function of the position of the sulfone moiety. While thermal stability enhancement is observed for bis-functionalised phospholipids, it is observed for neither lipids functionalised on only one chain nor for lipids functionalised with sulfide, sulfoxide or keto groups. It is proposed that the large dipole moment of the sulfone moiety leads to the observed behaviour. Apparent cross-linking by the sulfone dipole in liposomes is consistent with the observed properties. In mixed lipid systems, the bis-sulfone lipid exhibits extensive phase separation (lateral heterogeneity) over the entire range of compositions studied. This behaviour is attributed to long-range dipole-dipole interactions. Mono-functionalised lipids do not exhibit such extensive phase separation and are shown to mix with DSPC at larger mole fraction values. Both a large in plane dipole moment and the ability to maintain cooperative interactions between polar groups is shown to be required for observation of enhanced vesicle thermal stability of lipid vesicles.

#### 2.1. Introduction

The fluid mosaic model<sup>1</sup> provides a useful starting point for detailed molecular studies of lipid membranes. Because phospholipids are the main structural component of the cell membrane, this model continues to be modified as the understanding of the structural and functional role of the lipids broadens. Phospholipids are chemically diverse allowing membrane lipids to have both structural and functional roles in cell processes. The relationship between membrane dynamics and cell function has become of increasing interest given that the lateral heterogeneity of membrane phospholipids controls the location and function of integral membrane proteins.<sup>2,3</sup> Lateral heterogeneity can be viewed as a fluctuation in the surface density, surface charge, morphology, or composition of the component phospholipids.<sup>2,3</sup> A cell can control the location and function of integral membrane proteins, the association of extrinsic proteins and antigens, and functions such as cell fusion, division and cellular transport via lateral heterogeneity.

Phospholipids will spontaneously aggregate into lamellar (bilayer), hexagonal, and cubic phases when dispersed in a non-solvent such as water. The organization of lipids into a bilayer configuration is most common for biologically important phospholipids. The enthalpic (ΔH) gain accrued on aggregation is compensated for by the unfavorable loss in entropy which occurs as a result of the organization of both the lipid and water molecules at the lipid/water interface. The ΔH gain arises from a combination of the electrostatic interactions of the lipid headgroups and the van der Waals interactions between the acyl chains. The interactions of modified lipid chains are the subject of our attention here. Details concerning the role played by headgroup interactions in the ordering of lipids into bilayer assemblies have been studied in great detail and are reviewed elsewhere.<sup>4</sup>

Phospholipid aggregates often exhibit a cooperative phase transition. Differential scanning calorimetry (DSC) is one of the primary tools used to study these phase transitions and its use in this regard has been extensively reviewed.<sup>5-7</sup> Of principal interest is the thermally induced main phase transition of lipid bilayers (T<sub>m</sub>). A relatively ordered

gel phase  $(L_{\beta})$  is transformed to a relatively disordered, fluid-like liquid-crystalline phase  $(L_{\alpha})$  at  $T_m$ . A pre-transition  $(T_p)$ , (I to 10°C lower than the  $T_m$ ), is often observed and is associated with a chain orientation transition (the  $P_{\beta}$ ' phase). The  $T_m$  is governed by the structure of the lipid acyl chains and is less sensitive to the lipid headgroup structure. The  $T_m$  value is frequently used as a diagnostic of the stability of liposomes and is useful in deriving structure/function correlations of the acyl chains. The enthalpy of the transition is also useful in understanding the phase transition and can be obtained through integration of the endotherm. The main phase transition is measured under conditions such that  $\Delta G = 0$  and  $\Delta H = T \cdot \Delta S$ ;  $\Delta S$  can thus be determined from DSC enthalpy data.

An increase in  $T_m$  is an indication that greater amounts of energy must be invested in the process involving a transition from the gel phase to the liquid-crystalline phase, due to the adoption of a more stable chain packing conformation. Alternatively, an increase in the  $T_m$  can be due to the difficulty in inducing kinks into the alkyl chains.<sup>8</sup>

Introduction of functional groups or heteroatoms in the fatty acyl chains yields a host of different phospholipids with distinct phase and thermal properties. The consequence of systematically changing the structure of acyl chain(s) has been studied in a variety of systems<sup>6,9-16</sup> and several trends have been well documented. For example the phase transition temperatures of phospholipid vesicles systematically increase with acyl chain length for a given headgroup. The position and number of double bonds in the acyl chains of unsaturated lipids have been shown to have a profound effect on the T<sub>m</sub>, with the T<sub>m</sub> reaching a minimum value when a double bond is placed at the midpoint of the acyl chain. The effect of methyl groups, keto and hydroxy groups has also been reported but not extensively studied. Finally, an odd/even chain length effect has been observed for ω-terminated anteisobranched lipids. 17

The importance of artificial lipid analogs lies in their capacity to extend our understanding of the structural basis of lipid function. Lipid analogs also have applications

#### Chapter 2

in medicine as potential agents against bacterial and viral infections <sup>15,18,19</sup> and are widely studied as potential drug delivery agents. <sup>20</sup>

The present study takes a different perspective in that it investigates the effect of incorporating of a sulfone moiety into the acyl chain(s) of distearoylphosphatidylcholine (DSPC). The sulfone lipid systems represent a novel type of lipid with complex thermal and physical properties. We are concerned with several issues:

- (1) What influence does the SO<sub>2</sub> group have on the stability of component liposomes, in comparison to the unfunctionalised lipid DC<sub>18</sub>PC?
- (2) How is the phase transition of the functionalised lipids affected by the position of the SO<sub>2</sub> group?
- (3) What are the properties of binary lipid mixtures incorporating these functionalised lipids?

Differential scanning calorimetry (DSC) was used to measure the phase transition temperatures of a series of phospholipids derived from the parent molecule sn-1 lyso DSPC which incorporates a sulfone-containing acyl chain at positions 5, 7, 9, and 11. The properties of these lipids are discussed and compared to other lipid analogs possessing functional groups such as sulfoxide (SO), sulfide (S) and keto groups (>C=O). The phase behaviour of binary lipid mixtures containing bis- and mono-substituted sulfone lipids is also reported.

#### 2.2. Materials and Methods

#### 2.21. Differential Scanning Calorimetry

Experiments were conducted using a Perkin Elmer DSC VII in a nitrogen atmosphere. Lipid samples were dried from chloroform prior to suspension in Millipore Milli-Q water (18 mΩcm<sup>-1</sup>) at 10 mg/100 mL in the DSC sample pan. Mixtures of lipids were prepared by first dissolving the two components in chloroform and then combining the solutions to achieve the appropriate lipid composition. Chloroform was removed under vacuum. Samples saturated with water in sealed DSC sample pans were submitted to sonication for 20 minutes and four freeze-thaw cycles (-70 to 65 °C). Samples were stored at -20 °C for 48 hours prior to thermal analysis. A two point calibration of the instrument was conducted with octadecane (onset 28.4°C) and indium (onset 154.6°C). All DSC runs were performed at a rate of 1.25 °C/min. Measurements were conducted over a temperature range of 5 to 85°C.

A number of DSPC analogs functionalised at either the sn-1 chain or at both the sn-1 and sn-2 chains (Figure 1.1) were studied. Keto phospholipids were synthesized using procedures previously reported by Menger and co-workers. Phospholipids incorporating either sulfide, sulfone and sulfoxide moieties in the acyl chains were synthesized in our lab by the same methods. The synthesis of the sulfone and sulfoxide-functionalised fatty acid used in the partial synthesis of the sulfone-functionalised phospholipids has been described elsewhere. The sulfides used in the partial synthesis were purchased from Aldrich. Their composition was established by FAB-MS, and their purity monitored using NMR (300 MHz and 500 MHz) and thin layer chromatography (TLC) (70:26:4 CHCl<sub>3</sub>:MeOH:H<sub>2</sub>O). Purity was estimated to be >99% from these measurements.

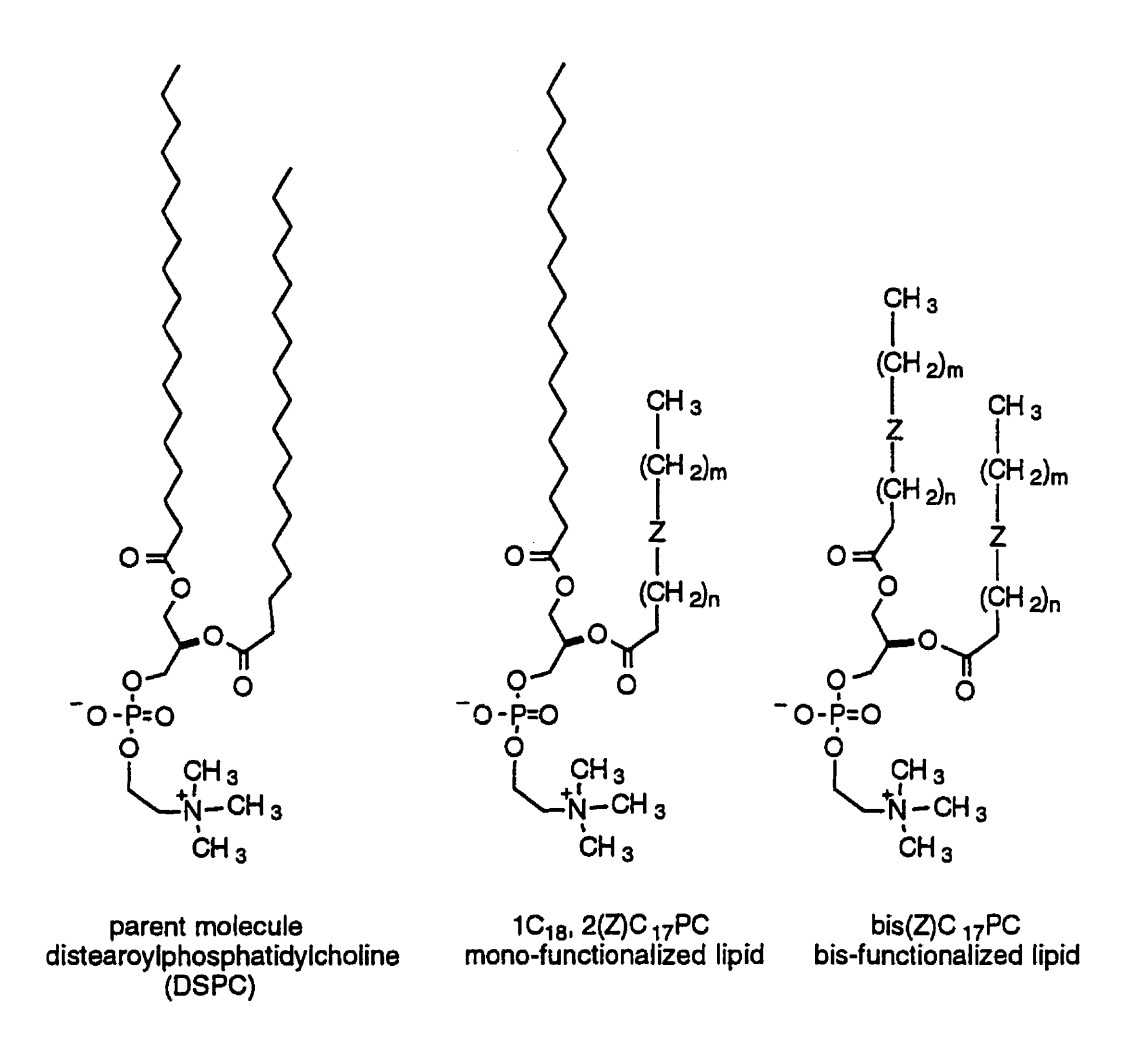


Figure 2.1. Distearoylphosphatidylcholine (DSPC) and phospholipid analogs used in the present study (n+m=14),  $Z = SO_2$ , SO, S or >C=0.

#### $2.22.\,^{31}P-NMR$

 $^{31}$ P-NMR spectra of  $^{1}$ C<sub>18</sub>,2(9SO<sub>2</sub>)C<sub>17</sub>-PC and bis(11SO<sub>2</sub>)C<sub>17</sub>-PC lipids both below (25 °C) and above (80°C) the DSC-determined  $^{1}$ T<sub>m</sub> values were obtained using a CheMagnetics CMX-300 spectrometer operating at 121.3 MHz. Samples were placed in short 5 mm tubes, saturated with Millipore Milli-Q water and sealed with epoxy. The sealed samples were heated, sonicated and driven through 4 freeze-thaw cycles prior to analysis. Sealed samples were sonicated between freeze-thaw cycles. Spectra were obtained with 90° pulses of 5  $\mu$ s duration with recycle times of 0.5 s. Typically, 600 transients were collected. The samples were static and high power  $^{1}$ H decoupling was employed during the acquisition. The temperature was maintained to  $\pm$  1°C by a CheMagnetics temperature controller.

#### 2.3. Results and Discussion

The phospholipid lamellar gel phase has a high degree of order at all positions along the acyl chains. The chains exist in an all-trans conformation so as to increase stabilizing van der Waals interactions. The chain disorder which is characteristic of the liquid crystalline phase begins at the chain ends and moves towards the center of the chain with an increase in temperature.<sup>24</sup> Order parameters obtained from NMR establish that from the acyl carbon (C1) to the C10 region the chains are relatively ordered, in the case of n-alkyl chains, and from C10 to C18 the molecular motions increase rapidly and uniformly.<sup>25-27</sup> The effect of a chain modification in these two regions will therefore be different. An order-inducing modification will have a greater effect if placed in the C10-C18 region and a disorder-inducing group will have a greater effect in the C1-C10 region. An increase in  $T_m$  can be attributed to either a stabilization of the gel phase or to a destabilization of the liquid-crystalline phase. The gel phase is stabilized by ordering and the liquid-crystalline phase is destabilized by ordering (both resulting in an increased T<sub>m</sub>) so although it is difficult to specify which phase is being affected, the effect of a structural modification can be assigned as an ordering or disordering one. The opposite argument is, of course, true for a decrease in T<sub>m</sub>.

The incorporation of the polar sulfone group into phospholipids and its effect on phospholipid cooperative properties have not been previously reported. The incorporation of the sulfone group into the alkyl chains of alkyl thiols in self-assembled monolayers has been studied. The dependence of the monolayer properties were studied by FT-IR spectroscopy and X-ray photoelectron spectroscopy (XPS). The perturbation caused by the steric bulk of the sulfone group was found to be partially compensated for by chain-ordering induced through dipole-dipole interactions. In another study the presence of multiple sulfone groups in the alkyl-thiol chain was shown to repel the adsorption of proteins to the alkyl-thiol monolayer. <sup>29</sup>

The SO<sub>2</sub>-functionalised lipids studied here provide another detailed example of a molecular assembly incorporating strong dipoles into the alkyl chain. The effect of the functional group and its position in the chain on the temperature, enthalpy, and entropy of the main phase transition of lipid bilayers with respect to DSPC is discussed. The trends observed in the sulfone series are compared with those of the sulfoxide, sulfide and keto lipids. How the steric bulk and the polarity of these functional groups modulates lipid-lipid interactions is of particular interest.

### 2.31. Effect of $SO_2$ groups on the thermal properties of functionalised lipids: $bis(nSO_2)C_{17}$ -PC series

A position-dependent increase in  $T_m$  is observed for bis(nSO<sub>2</sub>)C<sub>17</sub>-PC lipids (Table 2.1) with respect to DSPC. By the arguments presented above the bilayer is therefore shown to be more ordered for bis(nSO<sub>2</sub>)C<sub>17</sub>-PC vesicles than for DSPC vesicles. The ordering effect is attributed to the presence of the two SO<sub>2</sub> groups. The  $T_m$ 's of bis(5SO<sub>2</sub>)C<sub>17</sub>-PC and bis(7SO<sub>2</sub>)C<sub>17</sub>-PC are respectively 4°C and 5°C greater than the  $T_m$  of DSPC. Much greater  $T_m$  increases of 14°C and 22 °C are observed for bis(9SO<sub>2</sub>)C<sub>17</sub>-PC and bis(11SO<sub>2</sub>)C<sub>17</sub>-PC respectively. Sulfone functionalisation at the 9 and 11 positions is in the midpoint region of the chain where disorder markedly increases above the  $T_m$ . Introduction of the sulfone group into this region therefore has a greater effect than locating it in the more ordered region near the headgroup.

Table 2.1. Thermophysical data for the bis(nSO<sub>2</sub>)C<sub>17</sub>-PC lipid series

lipid	T <sub>m</sub> (°C)	ΔH <sup>I</sup> (kJ/mol)	ΔS <sup>1</sup> (J/mol.K)
DSPC	54.3	44	135
bis (5SO <sub>2</sub> ) PC	58.5	56	170
bis (7SO <sub>2</sub> ) PC	59.6	60	180
bis (9 SO <sub>2</sub> ) PC	68.2	68	200
bis (11SO <sub>2</sub> ) PC	75.9	64	185

 $<sup>^{1}\</sup>Delta G = \Delta H - T\Delta S$ ,  $\Delta G = 0$  at  $T_{m}$ .

### 2.32. Relationship between position of the functional group and $T_m$ for the $1C_{18}$ , $2(nSO_2)C_{17}$ -PC series

In contrast to the large increase in the  $T_m$  observed for the bis-sulfone series, introduction of a single SO<sub>2</sub> group on the sn-2 chain of DSPC causes a reduction in  $T_m$ . The  $T_m$  reduction also exhibits a strong dependence on the SO<sub>2</sub> position (Table 2.2). Greater decreases in the  $T_m$  arise when SO<sub>2</sub> is placed near the headgroup ( $\Delta T_m^{5SO2} = -13.6$  °C,  $\Delta T_m^{7SO2} = -14.7$  °C), than when placed near either the midpoint of the chain ( $\Delta T_m^{9SO2} = -6.7$  °C,  $\Delta T_m^{11SO2} = -3.4$  °C) or near the chain terminus ( $\Delta T_m^{16SO2} = -2.9$  °C). Both the decrease in  $T_m$  with respect to DSPC and the positional dependence of the  $T_m$  support a disorder inducing effect of the SO<sub>2</sub> group when placed in only one chain. The  $\Delta T_m$  is greater at positions closer to the headgroup since this is a highly ordered region.

Table 2.2. Thermophysical properties of the 1C<sub>18</sub>,2(nSO<sub>2</sub>)C<sub>17</sub>-PC lipid series

lipid	T <sub>m</sub> (°C)	ΔH (kJ/mol)	ΔS (kJ/mol·K)
1C <sub>18</sub> ,2(5SO <sub>2</sub> )C <sub>17</sub> -PC	40.7	34	110
1C <sub>18</sub> ,2(7SO <sub>2</sub> )C <sub>17</sub> -PC	39.6	57	182
1C <sub>18</sub> ,2(9SO <sub>2</sub> )C <sub>17</sub> -PC	47.6	58	180
1C <sub>18</sub> ,2(11SO <sub>2</sub> )C <sub>17</sub> -PC	50.9	88	270
1C <sub>18</sub> ,2(16SO <sub>2</sub> )C <sub>17</sub> -PC	51.4	a	a

a not measured due to broadness of peak

#### 2.33. Thermodynamics of the phospholipid main transition.

Bis-functionalised lipids exhibit an increase in  $\Delta H$  and  $\Delta S$  of the transition with respect to DSPC (Table 2.1). The variations in enthalpy and entropy with SO<sub>2</sub> position are much less pronounced than for the mono-functionalised lipids (Table 2.2). The increase in  $\Delta H$  of SO<sub>2</sub>-functionalized lipids with respect to that of DSPC may be attributed to an increase in  $H_{gel}$  since  $\Delta H = H_{gel} - H_{lc}$ . The absence of a significant position dependence in  $\Delta H$  for SO<sub>2</sub> bis-functionalised lipids may imply constant  $H_{gel}$  for all SO<sub>2</sub> positions or  $H_{lc}$  may increase with  $H_{gel}$ . An increase in  $H_{lc}$  may be rationalized by an ordered melt (preservation of chain-chain cohesive interactions in the liquid-crystalline phase).

Despite the decrease in  $T_m$  with respect to DSPC, increases in  $\Delta H$  and  $\Delta S$  are observed for all but n=5 in the  $1C_{18},2(nSO_2)C_{17}$ -PC series. Unlike the bis-SO<sub>2</sub> series, which exhibits small changes in  $\Delta H$  across the entire series, the mono-functionalised lipids exhibit a strong positional dependence in both  $\Delta H$  and  $\Delta S$ . The enthalpy and entropy difference between the gel and liquid-crystalline states widens as the  $T_m$  increases for the mono-functionalised lipids. An increase in  $H_{gel}$  and constant  $H_{lc}$  is consistent with this trend and may be rationalized by considering the chain order parameter.

In comparison to the increases in  $\Delta H$  and  $\Delta S$  shown for  $SO_2$ -functionalised lipids, the introduction of one or two methyl groups into the lipid chains (reported elsewhere)<sup>9</sup> resulted in decrease in both  $\Delta H$  and  $\Delta S$  of the transition with respect to DSPC. This suggests that different factors are at play in the  $SO_2$  and branched methyl systems. This issue will be addressed further in the discussion.

## 2.34. Phase behaviour in binary lipid mixtures of bis(11SO<sub>2</sub>) $C_{17}$ -PC/DSPC binary mixture

Thermograms obtained for binary mixtures of DSPC and bis(11SO<sub>2</sub>)C<sub>17</sub>-PC show that phase heterogeneity is maintained over a wide composition range. Between f = 0.1 to 0.2 bis(11SO<sub>2</sub>)C<sub>17</sub>-PC ( $f = X_{lipid}/(X_{lipid}+X_{DSPC})$ ) where X is moles of lipid) a second endotherm appears at 75 °C (Figure 2.2.). At f = 0.3, the thermogram becomes complex with 4-5 clear maxima. Between f = 0.1 and 0.9 two melting transitions are observed consistent with the occurrence of phase separation. In general, no melting point depression of either component is noted with the exception of a modest effect in DSPC from f = 0.6 to 0.8. At these compositions the DSPC endotherm occurs at ( $T_m - 2$ °C). Figure 2.2 shows that the single transition observed at f = 0.1 is at the same temperature as for pure DSPC. Likewise, for f = 0.9 bis(11SO<sub>2</sub>)C<sub>17</sub>-PC, a single transition is observed which is at the same temperature as for pure bis(11SO<sub>2</sub>)C<sub>17</sub>-PC.

The observed transitions may be represented as:

$$A_S + B_S ----> A_1 + B_3 ----> A_1 + B_1$$

for a situation in which no mixing in the liquid-crystalline state occurs. If mixing in the liquid-crystalline state is taking place then:

$$A_S + B_S ----> L + B_S ----> L$$

applies, where A and B represent the gel phases of DSPC and bis(11SO<sub>2</sub>)C<sub>17</sub>-PC, respectively, and the subscripts s and l represent the solid and liquid phases respectively.

(L + B<sub>S</sub>) represents the region between the two peaks, where domains of DSPC are disordered (L) and domains of bis(11SO<sub>2</sub>)C<sub>17</sub>-PC are not. L represents the liquid crystalline phase (lc) where the liquid-crystalline phases of both lipids exist. Whether or not the lipids mix in the liquid crystalline phase cannot be determined from these experiments. The absence of an endotherm at 75 °C (f = 0.1) and at 55°C (f = 0.9, Figure 2.2) suggests that either (i) bis(11SO<sub>2</sub>)C<sub>17</sub>-PC and DSPC are mixing at these compositions or (ii) that the phase separated domains are too small to be manifested as a DSC-detectable phase. The absence of any freezing point depression at f = 0.1 and 0.9 shows that the functionalised lipid is completely excluded from the DSPC phase (f = 0.1) and forms domains too small to be detected by the DSC (phase separation), likewise for f = 0.9. This model involving phase separation in the liquid-crystalline phase is assumed to be operative although it describes an uncommon situation (in lipid chemistry) of extreme non-ideality.

Cooperativity is a measure of the number of lipids which undergo the phase transition simultaneously.<sup>6,31</sup> In an ideal first-order transition all lipid molecules are involved in the phase transition and the endotherm is infinitely narrow. In practice, endotherms display a finite width as the number of lipids undergoing the transition is finite. The full width at half maximum (FWHM) is proportional to the cooperativity of the transition;<sup>6</sup> qualitatively, a larger peak width indicates a lower degree of cooperativity in the transition.

A distinct broadening of the transitions occurs upon addition of the  $SO_2$ functionalised lipid component to pure DSPC (Figure 2.2). The degree of broadening
remains constant as n increases, indicating that the degree of cooperativity of the mixed
systems does not vary with a change in composition. The ratio of the peak areas in the
thermograms reflects the composition of the lipid component in the mixture.

The non-ideal mixing observed for the bis(11SO<sub>2</sub>) $C_{17}$ -PC/ DSPC mixture reveals that the pure compounds are physically distinct. Lipids which are similar in structure will mix and a single endotherm of the mixture occurs at a position between the  $T_{\rm m}$ s of the pure

#### Chapter 2

pure components.<sup>32</sup> Phase separation has been reported in mixed lipid systems where the difference in chain length is 4 carbons or more<sup>7,31</sup> but the phase separation was not reported over a range of compositions. Hydrophobic mismatch has been proposed to account for this type of phase separation<sup>33</sup> and may also explain the phase separation observed in the bis(11SO<sub>2</sub>)C<sub>17</sub>-PC/DSPC system. The phase separation in this case occurs so that the system can optimize its bilayer packing by maximizing the van der Waals interactions.

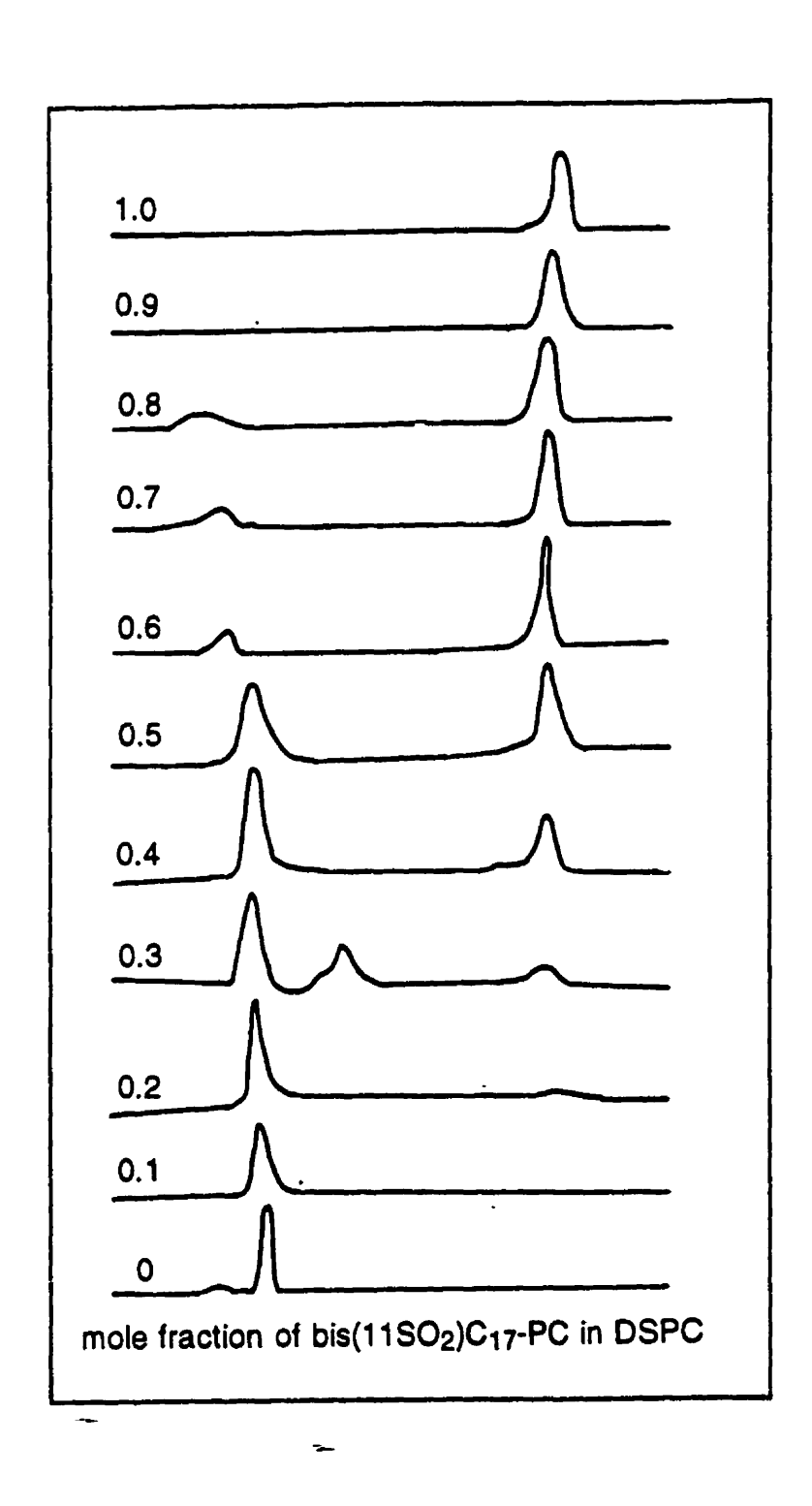


Figure 2.2. Binary mixtures of bis( $11SO_2$ )C<sub>17</sub>-PC with DSPC at various values of f.

#### 2.35. Phase behaviour of IC18,2(9SO2)C17-PC/DSPC binary mixture

The mixing behaviour of the  $1C_{18}$ , $2(9SO_2)C_{17}$ -PC/DSPC system is much more complex, and unlike the bis( $11SO_2$ )C<sub>17</sub>-PC/DSPC system, complete mixing of the lipid components is observed at f > 0.5 accompanied by a freezing point depression of the mixture with respect to pure  $1C_{18}$ , $2(9SO_2)C_{17}$ -PC (Figure 2.3). The transitions above f = 0.5 all occur at the same temperature (40 °C), which is 7 °C less than that of pure  $1C_{18}$ , $2(9SO_2)C_{17}$ -PC. The freezing point depression and the presence of the single transition for the binary lipid mixture demonstrate that the lipids mix ideally in the gel phase. The mono-substituted  $SO_2$  lipid can thus be accommodated within the DSPC phase (and vice-versa). At  $f \le 0.5$  for ( $1C_{18}$ , $2(9SO_2)C_{17}$ -PC), complex behaviour is observed in which phase separation is apparent.

A considerable loss in the cooperativity also accompanies these transitions as is evident from the broadness of the endotherms (Figure 2.3). Although phase separation persists, the number of lipid molecules which simultaneously undergo the transition is low. The decrease in cooperativity may be attributed to the co-existence of small domains of the two lipids and a state of limited mixing. The complexity of the phase separation in this mole fraction region cannot be rationalized without additional structural information (such as diffraction data), but may also be due to the introduction of different lipid morphologies or metastable states. In addition it should be noted that for f = 0.1 to 0.3, the final transition occurs at temperatures higher than for either lipid component in its pure state.

The placement of the SO<sub>2</sub> group along only one chain therefore yields a lipid which exhibits compositional homogeneity with an unfunctionalised lipid over a wide range of compositions. This illustrates that the difference in the way the mono-functionalised lipids and the unfunctionalised lipids pack is small.

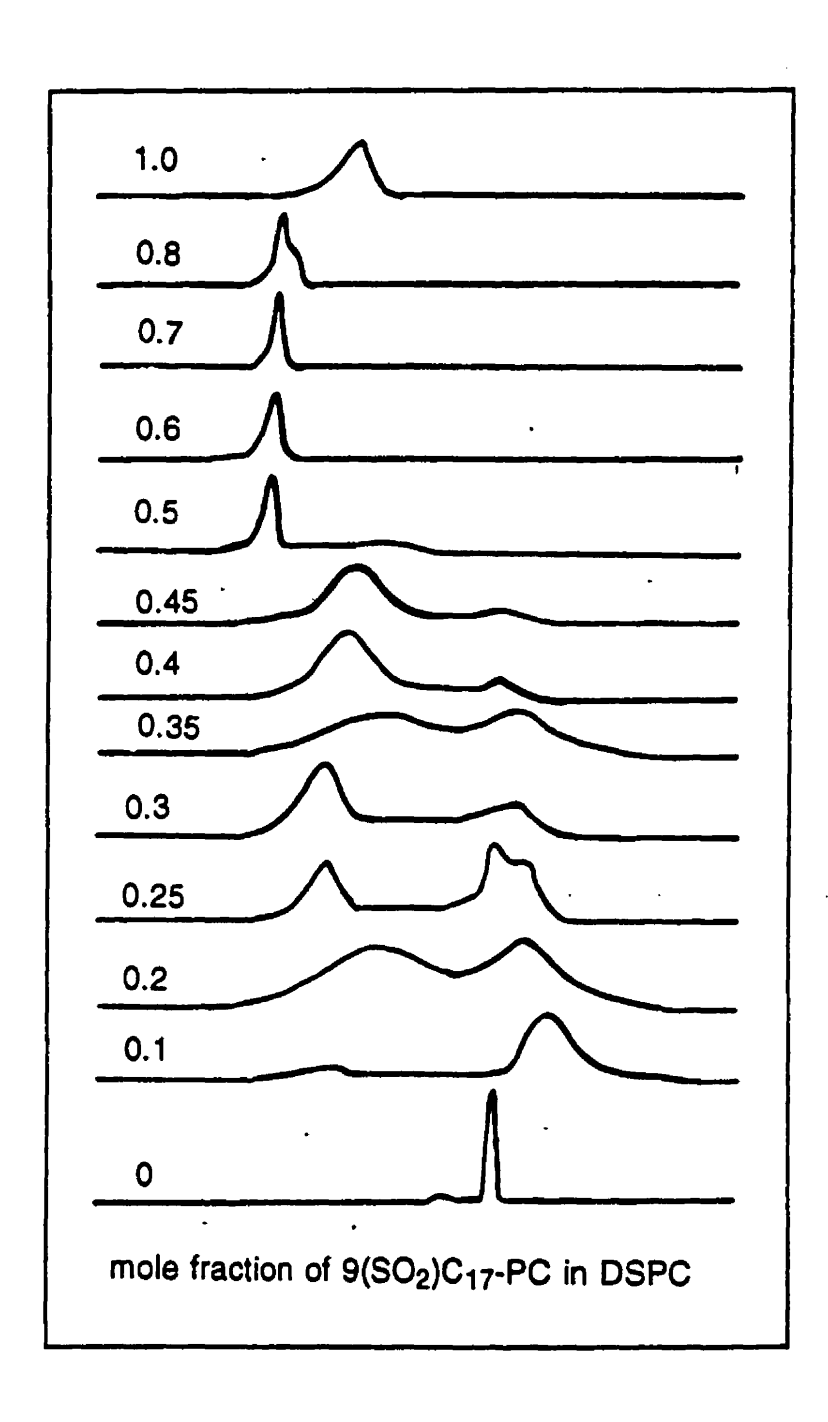


Figure 2.3. Binary mixtures of bipolar lipid  $1C_{18}$ ,  $2(9SO_2)C_{17}$ -PC and DSPC at different values of f.

# 2.36. Comparison of observed trends with those of other functionalised lipid systems

To assess the role of the sulfone group in the properties displayed by these functionalised lipids, the thermal properties of like-substituted lipids were compared, where the functional groups introduced into the chain included sulfoxide, sulfide, and keto groups (Table 2.3 and Table 2.4).

With the exception of the keto functionality, the  $T_m$  of the mono-substituted lipids exhibit a strong positional dependence. The trends observed in the variation of  $T_m$  with substituent position for each series show that the degree of perturbation (measured as a depression in  $T_m$ ) is a function of the position of the substituent. Similar trends were described for the sulfone and sulfoxide lipids (Sections 2.3.1-2.3.3). The  $T_m$  values of the SO-mono-functionalised lipids are however shifted downwards by 7-8°C with respect to the sulfone series (Table 2.3). These results show that for both the sulfone and sulfoxide lipids a greater perturbation of the lipid bilayer generally occurs as the substitution approaches the glycerol backbone.

The sulfide functionality does not yield the same trend in  $T_m$ , but rather parallels the positional dependence of alkene incorporation into the chain  $^{16}$  (Table 2.5). Instead of the  $T_m$  being most reduced near the headgroup, it produces the greatest extent of bilayer packing destabilisation when the sulfide moiety is positioned near the chain midpoint. The sulfide moiety, like the alkene functionality, can be viewed as dividing the lipid alkyl chain into two smaller segments. The observed  $T_m$  value of a sulfide lipid approximately reflects the largest number of contiguous carbons; placing the sulfide or alkene at the 5 or 16 positions leaves alkyl chain lengths of 12 carbons and 14 carbons respectively can be involved in favorable van der Waals interactions. The greatest  $T_m$  reduction is observed for substitution at the chain center since two smaller segments (i.e. C9) result from this substitution.

The van-der Waals area of the sulfone group is 25-55% larger than either the methylene or the sulfoxide group (Table 2.6). The effect of the size of the SO<sub>2</sub> group on the thermal properties can be compared to the results presented elsewhere for methylbranched analogs. The trend observed for mono-functionalised SO<sub>2</sub> lipids (Table 2.3) differs from that of the analogous methyl-branched series (Table 2.3). For example, the SO<sub>2</sub> past the midpoint of the sn-2 chain (11) has the greatest T<sub>m</sub> value of the 5, 7, 9, and 11 lipids whereas the T<sub>m</sub> of methyl branched lipids reaches a minimum near this position (C10, Table 2.5). The trend of the methyl-branched lipids parallels that of unsaturated and sulfide lipids and can also be rationalized by the "maximum number of contiguous carbons" argument. Menger explained the trend by viewing the methyl group as a probe of the gauche bonds or "kinks" in the alkyl chain. The greatest depression in the T<sub>m</sub> was observed at the midpoint of the chain where a cooperative chain bending was proposed to occur. The trend observed for methyl-branched lipids is thus not attributable to the steric bulk of the methyl group.

The positional dependence of the  $SO_2$ -mono-functionalised lipids  $T_m$  can be rationalized on steric grounds as previously discussed. At this point the thermodynamic data discussed in section 2.33 is useful to highlight the difference in behaviour between the methyl-branched and  $SO_2$ -functionalised lipid systems. Whereas  $\Delta H$  decreases in the methyl-branched lipid series (with respect to DSPC),  $\Delta H$  increases with position of  $SO_2$  in the mono-functionalised series. The introduction of methyl groups disrupts van der Waals interactions which stabilize the bilayer whereas  $SO_2$  enhances them. Although we do not fully understand why the enhancement in van der Waals interactions is not manifested in an increased  $T_m$  value for the mono-functionalised lipids (and for the SO lipids) it may be related to a loss of order in the liquid-crystalline phase ( $\Delta S$  also increases, where  $T_m$  -  $\Delta H$ .  $\Delta S$ ).

#### 2.37 Morphology of SO2-functionalised lipid aggregates

The DSPC endotherm feature observed at (T<sub>m</sub>-10°C) is a P<sub>β</sub>'-to-L<sub>β</sub> transition.<sup>31</sup> In structural terms this is associated with an untilting of the lipid molecules which occurs prior to the melting of the alkyl chains.<sup>31</sup> This pre-transition is observed in neither the mono-SO<sub>2</sub> nor the bis-SO<sub>2</sub> series. Phosphatidylcholines assume the tilted orientation to maximize packing to compensate for the relatively large cross-sectional area occupied by the headgroup, compared to that of the chains. The absence of the pre-transition in the sulfone and sulfoxide lipids suggests that the bulky polar groups change these area balance requirements.

The steric bulk of the substituent has been shown to effect the phase and packing behaviour of phospholipids. For example lipids possessing branched groups near the polar headgroup (i.e. C2) have been shown to exhibit hexagonal or cubic phases above the T<sub>m</sub> due to the packing properties of the acyl chains. Another study reports the presence of an orthorhombic phase for branched-chain di-isopalmitoylphosphatidylcholine, phosphatidylethanolamine, and phosphatidyl-glycerol. The adoption of these morphologies is due to the particular shapes of the lipid molecules. Changes from the cylindrical geometry required for the lamellar morphology are caused by the presence and the position of the bulky substituent.

Previous reports have dealt with aspects of the unusual behaviour of alkyl-chain functionalised lipids. For example, phospholipids such as 1,2-bis(12-methoxy-dodecanoyl)-sn-3-phosphocholine (L-AC2), which contains oxygens in the acyl chain have been shown to possess anti-HIV activity. <sup>15,18</sup> In this case, the main transition temperature of parent molecule dimyristoylphosphatidylcholine (DMPC) is shifted from 23.6 °C to 40.9 °C for L-AC2. Dipole-dipole interactions of the adjacent ether atoms have been invoked to rationalize the tighter packing of the alkyl chains which lead to the increased  $T_m$  value. The dialkyl ether dipole moment (Table 2.6) is small however, and is considerably less than the dipole moment of either the dialkyl sulfone or sulfoxides presented here. It is

therefore questionable as to whether induced dipole arguments are valid in the L-AC2 case. An increase in the  $T_m$  may also be due to a decrease in the stability of the liquid-crystalline phase. This argument may be more reasonable since L-AC2 vesicles revert to thermally unstable micelles above the  $T_m$ . Although the dipole-dipole interactions may be responsible for some of the  $T_m$  enhancement, the observation that the ether lipids form micelles instead of bilayers above the phase transition temperature supports a liquid-crystalline phase destabilization argument.

Such an argument cannot be extended to the bis-SO<sub>2</sub> lipids since <sup>31</sup>P-NMR of aqueous suspensions of these lipids has established that a lamellar morphology occurs both below and above the main phase transition (Figure 2.4). The validity of using <sup>31</sup>P-NMR to establish lipid morphology has been addressed in the literature. <sup>14,35,36</sup> Specifically an axially symmetric powder pattern characteristic of a lamellar gel phase is obtained below the T<sub>m</sub>. The broad spectra exhibited by these compounds is due to the slow asymmetric motion of the phosphate headgroup on the <sup>31</sup>P-NMR time scale. The peak sharpens upon heating and the spectrum narrows approaching the shape characteristic of a phosphate headgroup undergoing symmetric motions in a bilayer environment. The bulky SO<sub>2</sub> group does not appear to impart a change in the geometry of the lipid which would typically result in a morphology change.

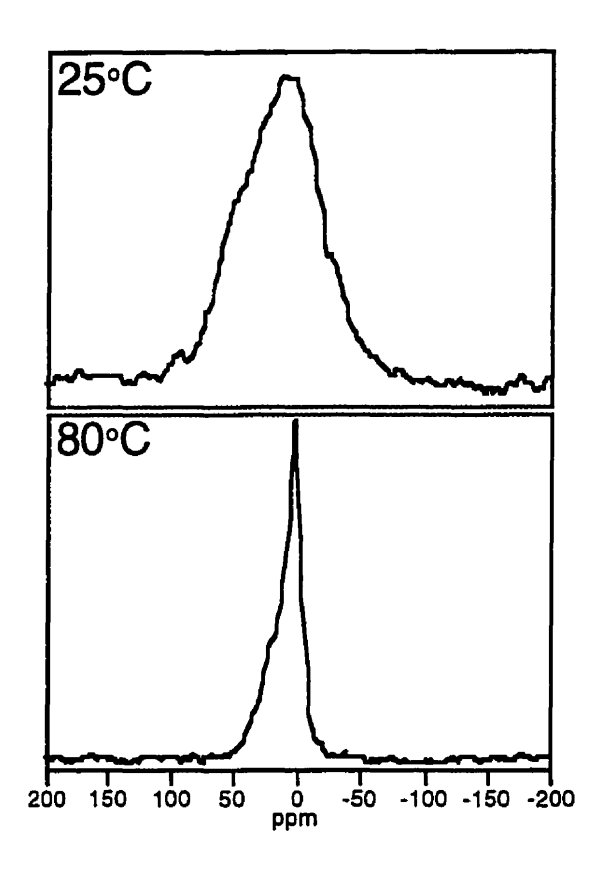


Figure 2.4. Proton-decoupled <sup>31</sup>P solid-state NMR of hydrated bisSO<sub>2</sub>-functionalised lipids. Spectra were measured at the temperatures indicated in a heating sequence which parallels the DSC experiment. Sample was incubated for 4 weeks at -20°C before measurement to ensure samples were at equilibrium. Spectra were obtained for lipids bearing SO<sub>2</sub> at positions 5 and 9 and found to be identical.

Although a sterically induced destabilisation is observed for mono-SO<sub>2</sub> lipids, a second SO<sub>2</sub> group has a stabilizing effect as shown by the marked increase in T<sub>m</sub>. Introduction of two bulky sulfone groups into the hydrophobic region of lipid bilayers apparently enhances the thermal stability via some additional factor. The most likely enhancement factor is a dipole-dipole cross-linking between the SO<sub>2</sub> groups. Although dipole-dipole interactions are usually not sufficient to lead to any strong mutual alignment

of polar molecules in a bulk liquid state,  $^{37}$  alignment nevertheless is possible since the bilayer state of the lipids is already quite ordered. Given the  $T_m$  enhancement, it appears that this dipole-dipole crosslinking is equivalent to increasing the DSPC hydrocarbon chain length by 4 carbons in length as the  $T_m$  of bis(11SO<sub>2</sub>)C<sub>17</sub>-PC is 75.9°C and the  $T_m$  of DC<sub>22</sub>PC is 74.8°C.  $^{38}$  This added electrostatic attraction is particularly interesting because evidently it has a large effect and explains the extensive phase separation observed in the bis(11SO<sub>2</sub>)C<sub>17</sub>-P/DSPC system.

Enhancement of liposome stability is observed for the bis-SO<sub>2</sub>-functionalised lipids. Although the SO group possesses a dipole moment comparable to than that of SO<sub>2</sub>, the bis-SO lipids show no equivalent stability enhancement (Table 2.5). Clearly the stability enhancement observed for bis-SO<sub>2</sub> lipids cannot be justified solely by consideration of the large dipole of the SO<sub>2</sub> group. The positional dependence of the T<sub>m</sub> of bis(nSO)C<sub>17</sub>-PC lipids however, parallels that of mono-functionalised sulfoxide and sulfone lipids indicating that it is the steric bulk of the SO group and not the dipole-dipole interaction that is dictating the thermal behaviour. The T<sub>m</sub> enhancement observed in bis(nSO<sub>2</sub>)C<sub>17</sub>-PC therefore appears to depend both upon the chemical nature of the group and upon the presence of polar groups in one or both lipid chains.

The absence of a T<sub>m</sub> enhancement for the SO series can be attributed to a lower *effective* dipole-dipole interaction. Maximum attraction occurs when two dipoles are aligned.<sup>37</sup> Given that the sulfoxide group is chiral, and that these samples are racemic, two dipole orientations are possible (Figure 2.5 (b)). Any cooperative alignment will be frustrated by the loss of dipole coherence. The energetic advantages from dipolar crosslinking are offset by the steric cost of the SO and SO<sub>2</sub> group when crosslinking is ineffective or diluted (Figure 2.5 (b) and (c)) and the functional group acts as a destabilizing moiety. The increased ΔH observed for mono-functionalised SO<sub>2</sub> lipids may be due to limited arrays of crosslinking in the gel state which are disrupted in the liquid-crystalline phase.

The symmetry of the  $SO_2$  group, on the other hand, does permit an alignment of the dipoles in a continuous manner (Figure 2.4.(a)). The increase in  $T_m$  and  $\Delta H$  observed for the bis-functionalised  $SO_2$  lipids may be due to an increase in both  $H_{gel}$  and  $H_{lc}$  implying that order persists in the liquid-crystalline phase due to the cooperative  $SO_2$  crosslinking.

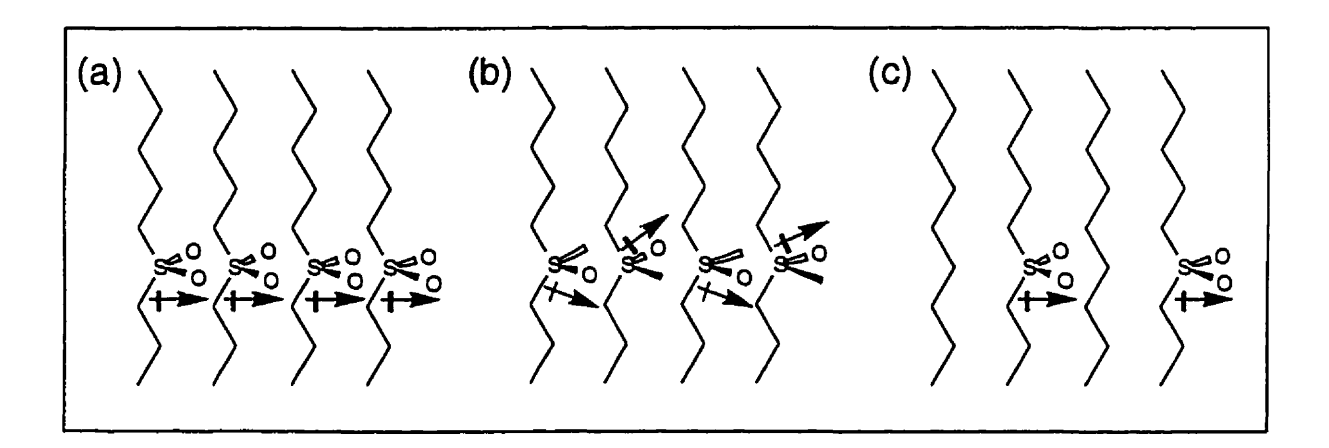
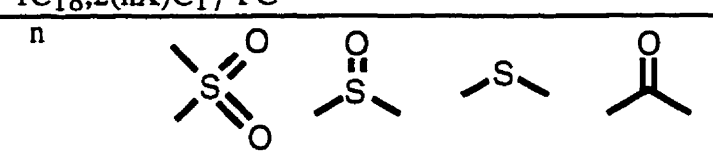


Figure 2.5. Schematic of alignment of (a) sulfone (b) sulfoxide groups (c) and monosubstituted lipids

Table 2.3.

Main transition temperatures of monofunctionalised phospholipids<sup>a</sup>
1C<sub>18</sub>,2(nX)C<sub>17</sub>-PC



		$T_{m}$ (°C)		
5	36.6	27.8	41.7	44.3
7	35.3	28.0	37.4	45.8
9	43.1	34.1	35.5	47.2
11	46.5	41.8	35.6	-
12	-	-	-	50.6
16	50.0		50.3	-

 $<sup>^{</sup>a}T_{m}$  (DSPC) is 54.3°C $^{31}$ 

Table 2.4.

Main transition temperatures of bis-substituted phospholipids, bis(nX)C17-PC

bis(nSO <sub>2</sub> )	S,O	O S	_S_

n		$T_{m}$ (°C)	
5	57.8	36.0	28.1
7	59.7	34.8	27.8
9	68.4	45.1	27.2
11	75.2	54.2	29.7

<sup>&</sup>lt;sup>a</sup>T<sub>m</sub> (DSPC) is 54.3°C<sup>31</sup>

Table 2.5. Main transition temperatures of branched chain and unsaturated lipids

Phospholipid Species	Z=Me <sup>9</sup>	$Z=(c\Delta)^{*39}$
	$T_{m}$ (°C)	
1C <sub>18</sub> ,2(4Z)C <sub>18</sub> -PC	41.5	-
1C <sub>18</sub> ,2(6Z)C <sub>18</sub> -PC	30.5	31
1C <sub>18</sub> ,2(8Z)C <sub>18</sub> -PC	18.6	•
$1C_{18,2}(9Z)C_{18-PC}$	-	5
$1C_{18},2(10Z)C_{18}-PC$	6.1	-
1C <sub>18</sub> ,2(12Z)C <sub>18</sub> -PC	8.0	19
1C <sub>18</sub> ,2(16Z)C <sub>18</sub> -PC	38.5	44

<sup>\*</sup> c∆ - cis double bond

Table 2.6. Physic	cal constants of functi	onal groups	
	dipole moment <sup>(a)</sup> (D)	dielectric constant(b)	group cross-sectional area <sup>(c)</sup> (Å <sup>2</sup> )
ethane	0		(CH <sub>2</sub> ) 2.5
dimethyl sulfone	4.00(1) 4.00(h)	47.39	(-SO <sub>2</sub> ) 4.5
dimethyl sulfoxide	3.16(1) 3.91(b)	47.24	(-SO) 3.4
dimethyl sulfide	1.43 <sub>(l)</sub>	6.7	(-S-) 3.1
acetone	3.09(1)	21.1	
dimethyl ether		25.3	(-O-) 1.7
diethyl ether	1.40(1) 1.11(cx)	4.27	(-O-) 1.7

<sup>(</sup>a) l=liquid, h=hexane, b=benzene, cx=cyclohexane<sup>40</sup>

<sup>(</sup>b) dielectric constants of liquids at 293.2 K<sup>41</sup>
(c) calculated from bond-length and van der Waals radii of elemental components as described elsewhere<sup>42</sup>

#### 2.4. Conclusions

The introduction of a polar functional group  $(SO_2)$  into the acyl chains of phospholipids results in an unusual thermal stability of the resulting phospholipid vesicles. The stability gain has been attributed to cross-linking of dipoles under specific conditions. The presence of functional groups with large dipoles in the acyl chains is not sufficient for the observation of thermal stability enhancement however. Phospholipids bearing sulfone groups on only one chain and lipids bearing sulfoxide groups in both chains did not exhibit  $T_m$  enhancement with respect to DSPC. The ability to form an extensive network of dipole cross-links is prevented in sulfoxide-functionalised lipids because the samples are racemic. In mono-functionalised sulfone lipids inhibition of a similar network is due to the interruption of interactions by the unfunctionalised sn-1 chain. Both the presence of a large dipole and the ability to form a contiguous network of interactions are required for a  $T_m$  increase to be observed.

Phase separation observed in binary lipid mixtures composed of bis(11SO<sub>2</sub>)C<sub>17</sub>-PC and DSPC also support the dipole-dipole cross-linking model. Phase separation exhibited by bisSO<sub>2</sub>/DSPC binary lipid mixtures represents an uncommon example of extreme non-ideal mixing which suggests that the matrix of the bis(SO<sub>2</sub>)-functionalised lipid bilayer is physically distinct from that of the unfunctionalised lipids. Monofunctionalised lipid 1C<sub>18</sub>,2(9SO<sub>2</sub>)C<sub>17</sub>-PC mixes with DSPC over a wide compositional range indicating the sulfone groups in this case do not participate in an extensive cross-linking due to the presence of the unfunctionalised chain. This points to the dipole-dipole cross-linking being responsible for the phase separation observed the bis(11SO<sub>2</sub>)C<sub>17</sub>/DSPC system. Optimization of van der Waals interactions must be greatest when bis(11SO<sub>2</sub>)C<sub>17</sub>-PC and DSPC exist in separate domains. The 'dipole-dipole' cross-linking would be interrupted upon mixing with a diluent lipid. Evidently the entropic energy which would be gained through mixing is lower than the enthalpy gained due to

#### Chapter 2

optimized van der Waals interactions when the lipids exist in phase separated, non-mixed states.

The phase separation and the enhanced liposome stability are related features which highlight the functional importance of the sulfone group. This paper presents a description of the effects that polar groups, especially sulfone and sulfoxide groups, may have on lipid assemblies. In particular the accessibility of thermally stable lipid vesicles through functionalisation of the acyl chains with the polar sulfone group is illustrated and attributed to an increase in order in both the gel and liquid-crystalline phases.

#### 2.5. References

- (1) Singer, S. J., Nicholson, G.L. Science 1972, 175, 720-731.
- (2) Mouritsen, O. G., Jørgensen, K., Hønger, T. *Permeability of lipid bilayers near the phase transition*; Mouritsen, O. G., Jørgensen, K., Hønger, T., Ed.; CRC Press: Boca Raton, 1994, pp 137-160.
- (3) Mouritsen, O. G. Chem. Phys. Lipids 1991, 57, 179-194.
- (4) Silvius, J. R. Chem. Phys. Lipids 1991, 57, 241-252.
- (5) Biltonen, R. L., Lichtenberg, D. Chem. Phys. Lipids 1993, 64, 129-142.
- (6) McElhaney, R. N. Chem. Phys. Lipids. 1982, 30, 229-259.
- (7) Ladbrooke, B. D., Chapman, D. Chem. Phys. Lipids 1969, 3, 304-367.
- (8) Nagle, J. F. J. Membrane. Biol 1976, 27, 233-250.
- (9) Menger, F. M., Wood M.G. Jr., Zhou Q.Z., Hopkins, H.P. J. Am. Chem. Soc. 1988, 110, 6804-6810.
- (10) Ingold, K. U., Chesseman, K. H., Emery, S., Maddix, S., Slater, T. F., Burton,
- G. W. Biochem. J. 1988, 250, 247-252.
- (11) Jacobs, R. E., Hudson, B., Anderson, H.C. Proc. Natl. Acad. Sci. USA 1975, 72, 3993-3997.
- (12) Blume, A. Chem. Phys. Lipids 1991, 57, 253-273.
- (13) Lamparski, H., Lee, Y., Sells, T. D., O'Brien, D. F. J. Am. Chem. Soc. 1993, 115, 8096-8102.
- (14) Lewis, N. A. H., McElhaney, R. N., Harper, P. E., Turner, D. C., Gruner, S. M. *Biophys. J.* 1994, 66, 1088-1103.
- (15) Pidgeon, C., Qiu, X. Biochemistry 1994, 33, 960-972.
- (16) Wang, G., Lin, H., Li, S., Huang, C. J. Biol. Chem. 1995, 39, 22738-22746.
- (17) McElhaney, R. N., Mannock, D.A. *Biophys. J.* **1994**, *66*, 734-740.
- (18) Pidgeon, C., Markovitch, R.J., Liu, M.D., Holzer, T.J., Novak, R.M., Keyer, K.A. J.Biol.Chem. 1993, 268, 7773-7778.
- (19) Fogler, W. E. Immunologic properties and activities of phospholipids; Fogler, W.
- E., Ed.; Marcel Dekker, Inc.: New York, 1993; Vol. I, pp 817-832.
- (20) Roger, R. C. Biological and biotechnological applications of phospholipids; Roger, R. C., Ed.; Marcel Dekker, Inc.: New York, 1993, pp 855-878.
- (21) Menger, F. M., Wood, M.G., Richardson, Jr. S., Zhou Q., Elrington A.R., Sherrod M.J. J. Am. Chem. Soc. 1988, 110, 6797-6803.
- (22) Berthiaume, G., unpublished results.

- (23) Georges, C., Lewis, J.T., Llewellyn, J.P., Salvago, S., Taylor, D.M., Stirling,
- J.M., Vogel, V. J. Chem. Soc. Faraday Trans. 1988, 84, 1531-1542.
- (24) Seelig, J., Browning, J. L. FEBS Lett. 1978, 92, 41-44.
- (25) Bloom, M., Evans, E., Mouritsen, O.G. Quarterly Rev. Biophys. 1991, 24, 293-397.
- (26) Mouritsen, O. G., Jorgensen, K. Chem. Phys. Lipids 1994, 73, 3-25.
- (27) Seelig, J. Quart. Rev. Biophys. 1977, 10, 353-418.
- (28) Evans, S. D., Goppert-Beraducci, K.E., Urankar, E., Gerenser, L.J., Ulman, A. Langmuir 1991, 7, 2700-2709.
- (29) Whitesides, G. M., Deng, L., Mrksich, M. J. Am. Chem. Soc. 1996, 118, 5136-5137.
- (30) Marsh, D. CRC Handbook of Lipid Bilayers; CRC Press: Boston, 1990.
- (31) Gennis, R. B. Biomembranes: Molecular Structure and Function; Springer-Verlag: London, 1989.
- (32) Blandamer, M., Briggs, B., Cullis, P.M., Engberts, J.B., Wagenaar, A., Smits,
- E., Hoekstra, D., Kacperska, A. J. Chem. Soc. Faraday. Trans. 1994, 90, 2703-2708.
- (33) Lehntonen, J. Y. A., Holopainen, J.M., Kinnunen, P.K.J. *Biophys. J.* 1996, 70, 1753-1760.
- (34) Silvius, J. R., Lyons, M., O'Leary, T.J. Biochemistry 1985, 24, 5388-5395.
- (35) Tilcock, C. P. S., Cullis, P.R., Gruner, S.M. Chem. Phys. Lipids 1986, 40, 47-56.
- (36) Mantsch, H. H., Madec, C. Biochemistry 1985, 24, 2440-2446.
- (37) Israelachvili, J. *Intermolecular and Surface Forces*; 2 ed.; Academic Press: New York, 1992.
- (38) Cevc, G. *Phospholipids Handbook*; Marcel Dekker, Inc.: New York, 1993; Vol. New York.
- (39) Boggs, J. M. Biochem. Cell Biol. 1986, 64, 50-57.
- (40) McClellan, A. L. Tables of Experimental Dipole Moments; Rahara Enterprises: San Francisco, 1977; Vol. 3.
- (41) Lides, D. R. CRC Handbook of Chemistry and Physics; 78 ed.; Lides, D. R., Ed.; CRC Press: New York, 1997-1998.
- (42) Williams, C. I., Whitehead, M.A. J. Phys. Chem. 1993, 97, 11652-11656.

#### Chapter 3

Bipolar phospholipid monolayers: Temperature dependence of the phase transition.

(co-authors: G. Berthiaume, L. Wei, and R.B. Lennox)

#### Abstract

Monolayer isotherms of a series of lipids which incorporate a sulfone (SO<sub>2</sub>) group into the alkyl chain at various positions were measured by the Langmuir film-balance technique (LFB). To establish the relationship between the monolayer phase transition and the bilayer phase transition the temperature dependence of the transition surface pressure is determined. The temperature dependence of the phase transitions was used to determine isothermal compressibilities  $(d\pi_1/dT)$  and critical temperatures  $(T_c)$  for the transitions. These values, along with dipole orientational changes reported elsewhere. show that the phase transition of simple diacyl phospholipids such as  $(DC_{14})$ , dipalmitoyl-  $(DC_{16})$  and distearoyl-  $(DC_{18})$ dimvristovlphosphatidylcholine (PC), and is an order-disorder process. If the phospholipid is derivatized on the acyl chain, but near the headgroup ( $n \le 7$ ) then the phase transition remains an order/disorder process. However lipids functionalised at positions at  $n \ge 9$  undergo a reorientational phase transition. Isotherms measured on a reduced temperature scale are plotted as reduced surface pressure  $(\pi/\pi_c)$  vs reduced surface area (A/A<sub>c</sub>). Isotherms of unfunctionalised lipids superimpose with this normalization process, but isotherms of functionalised lipids display a polar group-dependent  $\pi/\pi_c$  and reduced onset area  $(A_{on}/A_c)$ . The constancy of the transition area  $(\Delta A_t/A_c)$  in normalized isotherms reveals that the transition area reflects of the state of the lipid and not the area of the conformation adopted by the lipid at the interface. The virtue of the methodology proposed is in the clarification of the validity of using the monolayer isotherm for the extraction of relevant structural information and as a model of the cell membrane. The onset area and the transition pressure are shown to reflect structural differences whereas the transition area reflects the state of the lipid film. In addition the surface properties of a series of SO<sub>2</sub> functionalised lipids has revealed that the SO2 group served to destabilize the monolayer film as evidenced  $(\pi/\pi_c)$  values which increase with increasing distance of the functional group from the headgroup. This differs from the

#### Chapter 3

behaviour of lipids bilayers which experience a stabilizing effect of with increase in SO<sub>2</sub> position.<sup>2</sup> This highlights the limitations in using monolayers as models for lipid bilayers.

#### 3.1. Introduction

The relationship between lipid molecular structure and macroscopic properties such as the phase,  $^{3,4}$  morphology,  $^{5,6}$  and permeability of lipid vesicles  $^{7}$  provide insight into how a lipid may modulate macroscopic membrane function. Artificial lipid vesicles, monolayers formed at the air/water interface, and micellar phases have all been effective laboratory models of membranes in such studies. The Langmuir film-balance technique (LFB) provides a particularly convenient means of studying the lipid structure/function relationships using lipid monolayers. This technique and its versatility have been addressed in the literature. Briefly, a monolayer of lipid at the air/water interface is compressed by movable barriers while the surface tension is continuously recorded. The surface tension ( $\gamma$ ) (or surface pressure ( $\pi$ )) of the film is acquired as a function of the molecular area (A). Details of molecular packing and phases are accessible from this experiment.

The LFB technique has been extensively used in the field of membrane biophysics. The effect of lipid alkyl chain modification upon the packing properties of the lipid has been investigated for several systems including methyl branched lipids, <sup>10</sup> keto-functionalised lipids, <sup>11</sup> fluorinated lipids, <sup>12</sup> and fatty acids functionalised with a sulfoxide group. <sup>13</sup> Isotherms of modified lipids have usually been measured and compared at one defined temperature. This approach fails to take into account the different physical states of the lipids however. Isotherms contain structurally relevant information which is obscured due to differences in the well known temperature-dependent phase behaviour of lipids (*i.e.* different lipids possess different critical points which govern the temperature dependence of the monolayer isotherm). This report addresses this problem and presents a methodology which factors out phase variations so that one can compare isotherms of a series of structurally related phospholipids.

Lipids spontaneously aggregate upon dispersion in an aqueous medium. Long chain saturated phosphatidylcholine (PC's) form lamellar phases under standard temperature and pressure conditions. The most extensively studied phase transition is the

main gel-to-liquid-crystalline phase transition (Figure 3.1). This phase transition induced by changes in temperature, pH, pressure (P), and ionic strength (I) has been studied in great detail and has been established as an order-disorder transition for phospholipid vesicles. <sup>14, 15</sup> Most acyl lipids found in living systems exist in a chain melted state at the physiological temperatures. <sup>14</sup>

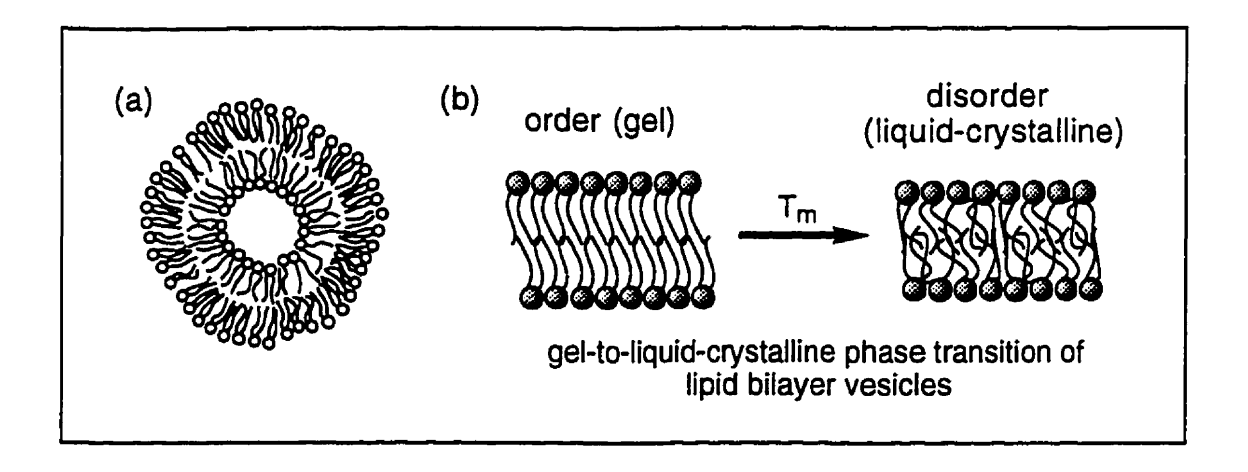


Figure 3.1. Schematic representation of (a) a bilayer lipid vesicle and (b) the order-disorder phase transition of lipid bilayers.

The phase properties of lipid monolayers have also been studied in great detail and a number of phases have been determined via diffraction techniques. The relationship between a given lipid phase and the conformation and orientation of the constituent lipid molecules is of particular interest. Figure 3.2. pictures an idealized  $\pi$ -A isotherms (adapted from  $^{15-17}$ ). A description of the basic terms used are shown and the reader is referred to the literature for a comprehensive review. Four isotherms are shown (Figure 3.2 (a)-(d)) which demonstrate schematically what happens to the isotherm as the temperature ( $T_{expt}$ ) is raised.

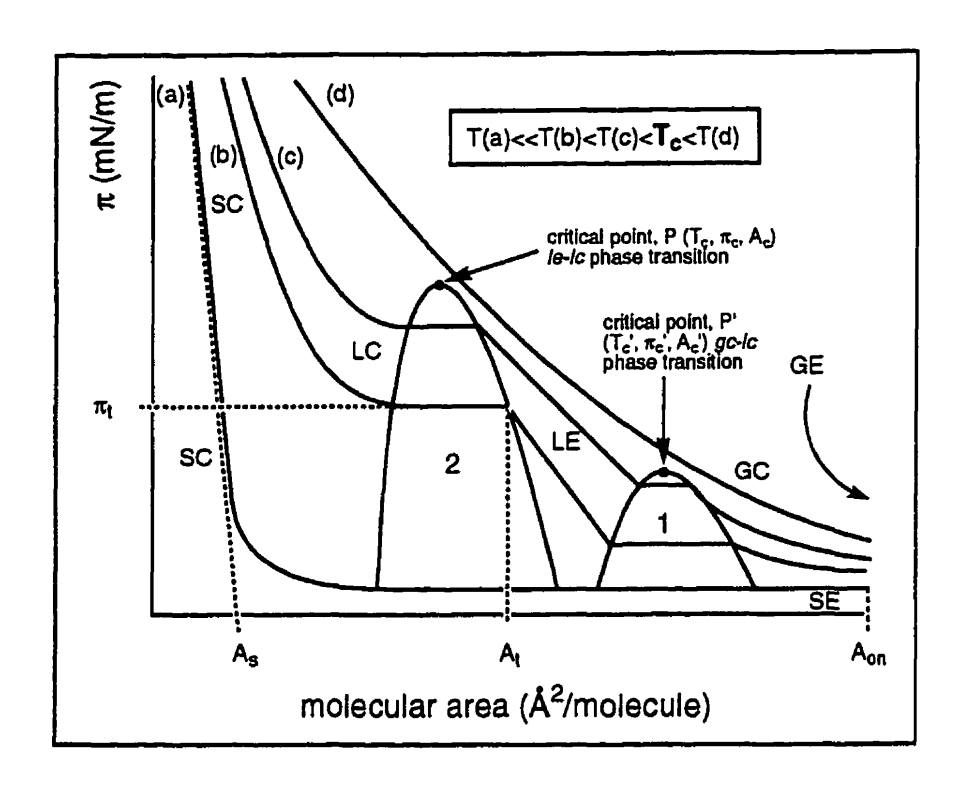


Figure 3.2. Schematic representation of the two-dimensional phase diagram of a phospholipid monolayer. Monolayer phases listed are GE (gas expanded), GC (gas condensed), SE (solid expanded), LE (liquid expanded), LC (liquid condensed), and SC (solid condensed). Two critical points are shown; P and P' with corresponding critical parameters  $\pi_c$ ,  $\pi_c$ ',  $A_c$ ,  $A_c$ ',  $T_c$  and  $T_c$ '. P is the critical point of the *le-lc* phase transition and P' is the critical point of the *gc-le* phase transition.  $A_s$  is the molecular area upon full compression and  $A_{on}$  is the area at which a rise in surface pressure is first detected. Curves (a)-(c) correspond to isotherms measured at increasingly higher temperatures. Curve (d) is measured above either  $T_c$  to  $T_c$ '.

Curve (a) (Figure 3.2) corresponds to an isotherm measured at a temperature far below the critical temperature ( $T_c$ ) of the lipid film. The film never attains a fluid state at this temperature. This film at low surface density is termed the solid-expanded phase (SE). The solid condensed phase (SC) corresponds to that part of the monolayer isotherm which is highly incompressible. The molecular area of the phospholipid in a vertical orientation is obtained by extrapolation of this part of the curve to the x axis and is termed the condensed area ( $A_s$ ).

When the temperature is increased, features appear in the isotherm which have been associated with either the liquid-expanded to liquid-condensed (le-lc) phase transition (second plateau, Figure 3.2) or the gas-condensed to liquid-condensed (gc-lc) phase transition (first plateau, Figure 3.2). The critical points of the transitions are P and P' respectively. The areas numbered 1 and 2 correspond to the two-phase coexistence region of the two transitions where above P or P' one phase persists. These are the transitions which are of particular interest to us. They are discussed in the literature but often have been given different designations.  $^{16-19}$  The molecular area and surface pressure at which the isotherm plateau begins are termed the transition area ( $A_t$ ) and transition pressure ( $\pi_t$ ) respectively. The difference between  $A_t$  and  $A_s$  decreases as the temperature is raised. When  $A_t$  -  $A_s \approx 0$  the critical point (P or P') is reached, and has an associated critical area ( $A_c$ ), a critical pressure ( $\pi_c$ ), and a critical temperature ( $T_c$ ). In the isotherms presented here only one plateau is evident (e.g. Figure 3.3). The assignment of the transition is addressed in this report. Theories dealing with the phase transition attribute the process to one of two categories: order/disorder and orientational.  $^{20}$ 

The le-lc phase transition has been extensively studied yet the nature of the transition remains controversial.  $^{15,16,18,20-24}$  In general it has been accepted that the conformational changes occurring during the le-lc phase transition are analogous to those occurring in bilayer lipid membranes (Figure 3.3) i.e. an order-disorder process  $^{25,26}$ . In the liquid-expanded film the hydrocarbon chains are depicted as being in a highly fluid and

mobile state analogous to the liquid-crystalline phase of lipid bilayers.<sup>21</sup> The chains in a solid film are ordered and are believed to be arranged similarly to the chains in the gel phase of a lipid bilayer.<sup>21</sup>

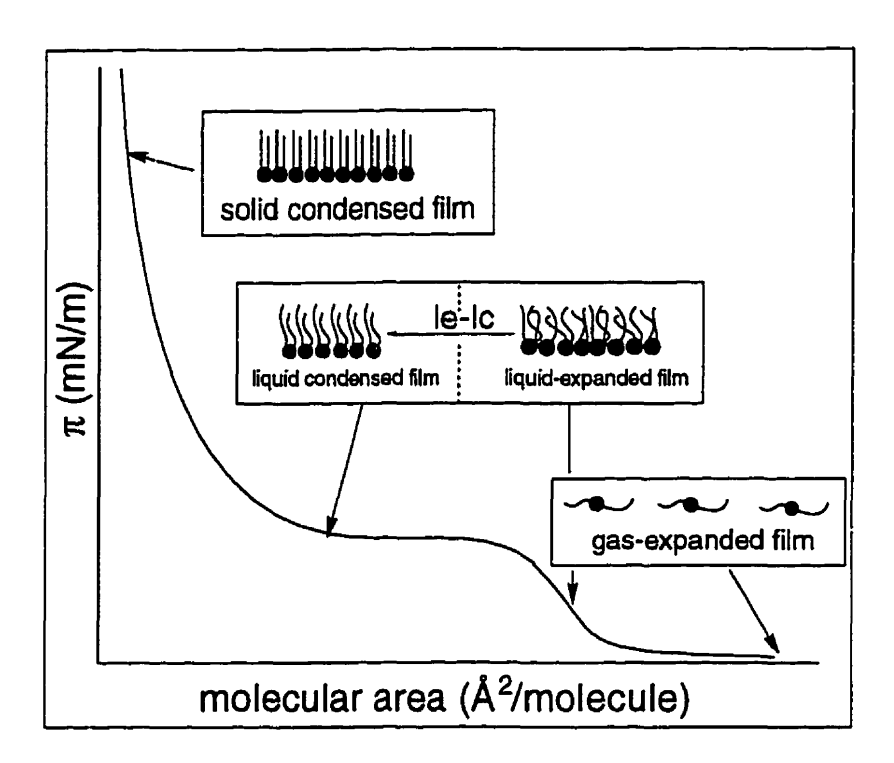


Figure 3.3. Generalized conformational changes which occur during compression of phospholipid monolayers. The plateau has been attributed to the liquid-expanded to liquid-condensed (le-lc) phase transition in many lipid films.

The gc-lc phase transition (Figure 3.2, first plateau) usually occurs at very low surface pressures and is therefore very difficult to observe for the saturated lipids studied. It has been attributed to a gas-liquid transition. At low surface densities hydrocarbon chains are usually depicted as lying horizontally at the air/water interface. As the surface density is increased, the polar groups remain in contact with the water while the hydrocarbon tails rise from the surface, eventually aligning themselves vertically while retaining a certain degree of disorder in the chain. This phase transition therefore involves a reorientation of the lipid at the interface. The gc-lc monolayer phase transition is

also temperature dependent and features a critical point (P') (Figure 3.2.). This critical point is distinct, however, from that associated with the le-lc phase transition. P' occurs at  $T_c'$ ,  $A_c'$  and  $\pi_c'$ .

A lipid monolayer is a two-dimensional solution which behaves as a gas at low surface densities and as such often obeys the two-dimensional ideal gas law at low surface pressure. 10 At higher surface densities deviations from ideality occur in much the same way as for three-dimensional gases. Specifically, lipid-lipid interactions and lipid-water interactions begin to dominate the phase behaviour. Ruckenstein recently introduced a model which is in qualitative agreement with experiment.<sup>29,30</sup> This model demonstrates that the nature of the phase transition can be modified by the balance between an interaction parameter (which globally describes lipid-lipid interactions) and the effect of lipid clustering or domain formation at the interface. The phase transition is controlled partially by the size and distribution of these domains which are temperature dependent.<sup>29-32</sup> The monolayer phase transition is described as diffuse first-order, meaning that the order/disorder transition is first-order within domains of limited size.<sup>22</sup> Fluorescence microscopy has confirmed the existence of coexisting phases during the le-lc transition.<sup>33</sup> The narrowing of the plateau in the monolayer isotherm with a rise in temperature can be associated with a decrease in the domain size of the condensed lipid domains (N.B. we do not imply that lipids adopt an all-trans conformation in these condensed domains, but that lipid-lipid interactions exist). As T<sub>c</sub> is approached the width of the plateau becomes smaller because the lc phase becomes less populated. At the Tc the phase transition occurs over a range of molecular areas of infinitely small width such that  $A_t \approx A_s$ . The lc phase approaches a population of zero at this point. Above T<sub>c</sub> the *lc* phase does not exist and the film collapses. The maximum temperature at which an lc phase is manifested in the isotherm is thus  $T_c$ .

Features of the monolayer phase transition are clearly temperature dependent. In comparing isotherms of structurally different materials however, it is important to

#### Chapter 3

understand how structural differences in the phospholipid affects the isotherm. To do this, the effect of temperature must be factored out of any analysis.

The analysis of bipolar lipids which possess a polar sulfone (SO<sub>2</sub>) group at positions 5, 7, 9 and 11 along the sn-2 alkyl chain is presented here. A methodology is introduced which permits direct comparison of their lipid monolayer isotherms through normalization with respect to the critical point of the phase transition. Knowledge of the temperature dependence of the monolayer phase transition is shown to be necessary for an understanding of the significance of the features of the isotherm. The critical temperature  $(T_c)$ , the  $d\pi_t/dT$  values, and other parameters which can be determined from the temperature dependence of the isotherm all provide insight into the nature of the transition and the effect of chemical modification of the lipid. This analysis permits the identification of the type of phase transitions responsible for the plateau.

#### 3.2. Materials and Methods

Samples studied consisted of distearoylphosphatidylcholine (DSPC) analogs functionalised in the *sn*-2 chain at positions 5, 7, 9 and 11. Phospholipids incorporating sulfone moieties in the acyl chain were synthesized in this lab. The partial synthesis of phospholipids has been previously described. The synthesis of sulfone-substituted fatty acids as used has been reported previously. The composition of this series was established by FAB-MS, and their purity was monitored using 300 MHz and 500 MHz NMR, and TLC in CHCl<sub>3</sub>. Purity was estimated to be >99%. Phospholipid standards dimyristoylphosphatidylcholine (DMPC), dipalmitoylphosphatidylcholine (DPPC) and DSPC were purchased from Avanti Polar Lipids (Alabaster, Alabama) and were used without further purification.

All isotherms were recorded using a KSV Instruments Langmuir film-balance (LFB), equipped with a 150 mm x 540 mm Teflon compartment (KSV, Helsinki, Finland.). A circulating bath provided thermal control of the subphase. 20 mg of each sample was dissolved in 10 mL CHCl<sub>3</sub> (BDH, Omnisolv). Samples were spread in a dropwise fashion (60μL aliquots) onto a subphase of Millipore Milli-Q water (18MΩcm<sup>-1</sup>). 15 minutes elapsed before compression was initiated so as to allow for solvent evaporation. A compression rate of 10 mm/min was used for each run. Compression rate did not affect the isotherms, as identical isotherms were obtained at rates of when the barrier compression was doubled or halved.

# 3.3. Results

The comparison of monolayer isotherms of different lipids is commonly performed so as to extract structural information from the characteristic features of the isotherm. This is conventionally done at a specific (fixed) temperature. 10-13,34 This practice however leads to serious ambiguities in the analysis as the structural variation and phase state of the monolayer become inexorably entwined. To this end, we have sought a means of deconvoluting the structural and phase effects for a series of functionalised lipids.

That phospholipids exist in different monolayer states which are temperature dependent has been extensively discussed in the literature. <sup>15,16</sup> For example DMPC possesses a T<sub>m</sub> of 24.0 °C, DPPC a T<sub>m</sub> of 40.5 °C, and DSPC a T<sub>m</sub> of 54.3 °C. <sup>35</sup> Comparison of the structural differences of these lipids using isotherms measured at 25 °C would be 1°C above, 16°C below and 24°C below the T<sub>m</sub> of DMPC, DPPC and DSPC respectively. The lipids clearly are in different physical states and thus structural information cannot be readily extracted from the monolayer isotherms unless the physical state of the lipid is taken into account. It is emphasized that a single isotherm reveals very little information and it is of more use to understand the thermal properties of the isotherm *i.e.* how the features of the isotherm change with temperature. Such an analysis is presented here.

We begin by assuming that if two lipids to be in the same state, the number of lipid molecules occupying ordered domains and amorphous domains are equal in the two materials. This concept is adopted from studies of the bilayer main phase transition and also follows naturally from clustering models of the monolayer phase transition. Such studies show that as the  $T_m$  is approached the ratio of lipid molecules in ordered, relative to amorphous, domains steadily decreases. When the  $T_m$  the ratio is 1:1. Clearly, the lipid state is controlled by temperature, so the comparison materials having different  $T_m$ 's requires a procedure to account for these thermal differences. This problem has been addressed in the study of the lipid order parameter where the concept of reduced

temperatures has been used. Specifically,  $^2H$ -NMR spectra were acquired at a reduced temperature ( $T_m$  - T) where T was fixed (at the same "distance" from the critical temperature).  $^{37}$  This ensures that the order parameters obtained for several lipids truly reflect the chain order and not the variations in lipids states.

To permit comparison of lipid isotherms the monolayers must also be compared when in corresponding states. Indeed Dervichian <sup>16</sup> states this very explicitly although no explicit means to effect the comparison were described. The monolayers are in "corresponding states" when (i) their isotherms are measured at  $T_{expt} = (T_c - T)$  where T is fixed and (ii) when the surface pressure and molecular area are represented in terms of reduced pressure,  $\pi_T = \pi/\pi_C$ , and reduced area,  $\alpha = A/A_C$  respectively. The use of a reduced pressure and reduced area accounts for differences in the van der Waals interactions and the finite area occupied by the lipid. The resulting isotherms are obtained at  $(T_c - T)$  and are plotted as  $\pi_T$  vs  $\alpha$ . The concept of reduced temperature and lipid monolayers has been mentioned previously <sup>15</sup>, but its application to the comparison of lipid isotherms has not been exploited.

Obviously, in order to normalize isotherms  $T_c$ ,  $\pi_c$  and  $A_c$  must first be determined. To do so the temperature dependence of monolayer isotherms of the saturated lipids DMPC, DPPC and DSPC were measured (Appendix I, Figure AI.1.) and the relevant data is listed in Table AI.1. Isotherms obtained for DMPC and DPPC are in excellent agreement with literature examples.  $^{15,17,20-22}$  The critical temperature can be obtained in two ways. Firstly, from the  $T_{expt}$  intercept of a plot of  $A_t$  -  $A_s$  versus  $T_{expt}$  or from the x intercept of a plot of  $Q_t$  vs  $T_{expt}$ . The latter treatment is obtained from the 2D Clausius-Clapeyron equation and is described elsewhere  $^{20,21}$  where Q is the heat of transition calculated for each isotherm ( $Q = \Delta A \cdot T \cdot d\pi/dT$ ). The critical pressure ( $\pi_c$ ) is obtained from the y intercept of a plot of  $\pi_t$  versus ( $T_{expt}$  -  $T_m$ )  $^{38}$ . The critical area is obtained from the x intercept of a plot of ( $A_t$  -  $A_s$ ) versus  $A_t$ . The graphs from which these parameters are obtained are included in Appendix I. The critical parameters obtained by these methods will have an

associated error dependent upon the fit of the data. A linear relationship is assumed. We found this approach very useful for *estimating* the critical point. Values obtained do differ from literature values<sup>15,16,39</sup> within experimental error.

Table 3.1 lists the critical parameters obtained from the temperature dependence of the plateau which are used in the isotherm normalization process. It was established that  $T_c \approx T_m$  for DMPC, DPPC, and DSPC in the present study and elsewhere  $^{15,16,20,40}$ . Isotherms of the lipids were then obtained at reduced temperatures,  $T_r$ , where  $T_r = (T_c - T)$  (Figure AI.1 (a)). The resulting isotherms (Figure 3.5.(b)) are plotted as reduced surface pressure  $(\pi_r)$  against reduced surface area  $(\alpha)$ . Normalized isotherms of DMPC, DPPC and DSPC (Figure 3.5 (b)) were obtained at  $T_r = (T_c - 15^{\circ}C)$ .

The temperature dependence of monolayer isotherms of  $1C_{18}$ ,  $2(nSO_2)C_{17}$ -PC ((nSO<sub>2</sub>)PC) was also measured (Figure 3.4., Table AI.1) and  $\pi_c$ ,  $A_c$  and  $T_c$  were determined as described above (Table 3.1). The  $T_c$  of the lipids functionalised at the 5 and 7 positions correspond very closely to the DSC-determined  $T_m$  value (Table 3.2) but  $T_c$  of the 9SO<sub>2</sub>- and 11SO<sub>2</sub>- functionalised lipids do not agree with the  $T_m$  measured by DSC (Table 3.1).

Table 3.1. Critical parameters obtained from the temperature dependence of the le-lc phase transition

transition.						
phospholipid	π <sub>c</sub> <sup>1</sup> (mN/m)	A <sub>c</sub> <sup>2</sup> (Å <sup>2</sup> /molec)	A <sub>S</sub> <sup>3</sup> (Å <sup>2</sup> /molec)	T <sub>c</sub> <sup>4</sup> (°C)	T <sub>c</sub> <sup>5</sup> (°C)	T <sub>m</sub> 6
	(11114/111)	(A-/molec)	(A-/molec)	( C)	( C)	( 0)
DMPC	54	39.3	44	27	27	24.0
DPPC	36	50.5	44	39	39	41.5
DSPC	25	44	44	49	49	54.3
1C <sub>18</sub> ,2(5SO <sub>2</sub> )C <sub>17</sub> -PC	32	49	50	38	39	39
1C <sub>18</sub> ,2(7SO <sub>2</sub> )C <sub>17</sub> -PC	57	50	50	37	39	38
1C <sub>18</sub> ,2(9SO <sub>2</sub> )C <sub>17</sub> -PC	58	50	55	52	58	44
1C <sub>18</sub> ,2(11SO <sub>2</sub> )C <sub>17</sub> -PC	50	44	60	66	84	49

 $<sup>^{1}</sup>$   $\pi_{c}$  is determined from the y intercept of the plot of transition pressure,  $\pi_{t}$ , against  $T_{m}$ -T. The critical point occurs when  $T_{m}$ -T is zero.

 $<sup>^2</sup>$   $A_c$  is determined from the x intercept of a plot of  $A_t$ - $A_s$  versus  $A_t$ . The critical point occurs when  $A_t$ - $A_s$  is zero.

 $<sup>^{3}</sup>$  A<sub>s</sub> is determined by extrapolating the curve at the solid section of the isotherm to the x axis.

<sup>&</sup>lt;sup>4</sup>  $T_c$  is determined from the x intercept of a plot of  $A_t$ - $A_s$  vs T.

 $<sup>^{5}</sup>$   $T_{c}$  is determined from the temperature dependence of the heat of transition  $Q_{t}$  as determined by the two dimensional Clausius-Clapeyron equation.

<sup>&</sup>lt;sup>6</sup> The main transition temperature of phospholipids has been determined by  $DSC^{35}$ . It is included in the table for comparison with  $T_c$ .

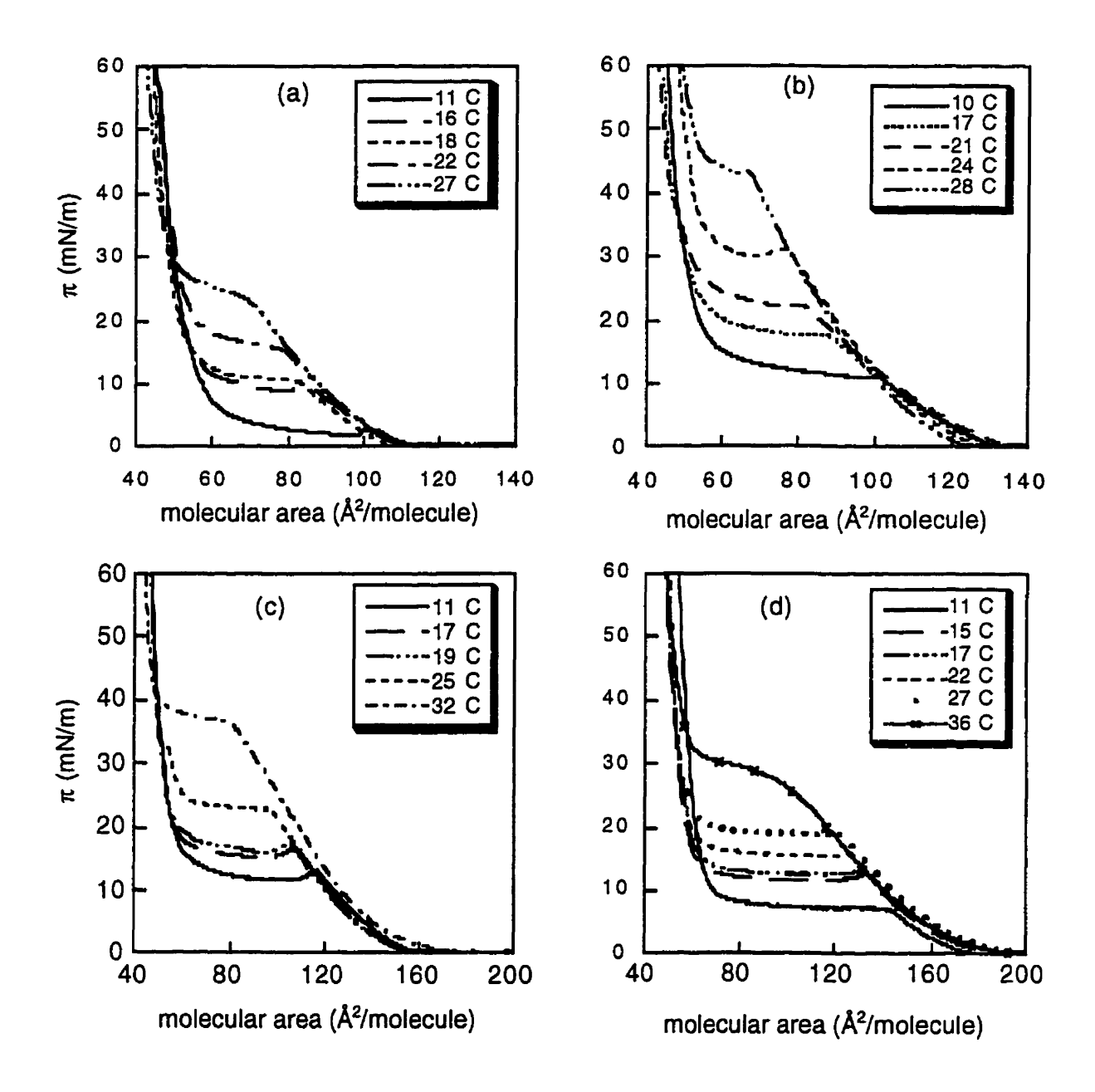
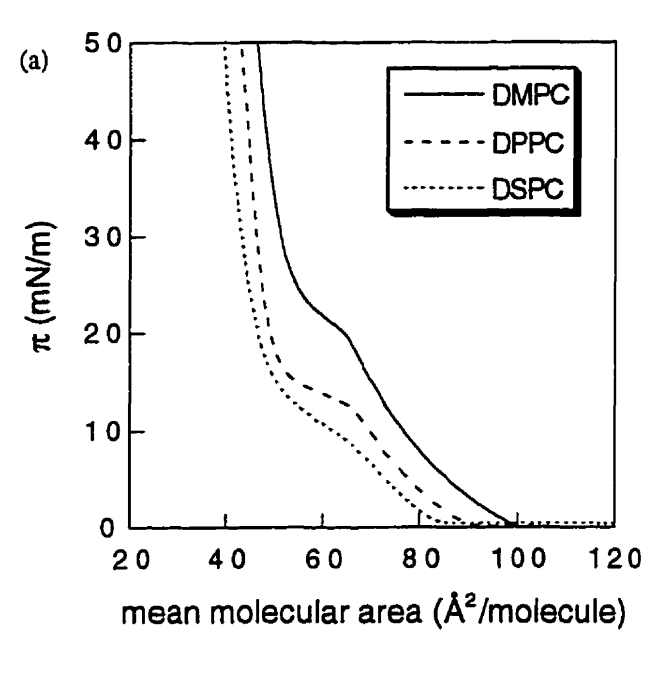


Figure 3.4. Temperature dependence of phospholipid isotherms (a)  $1C_{18}$ ,2(5SO<sub>2</sub>)C<sub>17</sub>-PC (b)  $1C_{18}$ ,2(7SO<sub>2</sub>)C<sub>17</sub>-PC (c)  $1C_{18}$ ,2(9SO<sub>2</sub>)C<sub>17</sub>-PC (d)  $1C_{18}$ ,2(11SO<sub>2</sub>)C<sub>17</sub>-PC on a water subphase.



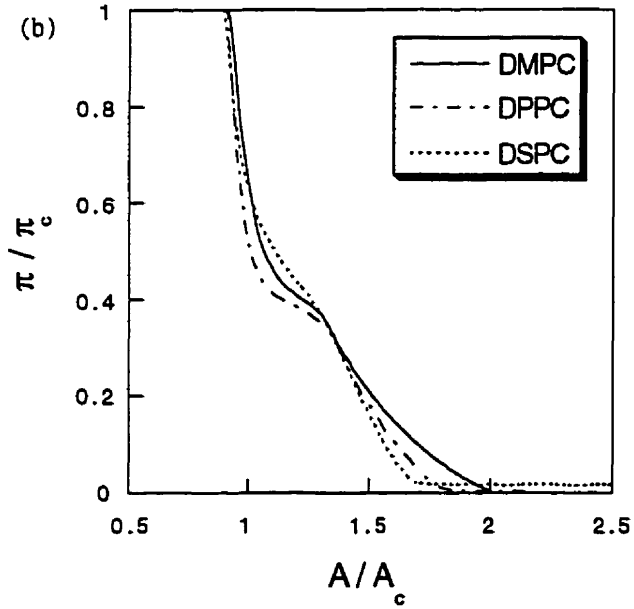


Figure 3.5. (a) Isotherms of lipid standards obtained at  $T_r = (T_m - 15^{\circ}C)$  (b)Normalized isotherms of lipid standards run at  $T_r = (T_m - 15^{\circ}C)$  on a water subphase.

The normalized isotherms of functionalised lipids report the effect of the substituent position on the features of the isotherms when the lipids are in corresponding states. The

normalized isotherms of DSPC,  $1C_{18}$ ,  $2(5SO_2)C_{17}$ -PC,  $1C_{18}$ ,  $2(7SO_2)C_{17}$ -PC and  $1C_{18}$ ,  $2(9SO_2)C_{17}$ -PC (Figure 3.6) were obtained at  $T_c$  -  $20^{\circ}$ C.

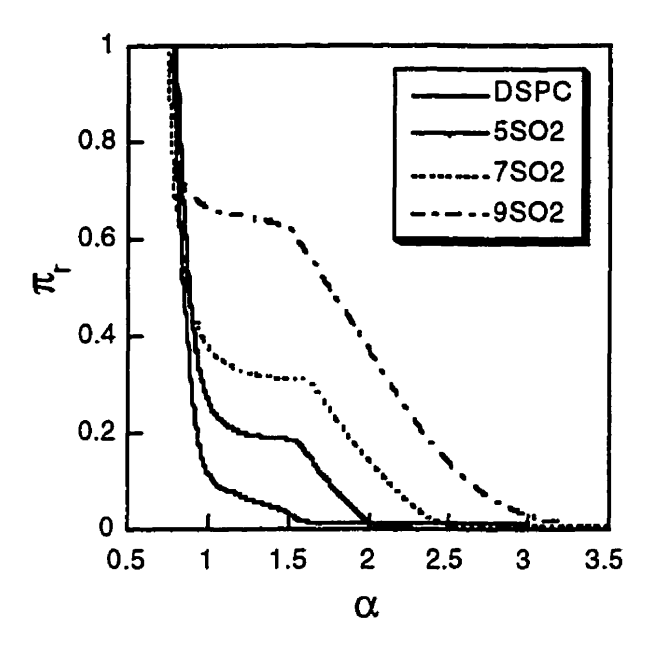


Figure 3.6. Normalized isotherms of DSPC (34°C),  $1C_{18}$ ,2(5SO<sub>2</sub>)C<sub>17</sub>-PC (18°C),  $1C_{18}$ ,2(7SO<sub>2</sub>)C<sub>17</sub>-PC (17 °C) and C<sub>18</sub>,2(9SO<sub>2</sub>)C<sub>17</sub>-PC (28°C) (T<sub>c</sub> - T = 20°C) on a water subphase.

Figure 3.6 shows that isotherms of functionalised lipids acquired on a reduced temperature scale do not superimpose upon each other.  $\pi_t$  and  $A_{on}$  are -SO<sub>2</sub> position dependent while  $A_t$  is fairly constant.

Figure 3.5 (b) and Figure 3.6 represent the isotherms at one fixed reduced temperature. It is not clear from these graphs if the observed behaviour (the coincidence of  $\Delta A_t$  for example) will be generally observed over a range of reduced temperatures. The normalization of monolayer isotherms can be evaluated at the phase transition over a range of temperatures by determining the relationship between the reduced transition pressures  $(\pi_t/\pi_c)$  and transition areas  $(\Delta A_t/A_c)$  using a reduced temperature scale (Figure 3.7). The superposition of the curves of  $\Delta A_t/A_c$  against  $(T_c - T)$  (Figure 3.7 (a)) demonstrates that upon normalization the transition area changes are roughly equal over the entire range of

# Chapter 3

temperatures for all lipid species. The transition pressure curves,  $\pi_t/\pi_c$  against ( $T_c$  - T), (Figure 3.7 (b)) reflect structural differences in the lipid molecules. The advantage of this representation is that it displays the coordinates of the phase transition ( $\pi_t$ ,  $A_t$ ) over a wide temperature range. The coincidence (or lack of) of  $\pi_t/\pi$  and  $\Delta A_t/A$  is revealed by the superposition of the curves obtained by a least squares fit of the points. It therefore becomes unnecessary to painstakingly acquire the isotherms at the strictly controlled temperatures ( $T_c$  - T) required for the plots shown in Figures 3.4. and 3.5.

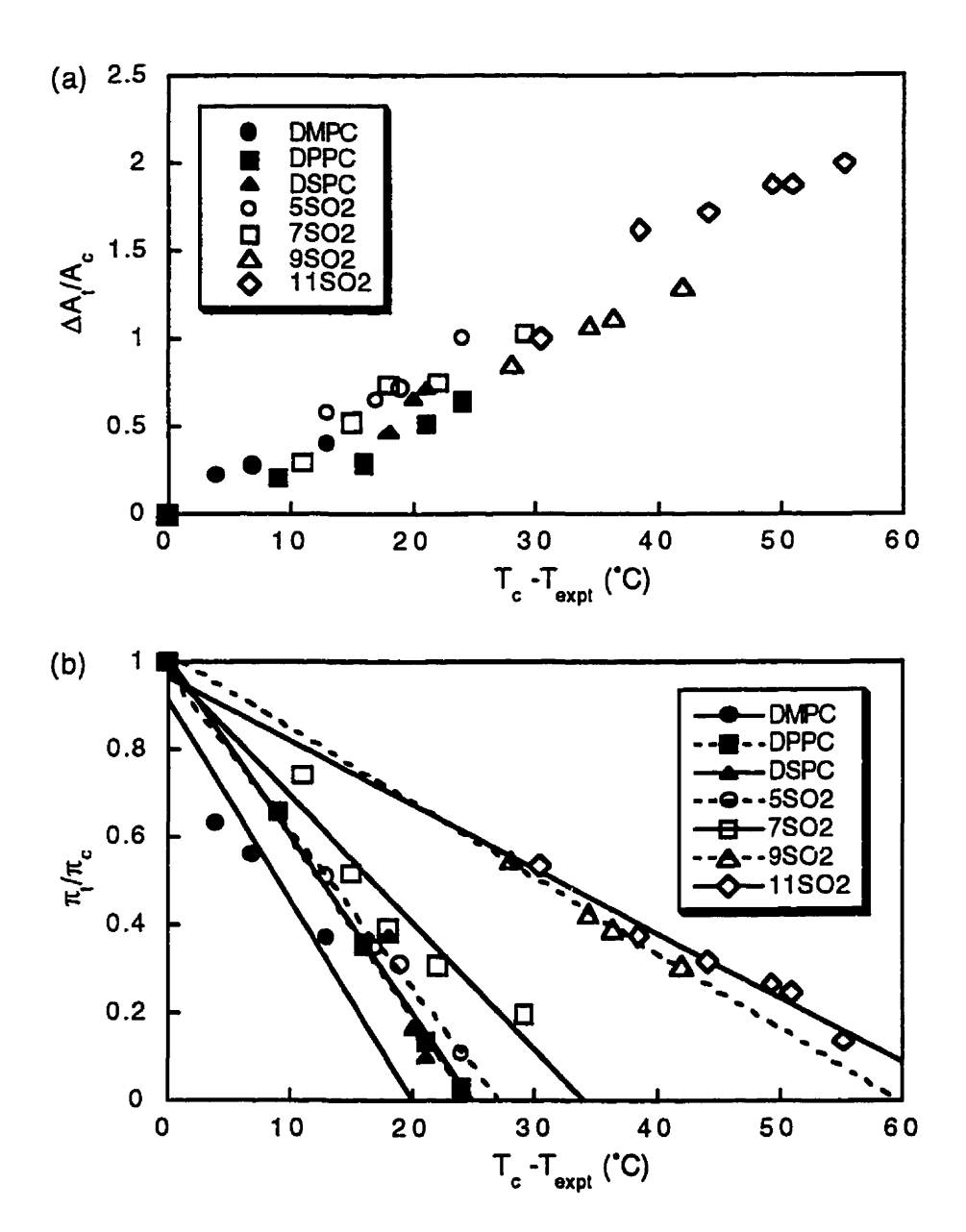


Figure 3.7. Isotherm normalization revealed though coincidence of the (a) reduced surface area of transition ( $\Delta A_t/A_c$ ) and (b) surface pressure ( $\pi_t/\pi_c$ ) curves on a reduced temperature scale. DMPC ( $\blacksquare$ ), DPPC ( $\blacksquare$ ), DSPC ( $\triangle$ ),  $1C_{18}$ ,  $2(nSO_2)C_{17}$ -PC, n=5 ( $\bigcirc$ ),  $7(\square)$ ,  $9(\Delta)$ , 11 ( $\lozenge$ ). As the temperature is increased the transition surface pressure increases until  $\pi_t = \pi_c$  and  $\pi_t/\pi_c \rightarrow 1$ . The area of the transition approaches zero as  $T_c$  is approached and  $(T_c-T) \rightarrow 0$ .

Table 3.2. Transition area and surface pressures of SO<sub>2</sub> functionalised lipid monolayers in two temperature ranges. The isothermal compressibility data is listed.

phospholipid	ΔA <sub>t</sub> <sup>21*</sup> (Å <sup>2</sup> / molec)	ΔA <sub>t</sub> <sup>11</sup> (Å <sup>2</sup> / molec)	$\pi_t^{21}$ (mN/m)	π <sub>t</sub> 11 (mN/m)	$d\pi_t/dT^a$ (mN m <sup>-1</sup> K <sup>-1</sup> )
DMPC	•	-	•	-	$2.2^{a}, 2.3^{24}, 1.26-1.90^{22}$
DPPC	-	-	-	-	1.4 <sup>a</sup> , 1.4, 2.35, 1.65-1.97 <sup>20</sup> ,
DSPC	-	-	-	-	1.14
1C <sub>18</sub> ,2(5SO <sub>2</sub> )C <sub>18</sub> -PC	19 21.5	45 10.7	15.6	2.8	1.2 <sup>a</sup>
1C <sub>18</sub> ,2(7SO <sub>2</sub> )C <sub>18</sub> -PC	23 20.5	47 9.5	22.4	10.6	1.6 <sup>a</sup>
1C <sub>18</sub> ,2(9SO <sub>2</sub> )C <sub>18</sub> -PC	38 25	56 11	22.8	13	0.9a
1C <sub>18</sub> ,2(11SO <sub>2</sub> )C <sub>18</sub> -PC	63 21.7	78 10.7	15.9	7.2	0.7a

<sup>\*</sup> superscript refers to the actual temperature at which the isotherm was measured

Figure 3.7.(b) reveals that the gradients of  $\pi_t/\pi_c$  vs ( $T_c$  -  $T_{expt}$ ) curves for 9SO<sub>2</sub>-and 11SO<sub>2</sub>-PC lipids are lower than observed for the other lipids studied. Likewise  $d\pi_t/dT$  values (Table 3.2), decrease with chain length and with n (position of the second polar group).  $d\pi_t/dT$  can be viewed as a measure of the rate at which a substance expands with temperature. This parallels the behaviour of other bipolar lipids reported elsewhere, indicating that the attenuation in temperature dependence of  $\pi_t$  is a characteristic of increasing bipolarity (Table 3.3<sup>22</sup>).  $T_0$  is the temperature at which a phase transition is no longer detected ( $\pi_t$  = 0); it is obtained from the x intercept of a plot of  $\pi$  versus T. From Table 3.4 it can be seen that the temperature required to obtain a featureless isotherm decreases significantly with the increasing position of the polar group.

a  $d\pi_t/dT$  determined experimentally in this work

Table 3.3. Representative literature values describing the phase transition of functionalised fatty acids<sup>22</sup>

phospholipid	To (°C)a	$d\pi/dT (mN m^{-1} K^{-1})$
hexadecanoic acidb	26.8	1.12
2-hydroxyhexadecanoic acid	28.6	1.41
3-hydroxyhexadecanoic acid	10	1.47
9-hydroxyhexadecanoic acid	-45.7	0.24
16-hydroxyhexadecanoic acid	-60.6	0.14
octadecanoic acid	38.1	1.09
	44.5	1.1
4-hydroxyoctadecanoic acid	8.2	0.83
12-hydroxyoctadecanoic acid	5.2	0.35

<sup>&</sup>lt;sup>a</sup> temperature at which no transition is observed ( $\pi_t = 0$ )

Several important observations can be drawn from the results presented. These observations permit the construction of a working model for the phase behaviour of phospholipid monolayers. These observations are:

- (1) The critical temperatures of the simple diacyl lipid standards are equal to the main bilayer phase transition temperatures ( $T_c = T_m$ ).
- (2) The isotherms of DMPC, DPPC and DSPC collapse upon one another upon normalization.  $\pi_t$  and  $A_t$  are constant.
- (3) In normalized isotherms of both DSPC and functionalised lipids  $1C_{18}$ ,  $2(nSO_2)C_{17}$ -PC (where n = 5, 7 and 9)  $\pi_t$  and  $A_{on}$  are  $SO_2$  position-dependent but  $A_t$  is a constant.
- (4) Information concerning the phase transitions of the normalized isotherms can be graphically represented over the entire experimental range of temperatures using the relationship between  $\pi_t/\pi_c$ ,  $\Delta A_t/A_c$  and the reduced temperature. The normalized transition pressure  $(\pi_t/\pi_c)$  and onset area  $(A_{0n}/A_c)$  of the normalized isotherms of  $1C_{18}$ ,2(nSO<sub>2</sub>)C<sub>17</sub>-PC are SO<sub>2</sub>-position dependent but the normalized transition area  $(\Delta A_t/A_c)$  is constant at a given reduced temperature.
- (5) The critical temperatures of functionalised lipids  $1C_{18}$ ,  $2(nSO_2)C_{17}$ -PC, where n = 9 and 11, are *not* equal to the main bilayer phase transition temperature ( $T_c \neq T_m$ ) (Table 3.2) (6)  $d\pi/dT$  values decrease with the increasing position of polar groups within the lipid acyl chain and with increasing chain length (Table 3.2 and 3.3)

In the light of these observations the relevance of the molecular structure of the lipid to the overall mechanism of the phase transition is considered in the following discussion.

b representative data

# 3.3. Discussion

The value of  $T_c$  is shown to be the same as the main transition melting temperature  $(T_m)$  (measured by differential scanning calorimetry, DSC) for lipids such as DMPC, DPPC, DSPC and those functionalised at the 5 and 7 positions (Table 3.2). In contrast,  $T_c$  values for lipid monolayers of 9SO<sub>2</sub>-PC and 11SO<sub>2</sub>-PC do not correspond to the  $T_m$  values. Two types of behaviour are thus exhibited by the phospholipids examined in this study;  $T_m = T_c$  and  $T_m \neq T_c$ . A correspondence between  $T_c$  and  $T_m$  has been noted previously and the implications to the relationship between monolayer and bilayer systems have been addressed. The implications of the relationship between  $T_m$  and  $T_c$  for the SO<sub>2</sub>-functionalized lipids are the topic of the following discussion.

# 3.31. The relationship between $T_m$ and $T_c$ and its significance to phospholipid monolayer film.

It is frequently assumed that a lipid bilayer is simply the sum of two monolayers with negligible transmonolayer interactions. The existence of a correspondence between the bilayer phase transition temperature and the monolayer phase transition temperature is one test of this assumption. Rationalization of differences in  $T_c$  and  $T_m$  values have also been addressed. 15,16,40 Albrecht proposed an expression which accounts for the monolayer-monolayer interaction in lipid bilayers where  $T_m = T_c - 2c_0/A_0$ . Differences between  $T_m$  and  $T_c$  arise either because of a breakdown in the assumption that the bilayer is made up of two independent monolayers  $(2c_0/A_0^{-15})$  or to differences between the monolayer and bilayer states at the phase transition.

The correlation between  $T_c$  and  $T_m$  suggests that the same energy demands control the monolayer and bilayer phase transitions and that by inference, the surface pressure in the bilayer and in the monolayer are the same at the phase transition. It is attractive to also conclude that the conformations of the lipid molecules are the same in the two states. The thermal energy required to reach the disordered state in both systems is the same suggesting that the transition mechanisms are the same as well. The bilayer phase transition is, of

course, a well studied order/disorder process.  $^{41-44}$  The monolayer surface pressure-induced phase transition from the liquid-expanded to liquid-condensed (le-lc) phases below the  $T_c$  has also been described as an order-disorder process  $^{18,24,39}$  and is supported by these results. The correspondence between  $T_c$  and  $T_m$  for DMPC, DPPC and DSPC lipid monolayers (Table 3.1) is consistent with the model of the bilayer as two independent monolayers. The additional "surface pressure factor" required to correlate the monolayer and bilayer phase transitions is negligible in the case of these lipids.  $^{40}$ 

Incorporation of an SO<sub>2</sub> group into the acyl chain results in a divergence of  $T_c$  and  $T_m$  values as n increases;  $T_c = T_m$  for n=5 and 7 but  $T_c > T_m$  for n=9 and 11. The bilayers formed from 5SO<sub>2</sub>-PC and 7SO<sub>2</sub>-PC are therefore composed of two non-interacting monolayers with the same conformations adopted in the monolayer and bilayer states. Because  $T_c > T_m$  for n = 9 and 11, the lipid bilayer is able to attain a disordered state at a lower temperature than can the lipid monolayer. The origin of the difference between  $T_c$  and  $T_m$  for 9SO<sub>2</sub>PC and 11SO<sub>2</sub>PC lies in factors which influence the  $T_c$  of lipid monolayers. For example, in the comparison of monolayer films of different lipids, the higher  $T_c$ 's observed in films of DPPA (and DPPE) compared to DPPC can be rationalized by both a decrease in the rotational isomerism and an increase in headgroup attractive interactions.<sup>40</sup>

If the substitution of a methylene group with an SO<sub>2</sub> group affects the rotational freedom of the chain, it will affect both the monolayer and bilayer states equally and therefore can be ruled out as a controlling factor. Moreover, decreases in rotational freedom have been shown to account for differences of up to 60°C.<sup>40</sup> The differences observed between 9SO<sub>2</sub>-PC and 11SO<sub>2</sub>-PC (10-20°C) are much smaller than this.

Headgroup interactions, however, produce much smaller changes in  $T_m$  values, and therefore may be considered a possible source of the difference between  $T_c$  and  $T_m$ . An increase in  $T_c$  with respect to  $T_m$  caused by an increase in attractive headgroup interactions must be due to a conformational change in the lipid in the monolayer state which does not

occur in the bilayer state. The conformational change must result in an increase in electrostatic or hydrogen bonding interactions between the headgroups. <sup>40</sup> The SO<sub>2</sub> group may form an attractive interaction with the headgroup via hydrogen bonds resulting in a looped conformation (Figure 3.8). Although the looped conformation has been displayed in terminally-functionalised surfactant micelles, <sup>45</sup> and has been linked to cell lysis in peroxidized lipid membranes, <sup>46</sup> the vesicles of 9SO<sub>2</sub>-PC and 11SO<sub>2</sub>-PC apparently do not contain the lipid in the looped conformation. The difference between T<sub>m</sub> and T<sub>c</sub> for these lipids can be attributed to headgroup-SO<sub>2</sub> interactions in the monolayer (looped conformation) which are not accessible in the bilayer. Such a configuration could result in loss of vesicle integrity (Figure 3.8, micellization) which was not found to occur in thermal studies of lipid vesicles. <sup>2</sup> The concurrence of T<sub>m</sub> and T<sub>c</sub> for 5SO<sub>2</sub>- and 7SO<sub>2</sub>-PC suggests that alternative headgroup interactions do not come into play in monolayers of these lipids. The looped conformation is therefore not believed to be found in any measurable population (relative to the vertical conformer). Surface dipole studies reported elsewhere <sup>1</sup> support this conclusion.

The discrepancy between  $T_c$  and  $T_m$  for 9SO<sub>2</sub>- and 11SO<sub>2</sub>PC could be due to interdigitation between the monolayers in the lipid bilayer not possible in the monolayer film (Figure 3.8). This option is disregarded for several reasons. Firstly, interdigitation would be expected to occur for n = 5-9 and cause a difference between  $T_m$  and  $T_c$  for all the lipids. Secondly, the looped conformation involved in the interdigitation process would result in loss of bilayer integrity and might result in micellization (Figure 3.8). This statement is supported by studies of peroxidized lipid bilayers in which migration of the polar-OOH group to the interface results in a lipid conformation which disrupts membrane integrity. <sup>46,47</sup> DSC and <sup>31</sup>P-NMR studies reported elsewhere do not support loss of bilayer integrity. Lastly, surface dipole studies and the normalized isotherm of functionalised lipids (Figure 3.6) support the existence of a looping conformation in the expanded monolayer film as an explanation for the high  $T_c$  observed for 9 and 11SO<sub>2</sub>-

functionalised lipids. The difference is thus attributed to a different conformation adopted by the lipid at the phase transition in the monolayer as compared to the bilayer (Figure 3.8).

# 3.32. The nature of the monolayer phase transition.

What does the conformational difference between DMPC, DPPC, DSPC, 5SO<sub>2</sub>, 7SO<sub>2</sub>, 9SO<sub>2</sub> and 11SO<sub>2</sub> lipids reveal about the phase transition? The monolayers of 9- and 11SO<sub>2</sub>-PC have been shown to adopt a looping conformation at the phase transition. Condensed areas (A<sub>s</sub>) of these lipids films are 55 and 60 Å<sup>2</sup>/molecule respectively (Table 3.1), very close to values obtained for 5 and 7 SO<sub>2</sub>-PC (50 Å<sup>2</sup>/molecule). The conformations adopted after the phase transition are therefore similar and are assigned the vertical conformation. The phase transition of 9- and 11SO<sub>2</sub>-PC is therefore a reorientational one (gc-lc).

The gc-lc (reorientational) phase transition is difficult to detect in mono-polar phospholipid monolayer isotherms because the  $T_c$ ' of mono-polar phospholipids is most likely too high for practical observation. The observation of the plateau corresponding to the phase transition is therefore rationalized by the lowering of  $T_c$ '. The incorporation of polar groups at positions 9 and 11 in the acyl chain effectively results in the decrease of  $T_c$ ' of lipid monolayers.

## 3.33. The significance of $d\pi_t/dT$ values to monolayer film properties.

What does the value of the expansion coefficient  $(d\pi_t/dT)$  reveal about the nature of the lipid film and the phase transition? The temperature dependence of the monolayer phase transition can help elucidate the nature of the lipid monolayer phase transition.  $^{15,20,23,24,39}$  Bipolar fatty acids exhibit decreasing  $d\pi_t/dT$  values with increasing position of the second polar group (Table 3.3). No such decrease is observed for lipids functionalised near the headgroup (Table 3.2 n=5,7 or Table 3.3. n <5). The  $d\pi_t/dT$  values of SO<sub>2</sub>-functionalised lipids follow the same trend with higher values observed for substitution near the headgroup at position 5 and 7 (1.2 and 1.6 mN m<sup>-1</sup> K<sup>-1</sup> respectively) compared to 9 and 11 functionalised lipids (0.9 and 0.7 mN m<sup>-1</sup> K<sup>-1</sup> respectively).

 $d\pi_t/dT$  values are proportional to the entropy of the transition  $(d\pi_t/dT \propto \Delta S_t = S_e - S_c)$ , where e refers to the expanded film, c refers to the condensed film and  $d\pi/dT = Q/T\Delta A$ ). The reduction in  $d\pi_t/dT$  for bipolar lipids (and for lipids with greater chain length) may be related to the destabilization of the condensed film by the presence of the polar group ( $S_c$  increase).

## 3.34. The consequence of normalization of phospholipid isotherms.

What does the superimposition of normalized isotherms of DMPC, DSPC, and DPPC reveal about the phase transition? Normalized isotherms of DMPC, DPPC, and DSPC at ( $T_c$  - 15 °C) and those of DSPC, 5SO<sub>2</sub>-, 7SO<sub>2</sub>- and 9SO<sub>2</sub>-PC at  $T_c$  - 20 °C can be viewed as being in corresponding states. This means that the temperature dependence of the features of the isotherm ( $A_t$ ,  $\pi_t$ ,  $A_{on}$ ) have been compensated for so that upon comparison differences in the isotherms truly reflect the structural influences on the monolayer behaviour. The isotherms of unfunctionalised lipids superimpose upon normalization (Figure 3.5(b)). The area (and the surface pressure) of the phase transitions and the onset areas are the same. Lipids with essentially the same structure but different  $T_m$  values exhibit similar features in their  $\pi/A$  isotherms. The merit of the normalization procedure is

demonstrated in the comparison of normalized isotherms of functionalised and unfunctionalised lipids (Figure 3.6). DSPC, 1C<sub>18</sub>,2(5SO<sub>2</sub>)C<sub>17</sub>-PC, 1C<sub>18</sub>,2(7SO<sub>2</sub>)C<sub>17</sub>-PC and 1C<sub>18</sub>,2(9SO<sub>2</sub>)C<sub>17</sub>-PC) are considered to be in corresponding states. They nonetheless exhibit differences in their reduced isotherms.

The reduced transition pressure  $(\pi_t/\pi_c)$  exhibits an SO<sub>2</sub> positional-dependency. The increasing  $\pi_t/\pi_c$  with SO<sub>2</sub> position can be related either to greater energies required to expel the polar group from the air-water interface or to a greater destabilisation of the condensed monolayer by the presence of the bulky functional group. The former scenario implies a reorientational phase transition whereas the latter does not. The 5SO<sub>2</sub>- and 7SO<sub>2</sub>-functionalised lipids do not however undergo a reorientational phase transition. Therefore, the destabilisation argument is favored as rationalization for the observed behaviour. This conclusion is supported by the  $d\pi_t/dT$  values of bipolar lipids discussed previously.

Of significance is the  $SO_2$  positional dependence of the onset area  $(A_{on})$  (Figure 3.6). The onset areas are not temperature dependent, and are constant for a given lipid (Figure 3.4). This phenomenon is not understood at present, but it may mean that the onset area reports the area of the lipid in the horizontal conformation (Figure 3.8).

The transition areas (A<sub>t</sub>) of the normalized isotherms of DSPC, 5, 7 and 9 functionalised lipids (Figure 3.6) are equivalent. The equivalence of the transition areas demonstrates that at the transition, the distribution of lipid domains is equivalent in these four lipids.

To illustrate the virtue of isotherm normalization, area changes of the functionalised lipids at two temperatures have been tabulated (Table 3.2). At  $\sim$ 11°C and at  $\sim$ 21°C the plateau areas of the *unnormalized* lipid isotherms increase with SO<sub>2</sub> position. The trend erroneously hints of a positional dependence of the plateau area. In fact the transition area in this case simply describes lipid films in different states with respect to the  $T_c$ .

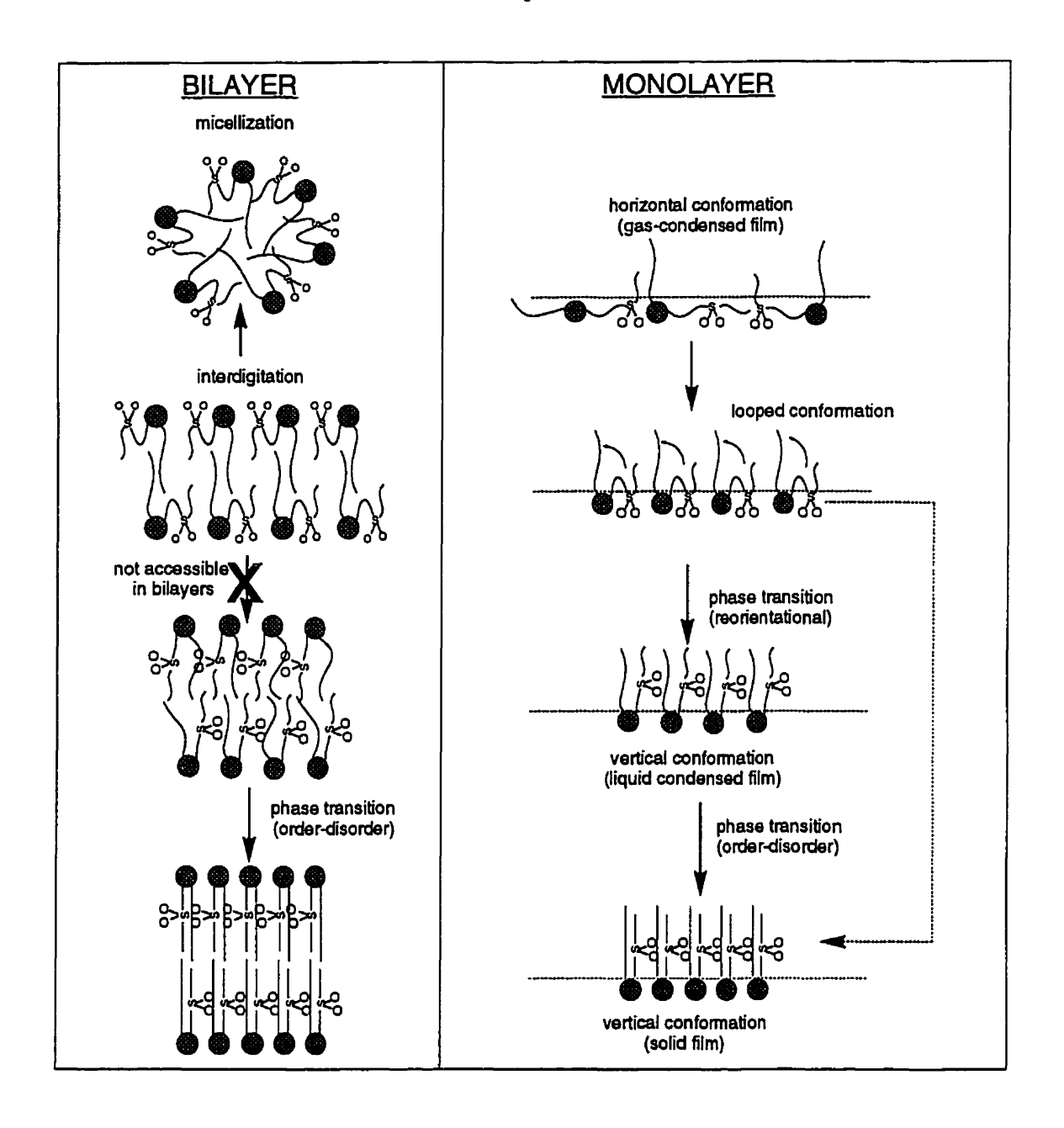


Figure 3.8. Schematic representation of bilayer and monolayer phase transitions shown in parallel to account for results obtained for  $SO_2$ -functionalised lipids. The difference between  $T_c$  and  $T_m$  for 9- and 11  $SO_2$ -PC is attributed to the looping conformation which can be adopted in the monolayer state, but which is unlikely in the bilayer. Such a lipid conformation is depicted as being disruptive to bilayer integrity resulting in micellization.

#### 3.4. Conclusions

The analogy between the le-lc phase transition and the gel-to-liquid-crystalline phase transition of lipid bilayers is supported by the excellent correspondence between the critical temperature of the monolayer phase transition and the  $T_m$  value ( $T_c = T_m$ ). This correlation shows that the condensation which occurs in monolayers is analogous to that which occurs in lipid bilayers. Above the  $T_m$  the lipids exist in a disordered state both in bilayer and monolayer conditions.

Some chain-functionalised lipids do not however display this equality between  $T_{\rm c}$  and  $T_{\rm m}$ . The divergence is attributed to increased cohesive interactions between the sulfone groups and the headgroup at the phase transition. These interactions increase the monolayer critical temperature with respect to the main bilayer phase transition temperature. The phase transition shifts towards a reorientational-type phase transition due to a conformational change. The relationship between the  $T_{\rm c}$  and the  $T_{\rm m}$  and the temperature dependence of the monolayer phase transition can be used to distinguish between the types of phase transition in the monolayer system.

This report emphasizes that structural information cannot be directly extracted from the phase transitions observed for isolated monolayer isotherms. A methodology is presented to allow comparison of monolayer isotherms for the purpose of extracting structural information. This methodology involves:

- (i) Determination of the temperature dependence of the phase transition of the lipids of interest.
- (ii) Determination of the critical parameters  $\pi_c$ ,  $A_c$  and  $T_c$ .
- (iii) Establish the nature of the phase transitions.
- (iv) Normalization of the isotherms with respect to the critical temperatures.

The LFB technique is a simple, yet powerful tool for the study of phospholipid morphology, yet comparison of data can be problematic. We have been able to show that

## Chapter 3

the introduction of polar functional groups into the acyl chains of phospholipids at an appropriate position yields lipids which express bipolar character. This bipolar character can be identified either by an elevated critical point with respect to the  $T_m$  of the lipid, or by decreased values of  $d\pi/dT$  with respect to the unfunctionalised lipid. The phase transition of bipolar lipids is not attributable to a conventional le-lc transition but has been assigned to the gc-lc phase transition which is usually difficult to detect in unfunctionalised lipids. The trends observed for the  $SO_2$  functionalised lipids have been observed previously for bipolar fatty acids, but the assignment of the monolayer phase transition of these lipids to the gc-le process has not been previously made. Perhaps with the study of additional structurally unique phospholipids new phase behaviour will be uncovered and contribute to the expansion of our understanding of phospholipid film morphology.

# 3.5. References

- (1) Heitner, T., Berthiaume, G., Lennox, R. B. Langmuir 1998, submitted.
- (2) Heitner, T., Berthiaume, G., Tanenbaum, D., Lennox, R. B. Biophys. J. 1998, submitted.
- (3) Hatta, I., Matuoka, S., Singer, M. A., Finegold, L. Chem. Phys. Lipids 1994, 69, 129-136.
- (4) Attard, G.S., McGuigan, C., Mackenzie, A. Chem. Phys. Lipids 1995, 76, 41-48.
- (5) Chung, H., Caffrey, M. Biophys. J. 1995, 69, 1951-1963.
- (6) Lindblom, G., Rilfors, L. Biochim. Biophys. Acta 1989, 988, 221-256.
- (7) Mouritsen, O.G., Jørgensen, K., Hønger, T. Permeability of lipid bilayers near the phase transition; Mouritsen, O.G., Jørgensen, K., Hønger, T., Ed.; CRC Press: Ann Arbor, 1995, pp 137-160.
- (8) Kuhn, H., Mobius, D. Monolayer Assemblies; Second Ed. ed.; Kuhn, H., Mobius, D., Ed., 1993; Vol. IXB, pp 375-544.
- (9) Rame, E. J. Coll. Interface Sci. 1997, 185, 245-251.
- (10) Menger, F.M., Wood M. G. Jr., Zhou Q. Z., Hopkins, H. P. J. Am. Chem. Soc. 1988, 110, 6804-6810.
- (11) Menger, F.M., Richardson, S. D., Wood, M. G., Sherrod, M. J. Langmuir 1989, 5, 833-838.
- (12) Rolland, J., Santaella, C., Vierling, P. Chem. Phys. Lipids 1996, 79, 71-77.
- (13) Georges, C., Lewis, J. T., Llewellyn, J. P., Salvago, S., Taylor, D. M., Stirling,
- J. M., Vogel, V. J. Chem. Soc. Faraday Trans. 1988, 84, 1531-1542.
- (14) Smaby, J.M., Brockman, H. L. Langmuir 1991, 7, 1031-1034.
- (15) Albrecht, O., Gruler, H., Sackmann, E. J. Physique 1978, 39, 301-313.
- (16) Derivichian, D.G. J. Chem. Phys. 1939, 7, 931-948.
- (17) Chattoraj, D.K., Birdi, K. S. Adsorption and the Gibbs Surface Excess; Plenum Press: New York, 1984.
- (18) Gaines, G.L. Insouble Monolayers at Liquid-Gas Interfaces; Interscience Publishers: New York, 1966.
- (19) Davies, J.T., Rideal, E. K. Interfacial Phenomenon; Academic Press: New York, 1961.
- (20) Cadenhead, D.A., Muller-Landeau, F., Kellner, B. M. J. *Phase transitions in one and two-component films at the air/water interface*; Cadenhead, D.A., Muller-Landeau, F., Kellner, B. M. J., Ed.; North Holland: New York, 1980, pp 73-81.

- (21) Phillips, M.C., Chapman, D. Biochim. Biophys. Acta 1968, 163, 301-313.
- (22) Cadenhead, D.A., Muller-Landau, F., Kellner, B. M. J. J. Coll. Interface Sci. 1978, 66, 597-601.
- (23) Birdi, K.S. Langmuir 1987, 3, 132-133.
- (24) Birdi, K.S. Lipid and Biopolymer Monolayers at Liquid Interfaces; 1 ed.; Plenum Press: New York, 1989.
- (25) Ladbrooke, B.D., Chapman, D. Chem. Phys. Lipids 1969, 3, 304-367.
- (26) Laggner, P., Kriechbaum, M. Chem. Phys. Lipids 1991, 57, 121-145.
- (27) Bois, A.G., Firpo, J. L., Dupin, J. J., Albinet, G., Baret, J. F. Coll. Polym. Sci. 1979, 257, 512-521.
- (28) Benedek, G.B., Hawkins, G. A. Phys. Rev. Lett. 1974, 32, 524-527.
- (29) Ruckenstein, E., Li, B. Langmuir 1995, 11, 3510-3515.
- (30) Ruckenstein, E., Li, B. Langmuir 1996, 12, 2308-2315.
- (31) Ruckenstein, E., Li, B. J. Phys. Chem. 1996, 100, 3108-3114.
- (32) Israelachvili, J. Langmuir 1994, 10, 3774-3781.
- (33) Klopper, K.J., Vanderlick, T. K. J. Coll. Interface Sci. 1996, 182, 220-229.
- (34) Paltauf, F., Hauser, H., Phillips, M. C. *Biochim. Biophys. Acta* 1971, 249, 539-547.
- (35) Marsh, D. CRC Handbook of Lipid Bilayers; CRC Press: Boston, 1990.
- (36) Mouritsen, O.G. Computer Studies of Phase Transitions and Critical Phenomena; Springer-Verlag: New York, 1984.
- (37) Seelig, J., Browning, J. L. FEBS Letters 1978, 92, 41-44.
- (38) Kim, M.W., Cannell, D. S. Phys. Rev. A 1976, 13, 411-416.
- (39) Mohwald, H. *Phospholipid Monolayers*; Mohwald, H., Ed.; Marcel Dekker, Inc.: New York, 1993, pp 579-602.
- (40) Nagle, J.F. J. Membrane Biol. 1976, 27, 233-50.
- (41) Cevc, G. Phospholipids Handbook; Marcel Dekker, Inc.:, 1993; Vol. New York.
- (42) Silvius, J.R. Chem. Phys. Lipids 1991, 57, 241-252.
- (43) Mouritsen, O.G. Chem. Phys. Lipids 1991, 57, 179-194.
- (44) Bloom, M., Evans, E., Mouritsen, O. G. Quart. Rev. Biophys. 1991, 24, 293-397.
- (45) Shobha, J., Balasubramanian, D. J. Phys. Chem. 1986, 90, 2800-2802.
- (46) Rice-Evans, C., Burdon, R. Prog. Lipid. Res. 1993, 32, 71-110.
- (47) Barclay, L.R.C. Can. J. Chem. 1993, 71, 1-16.

# Chapter 4

Surface dipole and pressure isotherms of sulfone-functionalised phospholipids reveal an orientational phase transition mechanism.

(co-authors: G. Berthiaume and R.B. Lennox)

#### Abstract

Surface pressure- and surface potential-area isotherms are presented for monolayers of phospholipids bearing polar groups (SO2, SO). The surface dipole moment changes which occur during the phase transition are determined from the surface potential isotherm using the Helmholtz model. From the types of changes in the calculated surface dipole which occur during the isotherm in the isotherm the nature of the phase transition is determined. Order/disorder transitions lead to constant surface dipole value during the transition for dipalmytoylphosphatidyl-choline (DPPC) and distearoylphosphatidylcholine(DSPC). A detailed study of the molecular structurefunction, dipole-surface pressure relationships for chain-substituted PC's allows one to assign average molecular orientations to the monolayer lipids. For example, the phase transition of functionalised lipids is accompanied by either a constant or sharp decrease in the surface dipole value depending on the position of the functionalisation and the experimental temperature. A sharp decrease in the surface dipole at the  $\pi$ -area transition indicates that a reorientation of the film dipole moment at the interface has occurred. An orientation change is proposed which is typical of bipolar amphiphiles. It arises due to the stabilization of a horizontally oriented (prone) lipid conformation of the lipid in the expanded state of the monolayer. Lipids functionalised near the headgroup display surface dipole isotherms comparable to unfunctionalised lipids (i.e. DPPC). This indicates that no orientational readjustment is required by the functional group of these lipids. The orientational phase transition is shown to be inducible, however, through an increase in temperature. The reorientation mechanism is therefore proposed to be accessible to lipids through the appropriate balance of temperature and position of functional group along the alkyl chain. The reorientational mechanism is favored (i) in lipids functionalised at positions remote from the head group and (ii) at higher temperatures. Surface dipole studies further indicate that the expanded lipid

# Chapter 4

film exists as a series of condensed domain islands rather than as a homogeneous, two-dimensional gas.

# 4-I. Introduction

Phospholipids bearing sulfone and sulfoxide groups in the hydrocarbon chain region have been shown to display unusual features in the surface pressure/molecular area monolayer isotherms. The temperature dependence of the phase transition leads to predictions of the critical temperature,  $T_c$ , which differ from the main transition temperature of lipid bilayers as measured by differential scanning calorimetry (DSC) for particular functionalised lipids. The monolayer phase transition of the sulfone functionalised phospholipids, which is manifested as a plateau in the isotherm, is not adequately described by an order-disorder mechanism however. To probe the detailed nature of this phase transition we have simultaneously measured the surface pressure  $(\pi)$  and surface potential isotherms of the lipid monolayers. Surface potential is related to the perpendicular dipole moment  $(\mu_L)$  of the film and the resulting  $\mu_L/\pi/a$ rea(A) relationships provide insight into molecular orientations of monolayer components.

A  $\pi/A$  isotherm of a 2D system is formally analogous to a pressure/volume isotherms of a 3D system. At low surface pressures the  $\pi/A$  isotherm can often be adequately described by the two-dimensional van der Waals equation<sup>2</sup>. At larger surface pressures isotherms exhibit discontinuities or plateaus which are referred to as phase transitions: a decrease in lipid mean molecular area occurs at constant or near constant surface pressure ( $d\pi/dA \approx 0$ ). It proves to be very challenging to establish what phases are involved in these "transitions". In addition to *in situ* diffraction techniques, the behaviour of the surface dipole moment,  $\mu$ , both at low surface pressures and during the plateau region provides insight into lipid states in the phase transition region.

Although surface potentials of monolayers are not simple quantities to interpret, the measured values have been effectively used to acquire detailed information about orientation of lipids in monolayers. As the surface density of a monolayer is increased the surface potential value increases due to the increase in the surface concentration of molecular dipoles at the interface. In order to relate the observed surface potential to the

properties of the molecules forming the monolayer, it is necessary to take these surface concentration changes into account. If the surface concentration is factored out as  $\Delta V \cdot A$  (where  $\Delta V$  is the difference between the surface potential of the monolayer and the surface potential of the clean air/water interface, and A is the lipid mean molecular area) then isotherms of different materials can be directly compared. The apparent surface dipole moment of a monolayer is calculated from the experimental surface potential values using the Helmholtz equation.<sup>3</sup> This procedure treats the surface adsorbed monolayer as a parallel plate condenser such that:

$$\mu_{\perp} = \Delta V A \qquad (4.1)$$

$$12\pi$$

where  $\mu_{\perp}$  is the component of the surface dipole moment normal to the interface and  $\Delta V$  is the difference in potential between a clean water surface and the lipid monolayer-coated water surface. This convention has been adopted for the representation of the monolayer surface dipole in this report. The calculated dipole moment is referred to as the *apparent* surface dipole moment,  $\mu_{app}$ .

In the Helmholtz model, the monolayer is treated as an assembly of molecular dipoles and is an average of all perpendicularly oriented dipoles in the monolayer. The surface potential is equal to the sum of the molecular dipoles ( $\Delta V \propto N\Delta\mu$ ). It is difficult however to differentiate the contributions made by individual components of the system to the measured surface potential value. For example, several reports attempt to calculate separate surface dipole contributions due to the aligned water at the interface ( $\mu_1$ ), the headgroup ( $\mu_2$ ), and the hydrophobic chain ( $\mu_3$ ) (Figure 4.1.).<sup>4-7</sup> For each model proposed, the correct assignment of the individual surface dipole component relies upon the appropriate assignment of the corresponding dielectric constant. This assignment in turn requires certain assumptions. The validity of some of these assumptions has been reviewed and is believed to be the origin of discrepancies between the calculated values in the literature.<sup>8</sup>

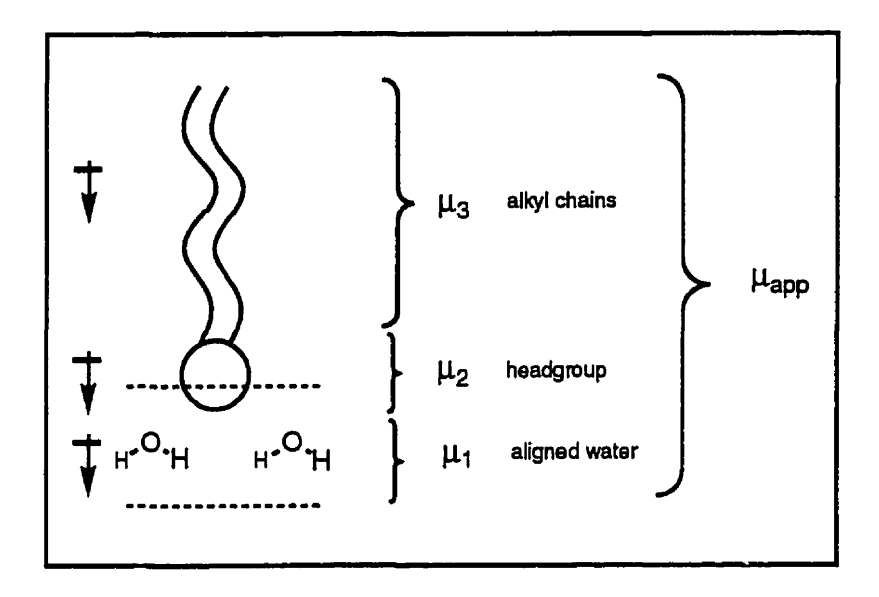


Figure 4.1. Contribution of component molecular dipoles of a phospholipid to the observed apparent dipole  $\mu_{app}$ .

Only dipoles which possess some component normal to the interface can be detected in the surface potential experiment. The average relative orientation of the sulfone and sulfoxide groups in the molecules studied here can thus be determined and used to describe an average conformation for the phospholipid at the interface. A systematic investigation of the changes in the surface dipole moment which take place during the monolayer compression for both sulfone- and sulfoxide-functionalised phospholipids is presented. Comparison with the surface dipole profiles and isotherms of DPPC and DSPC allow one to assess the importance of the position of the polar functional group and of its role in the phase transition of the monolayer. Of particular relevance to this investigation is the comparison of isotherms which exhibit a phase transition so that surface dipole changes during the transition can be compared.

Techniques such as synchrotron X-ray reflectivity<sup>9</sup> and grazing incidence<sup>10-13</sup> or polarized IR<sup>14-17</sup> have frequently been used to obtain information about chain conformations but are difficult to access because of instrumentation, complexity, and cost in the case of the X-ray experiments. The surface potential experiment on the other hand,

permits the convenient extraction of detailed information on the orientation of lipid acyl chains bearing polar functional groups.

It is well recognized that the dipole determined for a lipid monolayer ( $\mu_{app}$ ) is lower than predicted by summing the dipoles of the individual components of the molecules forming the monolayer <sup>5</sup>. The orientation of subphase water molecules by the lipid head groups has been proposed to account for this discrepancy (Figure 4.1.). When comparing any two lipids in this report it is assumed that any contributions from the oriented water molecules in the subphase, the headgroup, and the hydrocarbon tails are constant. Differences between surface dipole-area isotherms of functionalised and unfunctionalised lipids are thus assumed to be due solely to the functionalisation of the alkyl chains. Polarization effects between the headgroup and functional groups, in addition to the local dielectric properties of the environment, are included in the measured surface potential value. Differences in the surface dipole isotherms are therefore attributable to the sulfone or sulfoxide dipoles or to induced dipole effects caused by their presence.

The monolayer phase behaviour of bipolar amphiphiles has been studied using a number of different lipids in previous work. For example, the temperature dependence of the surface potential profile for HOOC-(CH<sub>2</sub>)<sub>16</sub>COOCH<sub>3</sub> (C18HE) was systematically studied and the nature of the phase transition was re-evaluated. Surface potential studies of fatty acids bearing sulfoxide groups have been studied. The surface potential profiles of octadecyl methyl sulfoxide (OMS) and (+)-octadecyl-p-tolyl sulfoxide (OTS) in addition to bipolar lipids HOOC-(CH<sub>2</sub>)<sub>16</sub>-COOCH<sub>3</sub>, laglycerol dialkyl nonitol tetraether (GDNT) and glycerol dialkyl glycerol tetraether (GDGT)<sup>20</sup> have also been reported. The present study focuses on the effect of a second (and third) polar group in the acyl chain of phospholipids. Both the positional dependence of the functional group and the temperature dependence of the monolayer phase transition have been investigated. A self-consistent model emerges from these structure-property variations which describes the phase behaviour of both functionalised and unfunctionalised phospholipids. A re-interpretation of

monolayer phase transitions of phospholipid films in light of information gained through the study of these systems is presented.

## 4-2. Materials and Methods

Samples studied consisted of distearoylphosphatidylcholine (DSPC) analogs functionalised at position 5, 7, 9 or 11. Phospholipids incorporating sulfone moieties in the acyl chain were synthesized in our lab. The partial synthesis of analogous phospholipids has been described elsewhere<sup>21</sup> as has the synthesis of the sulfone substituted fatty acids used<sup>19</sup>. The composition of this series was established by FAB-MS, and their purity was monitored using 300 MHz and 500 MHz NMR, and thin layer chromatography. Purity was estimated to be >99%. Phospholipid standards DC16PC and DC18PC were purchased from Avanti Polar Lipids (Birmingham, Alabama) and were used without further purification.

Isotherms were recorded using a KSV Instruments Langmuir film balance, equipped with a 150 mm x 540 mm Teflon compartment (KSV, Helsinki, Finland.). A circulating bath provided thermal control of the subphase. 20 mg of a sample was dissolved in 10 mL CHCl<sub>3</sub> (BDH, Omnisolv). Samples were spread in a dropwise fashion ( $60\mu$ L aliquots) onto a subphase of Millipore Milli-Q water ( $18M\Omega$ ). 15 minutes elapsed before compression was initiated so as to allow for solvent evaporation. A compression rate of 10 mm/min was used for each run. The compression rate did not affect the isotherms, as identical isotherms were obtained when the barrier compression rate was doubled or halved.

The surface potential and surface pressure of the lipid monolayers were recorded simultaneously. A vibrating plate capacitor device (KSV) was used for surface potential experiments. The principles of the vibrating plate method have been described elsewhere.<sup>3</sup> The upper electrode of the capacitor oscillates at a frequency of 80 to 120 Hz. The lower

platinum electrode is placed below the water surface. The measuring range of the meter was  $\pm 10$  V and values are quoted to an accuracy of  $\pm 5$  mV.

## 4-3. Results and Discussion

Surface dipole moment values obtained from the surface potential isotherms are used to derive information about the molecular orientations of the phospholipids at the interface. The surface dipole of the expanded film is at a maximum prior to the plateau feature of the surface pressure-area ( $\pi/A$ ) isotherm and thus is designated  $\mu_{app}^{max}$ . The surface dipole moment of the condensed film at full compression is designated  $\mu_{app}^{cond}$ . These values are listed in Table 4.1. The value of  $\mu_{app}$  max reflects the orientation all polar groups in the lipid molecule. However, if the isotherms of SO- and SO<sub>2</sub>-functionalised lipids are compared to those of unfunctionalised lipids, the differences in the surface dipole values can yield information concerning the orientation of the functional group in the monolayer. The difference  $\Delta \mu_{app} = \mu_{app}^{max} - \mu_{app}^{cond}$  is the change in surface dipole which occurs during the plateau of the  $\pi/A$  isotherm. The SO and SO<sub>2</sub> groups effectively act as probes for the surface potential experiment due to their large intrinsic dipole moments. The orientations of these groups serve to report the orientation(s) of the lipid chains. For monolayer phases in which no molecular reorientation is involved,  $\Delta \mu_{app} = 0$ . Reorientation of the dipole from a normal to parallel orientation with respect to the interface results in  $\Delta\mu_{app}$  values whose maximal values should be the dipole moment of the molecule. As mentioned in the Introduction, the SO and SO<sub>2</sub> dipoles will only be detected if there is some component oriented perpendicularly to the interface (Figure 4.5 (f), (h) and (i)).

# 4.31. Characterization of the expanded film

What does the surface dipole moment of the expanded monolayer of bis(11SO)C17-PC and bis(11SO<sub>2</sub>)C17-PC lipids reveal about the lipid conformations in this region of the isotherm? Ordinary diacyl phospholipids (i.e. DPPC and DSPC) exhibit only modest surface dipole moments in their expanded film states (0.8 and 1.0 D respectively) (Figure 4.2 (a) and (b)). The  $\mu_{app}$  of DPPC and DSPC is not specifically dependent upon the orientation of the lipid chain so it is not a direct measure of chain conformation in these molecules (Figure 4.5 (a)-(c)). For the functionalised lipids, however, the SO and SO<sub>2</sub> groups may contribute to  $\mu_{app}$ , the extent of contribution depending upon the orientations adopted. The surface dipole values for the expanded isotherms of bis11-SO and -SO<sub>2</sub> lipids (Figure 4.3 (a) and (b)) are 3.0 D and 2.5 D respectively (Table 4.1), much greater than for either DPPC or DSPC. It follows that the dipoles (or some component of them) are oriented normal to the interface and that the acyl chains must lie parallel to the interface. The lipid is in a prone conformation in this gas-expanded state (Figure 4.5 (h)).

What does the surface dipole of bis(5SO)C<sub>17</sub>-PC and bis(5SO<sub>2</sub>)C<sub>17</sub>-PC reveal about the properties of the expanded film? Like DPPC and DSPC, lipids bearing SO and SO<sub>2</sub> groups at the 5 position exhibit small surface dipole moments in the expanded monolayer state (0.75 and 1.35 D respectively, Table 4.1, Figure 4.4 (a)-(b)). This means that the SO and SO<sub>2</sub> groups are oriented parallel to the interface. It follows that the lipid chains are vertically oriented (Figure 4.5 (d)). Prior to the onset of surface pressure the film has been previously described as being in a "gaseous" state<sup>3,22-24</sup> in which lipids are isolated and lie with their acyl chains extended along the air/water interface. Clearly this is not the case for bis(5SO)C<sub>17</sub>-PC and bis(5SO<sub>2</sub>)C<sub>17</sub>-PC. The lipid monolayer film at this point most probably consists of islands of condensed domains with the lipids adopting a vertical conformation (Figure 4.8 (d)).

The existence of isolated domains in a liquid-expanded film has been noted previously. More recently the presence of lipid clusters has been theoretically predicted to explain the phase transitions observed in the  $\pi$ -A curves of phospholipids and the state of the expanded film. These clusters or domains act as the individual components of a two-dimensional gas making up a "gas-condensed" state. The hydrophobic force which stabilizes this gas-condensed state must be greater than the electrostatic attraction of the alkyl chain for the water. The behaviour of bis(5SO)C<sub>17</sub>-PC and bis(5SO<sub>2</sub>)C<sub>17</sub>-PC lipids supports a clustering model.  $^{2,27,28}$ 

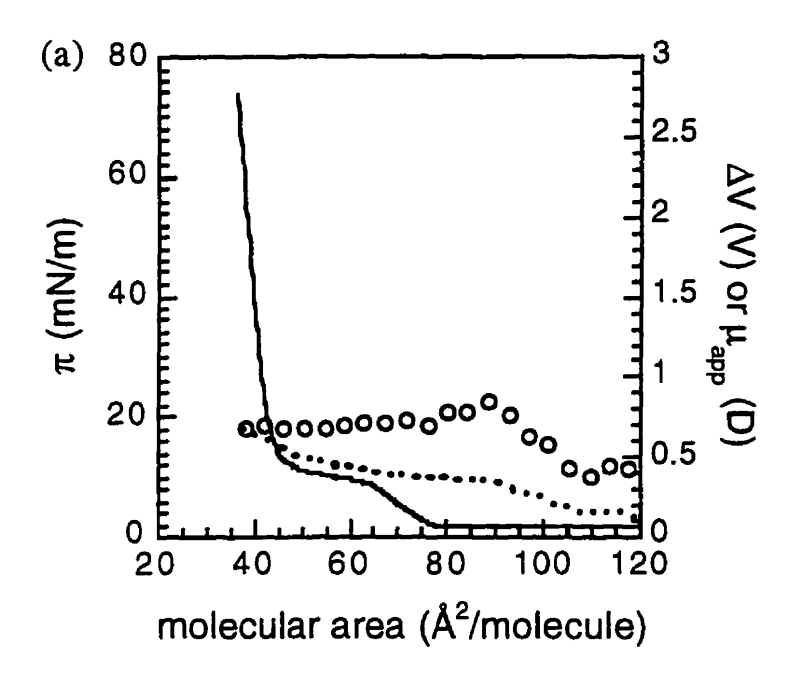
What does this say about the expanded films of DPPC and DSPC? The behaviour of the bis(5SO) and bis(5SO<sub>2</sub>) lipids describes the general arrangement of lipids in the expanded monolayer state. Surface dipole measurements of the 7SO<sub>2</sub>-PC monolayer parallels the behaviour of bis(5SO) and bis(5SO<sub>2</sub>)PC's. Their  $\mu_{app}^{max}$  and  $\Delta\mu_{app}$  values are similar (Table 4.1). The expanded film of 7SO<sub>2</sub>-PC can therefore also be described by islands of condensed domains (Figure 4.8.(d)). Because 7SO<sub>2</sub>-PC possesses a  $T_m$  (40 °C)<sup>29</sup> very close to that of DPPC (41 °C)<sup>30</sup> the isotherm of 7SO<sub>2</sub>-PC can be used to extract information about the expanded film of DPPC. The monolayer phase behaviour of DPPC and 7SO<sub>2</sub>-PC are similar (Figures 4.2 (a) and 4.6 (a)) so it is likely that the expanded DPPC film also exists in islands of condensed domains (clusters).

Table 4.1. Variation in the apparent surface dipole  $(\mu_{app})$  during the monolayer phase transition

phospholipid	T(°C)	μ <sub>app</sub> <sup>ma</sup> x (D)	μ <sub>app</sub> co mp. (D)	Δμ <sub>арр</sub> (D)	phase transition <sup>1</sup>
DPPC	23	0.76	0.72	0.2	O/D
DSPC	25	1	0.8	0.2	O/D
bis (11SO <sub>2</sub> )C <sub>17</sub> -PC	25	3	1	2	R
bis (11SO)C <sub>17</sub> -PC	25	2.5	0.5	2	R
bis (5SO <sub>2</sub> )C <sub>17</sub> -PC	27	0.75	0.75	0	O/D
bis (5SO)C <sub>17</sub> -PC	25	1.35	1	0.35	O/D
1C <sub>18</sub> ,2(7SO <sub>2</sub> )C <sub>17</sub> - PC	25	0.8	0.6	0.2	O/D
IC <sub>18</sub> ,2(11SO <sub>2</sub> )C <sub>17</sub> -PC	25	1.45	0.65	0.6	R/O/D <sup>2</sup>
bis (7SO <sub>2</sub> )C <sub>17</sub> -PC	25	1.1	0.7	0.4	O/D
bis (7SO <sub>2</sub> )C <sub>17</sub> -PC	33	2.5	0.7	1.8	R

<sup>&</sup>lt;sup>1</sup> low values of  $\Delta\mu_{app}$  implies an order/disorder phase transition (O/D) large values of  $\Delta\mu_{app}$  implies an orientational phase transition (R) <sup>2</sup> characteristics of both O/D and R phase transition is observed: decrease in  $\mu_{app}$  during the

phase transition and low  $\Delta\mu_{app}$ 



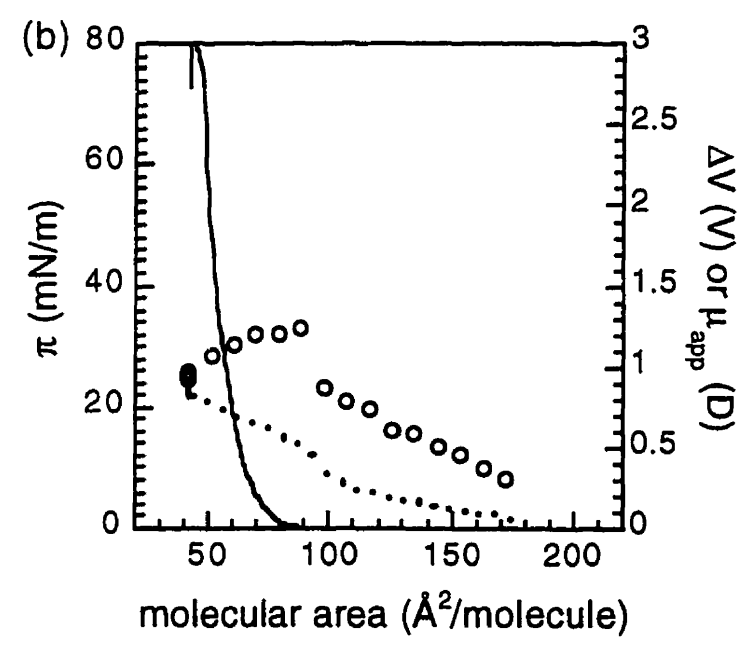


Figure 4.2. Isotherms of (a)DPPC (22 °C) and (b)DSPC (25 °C)monolayers at an air/water interface. Surface pressure (———) and surface potential (•••••) were recorded simultaneously. Surface dipole values (0000) were calculated from the measured surface potential using Equation 4.1.

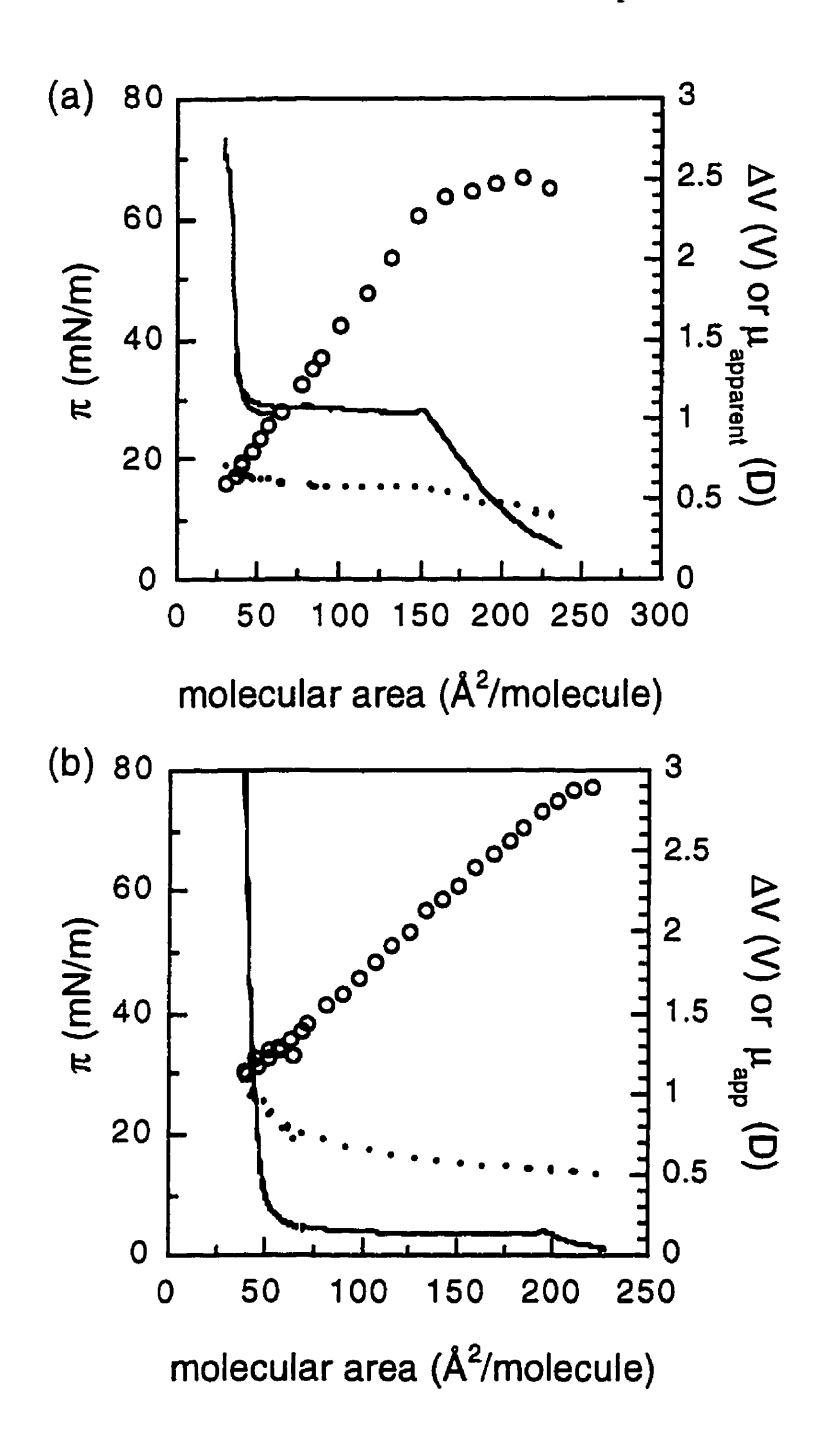


Figure 4.3. Isotherms of (a) bis(11SO)C<sub>17</sub>-PC and (b) bis(11SO<sub>2</sub>)C<sub>17</sub>-PC monolayers at an air/water interface at 25°C. Surface pressure (———) and surface potential ( $\bullet \bullet \bullet \bullet \bullet$ ) were recorded simultaneously. Surface dipole values ( $\circ \circ \circ \circ$ ) were calculated from the measured surface potential using Equation 4.1.

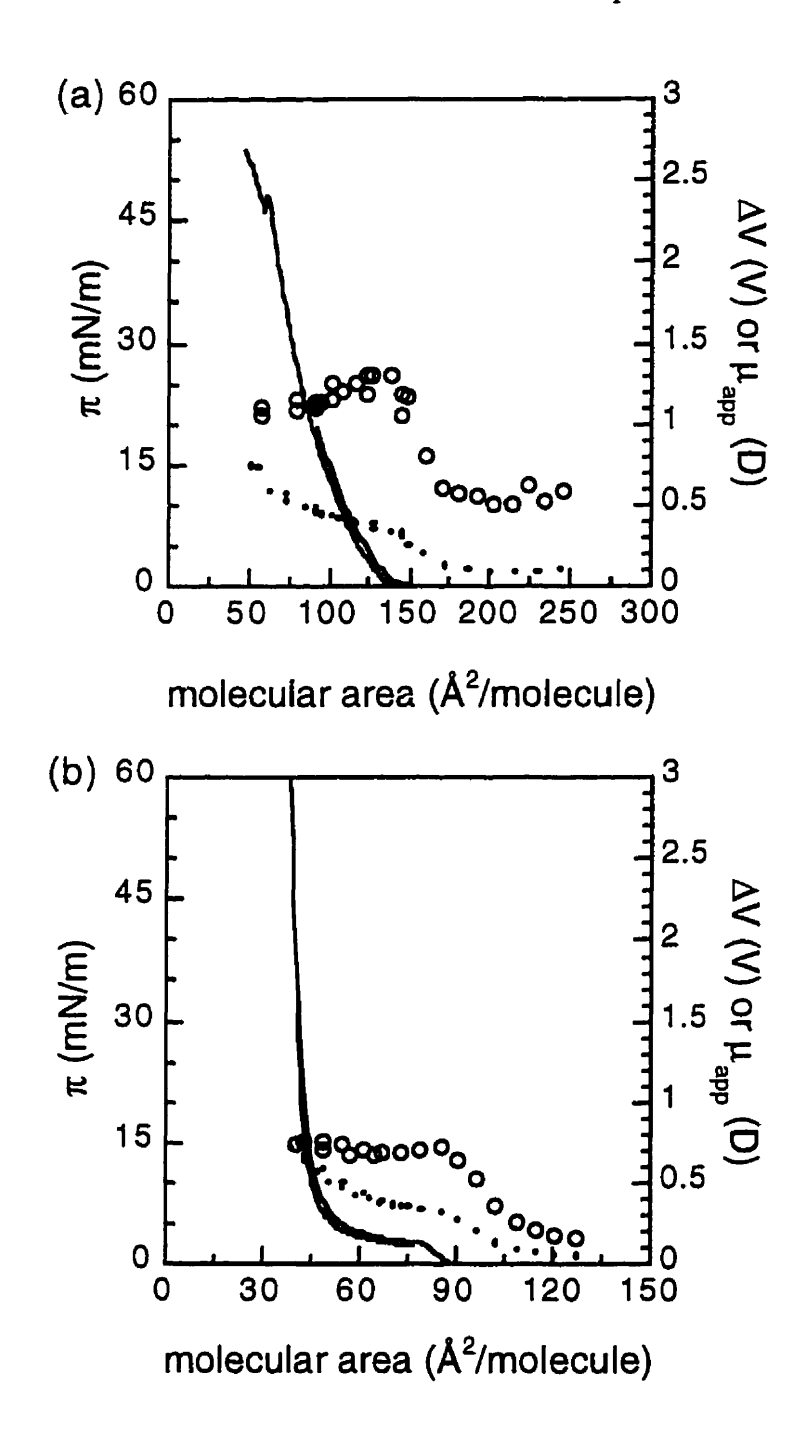


Figure 4.4. Isotherms of (a) bis(5SO)C<sub>17</sub>-PC and (b) bis(5SO<sub>2</sub>)C<sub>17</sub>-PC monolayers at an air/water interface at 25°C. Surface pressure (———) and surface potential ( $\bullet \bullet \bullet \bullet \bullet$ ) were recorded simultaneously. Surface dipole values ( $\circ \circ \circ \circ$ ) were calculated from the measured surface potential using Equation 4.1.

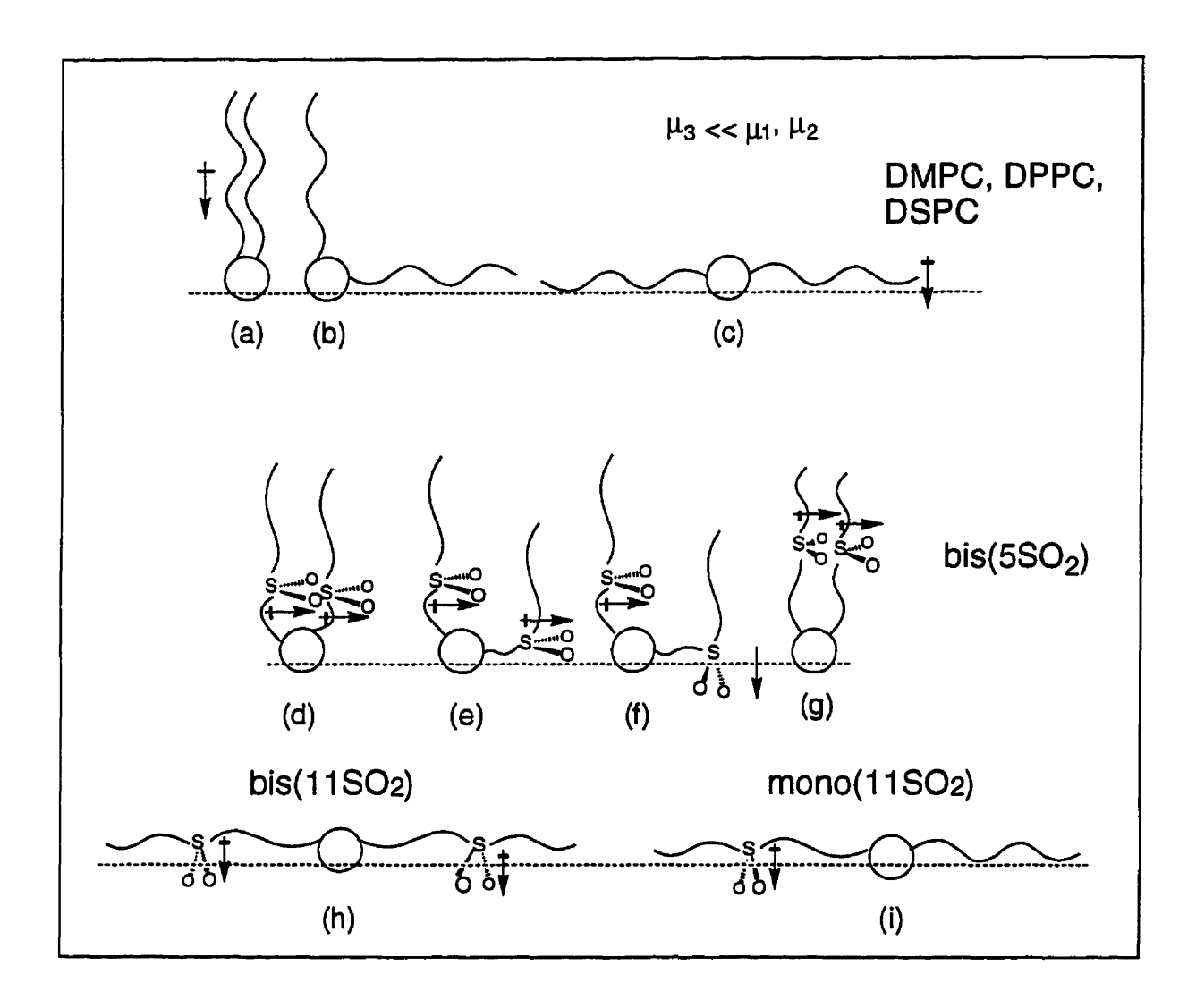


Figure 4.5. Possible conformations of lipids which could be adopted at the air/water interface in the expanded lipid film. (a)-(c) correspond to possible conformations of DPPC and DSPC. (d)-(g) correspond to possible conformations of bis(5SO)C<sub>17</sub>-PC and bis(5SO<sub>2</sub>)C<sub>17</sub>-PC and (h)-(i) show possible conformations of bis(11SO)C<sub>17</sub>-PC and bis(11SO<sub>2</sub>)C<sub>17</sub>-PC.

#### 4.32. Characterization of the fully compressed monolayer

What does the surface dipole of the fully compressed monolayer ( $\mu_{app}^{comp}$ ) reveal about lipid conformation? A vertical conformation of all the lipids in the compressed monolayer is confirmed by both the equality of the average molecular area of the lipids in the compressed film ( $A_s$ ) and the surface dipole values ( $\mu_{app}^{comp}$ ). The surface dipole moment of both the unfunctionalised and functionalised phospholipids in this vertical orientation is the same within experimental error (Table 4.1 ) consistent with the sulfone and sulfoxide groups being parallel to the interface (Figure 4.5 (a),(d) and (g)). The final value of 0.5 D obtained for bis11(SO)-PC is close to that obtained for the final value of DSPC (0.72 D) indicating that the structural arrangement of the two lipids in the 2D solid phase is similar.

# 4.33. Functionalisation of the lipid acyl chain and the nature of the phase transition.

What effect does the presence and position of the polar functional group have on the nature of the monolayer phase transition? It is the conformation of the lipid in the expanded film that ultimately governs the type of phase transition followed. Since the position of the polar group dictates the conformation adopted by the lipid (vertical or prone) in the expanded film, conformational changes which accompany the plateau feature of the isotherm are dictated by the position of the functional group. Only lipids which exhibit a plateau in their monolayer isotherms will be considered in this discussion. DSPC does not exhibit a plateau 19 °C below its T<sub>c</sub> (54°C). DPPC does, however, exhibit a liquid-expanded-to-liquid-condensed (*le-lc*) phase transition, and the surface dipole variations which occur in the phase transition region (plateau) of the isotherm and can be compared to the variations which occur during the plateau region of the functionalised lipids.

The  $\mu_{app}$  values are small ( $\mu_{app} \equiv 0.2$  D) and are roughly constant during the plateaus of both DPPC (Figure 4.2 (a)) and the 5SO<sub>2</sub>-functionalised lipid (Figure 4.3).

Apparently no dipole orientational changes occur during the compression of either DPPC or the 5SO- and 5SO<sub>2</sub>-functionalised lipids. When the polar functional group is situated near the lipid headgroup it is not "sensed" as being separate from the headgroup. The "looping" of the alkyl chain to the interface (Figure 4.5 (f)) is thus prevented. This parallels the behaviour of fatty acids bearing sulfoxide groups near the carboxylic acid headgroup. <sup>19</sup> The bis(5SO<sub>2</sub>)C<sub>18</sub>PC, and 1C<sub>18</sub>,2(7SO<sub>2</sub>)C<sub>18</sub>-PC phase transitions therefore corresponds to the crystallization of the lipid alkyl chains in the conventional manner. This is the liquid-expanded-to-liquid-condensed monolayer phase transition which is described as an order/disorder process. A number of gauche conformations can exist in the lipid acyl chains at low surface density. The lipids are in the all-trans conformation after the phase transition. <sup>13,31,32</sup>

In sharp contrast to the behaviour exhibited by bis(5SO<sub>2</sub>)C<sub>18</sub>PC the surface dipole  $(\Delta\mu_{app})$  of bis(11SO<sub>2</sub>)C<sub>17</sub>-PC, and bis(11SO<sub>2</sub>)C<sub>17</sub>-PC decreases by 2.0 D (Table 4.1). Since the surface dipole decreases a reorientation of the polar group from a perpendicular orientation (with respect to the air/water interface,  $\mu_{\perp}$ SO<sub>2</sub>SO<sub>2</sub> > 0) to a parallel orientation ( $\mu_{\perp}$ SO<sub>2</sub>SO<sub>2</sub> = 0) can be assigned. This corresponds to a change in the hydrocarbon chain orientation from prone (horizontal) (Figure 4.8.(a)) to vertical (Figure 4.8.(c)). Orientational changes involving the headgroup can be disregarded since no such changes are observed in the isotherm of DPPC (which has the same headgroup). The change is thus attributed solely to the reorientation of the SO and SO<sub>2</sub> functional groups. This reorientation corresponds to the *gc-lc* phase transition.

# 4.34. Surface dipole studies of mono-functionalised lipids

Mono-functionalised lipids ( $1C_{18}$ ,2( $nSO_2$ ) $C_{18}$ -PC n=7 or 11) also demonstrate a positional dependence in the surface dipole value, but these effects are not as pronounced as those observed for bis-functionalised lipids (Figure 4.4.(a) and (b)). The  $\mu_{app}$  value (0.8 D) determined for the expanded film of  $1C_{18}$ ,2(7SO<sub>2</sub>) $C_{17}$ -PC is comparable to values

obtained for unfunctionalised lipids and therefore suggests that a vertical conformation is adopted. However, mono-functionalisation at the 11 position yields behaviour approaching that of the bis-functionalised lipids discussed earlier where  $\mu_{app}^{max}(1C_{18},2(11SO_2)C_{17}-PC) = 1.5$  D. Since  $1C_{18},2(11SO_2)C_{17}-PC$  possesses only one sulfone group,  $\mu_{app}$  measured is half that measured for the bis-functionalised lipid ( $\mu_{app}^{max}$ (bis(11SO<sub>2</sub>)C<sub>17</sub>-PC) = 3.0 D). The functionalised chain must therefore lie horizontally such that the SO<sub>2</sub> dipole is perpendicular to the interface (Figure 4.5.(i)).

 $\Delta\mu_{app}$  values (Table 4.1.) are 0.2 D and 0.6 D for  $1C_{18}$ ,2(7SO<sub>2</sub>)C<sub>18</sub>-PC and  $1C_{18}$ ,2(11SO<sub>2</sub>)C<sub>18</sub>-PC respectively, the first value is similar to that observed for DPPC and DSPC. The surface dipole of the mono 7-functionalised lipid is constant during the plateau whereas the mono 11-functionalised lipid exhibits a decrease during the plateau (Figure 4.6.(a) and (b)). Using the same arguments previously presented,  $1C_{18}$ ,2(11SO<sub>2</sub>)C<sub>18</sub>-PC undergoes a reorientation of the SO<sub>2</sub> group during the phase transition. It is also likely that for  $1C_{18}$ ,2(11SO<sub>2</sub>)C<sub>17</sub>-PC the conformational changes which occur during the phase transition involve a combination of both order-disorder and reorientational changes since it possesses both a functionalised and unfunctionalised chain. The  $1C_{18}$ ,2(7SO<sub>2</sub>)C<sub>17</sub>-PC film adheres to the conventional order/disorder phase transition model. This is supported by the temperature dependence of the phase transition of  $1C_{18}$ ,2(nSO<sub>2</sub>)C<sub>18</sub>-PC, which predicts a critical temperature much greater than the DSC-determined  $T_m$  for n = 11 but which is equal to  $T_m$  for n = 5.<sup>29</sup>

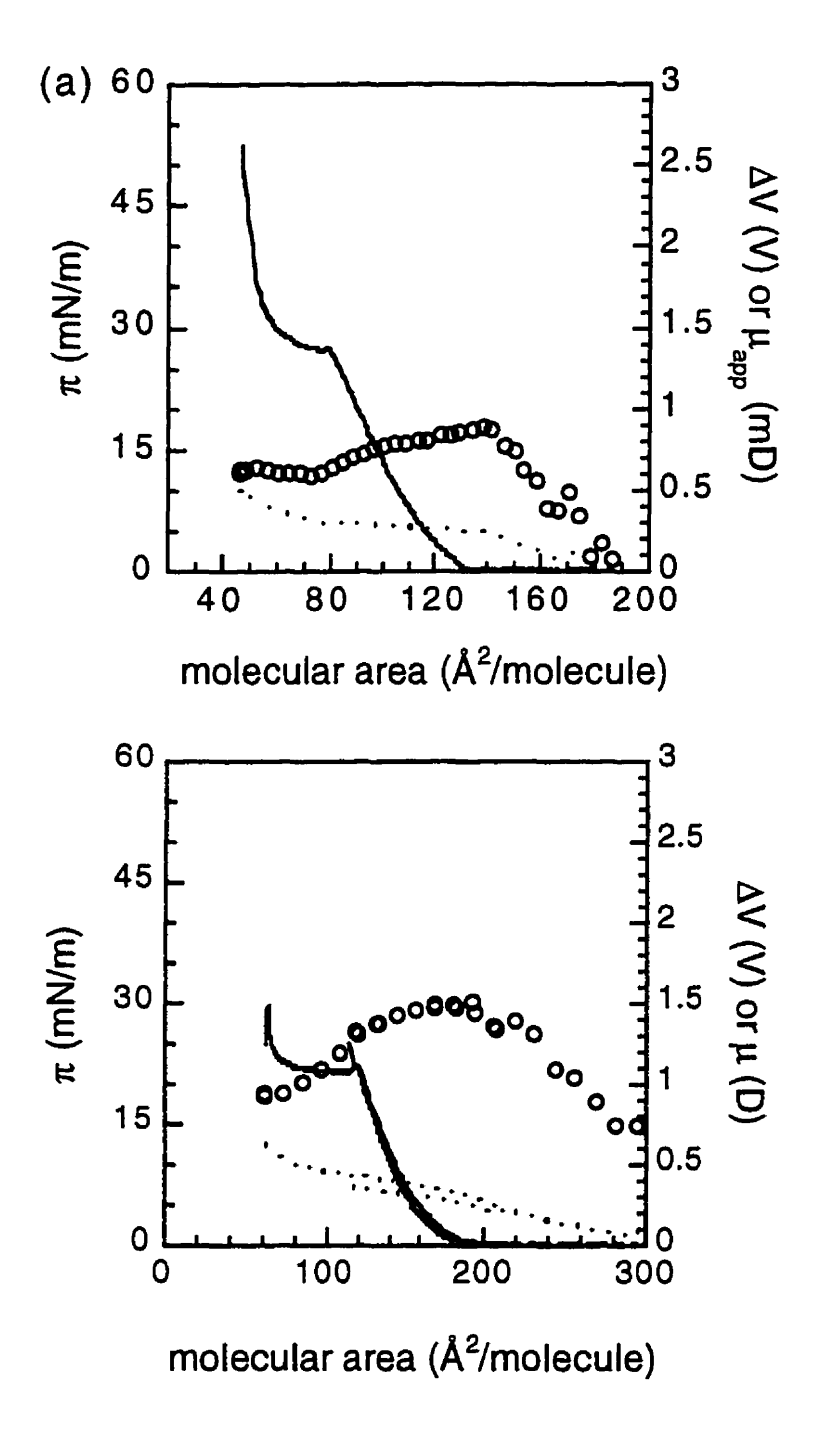


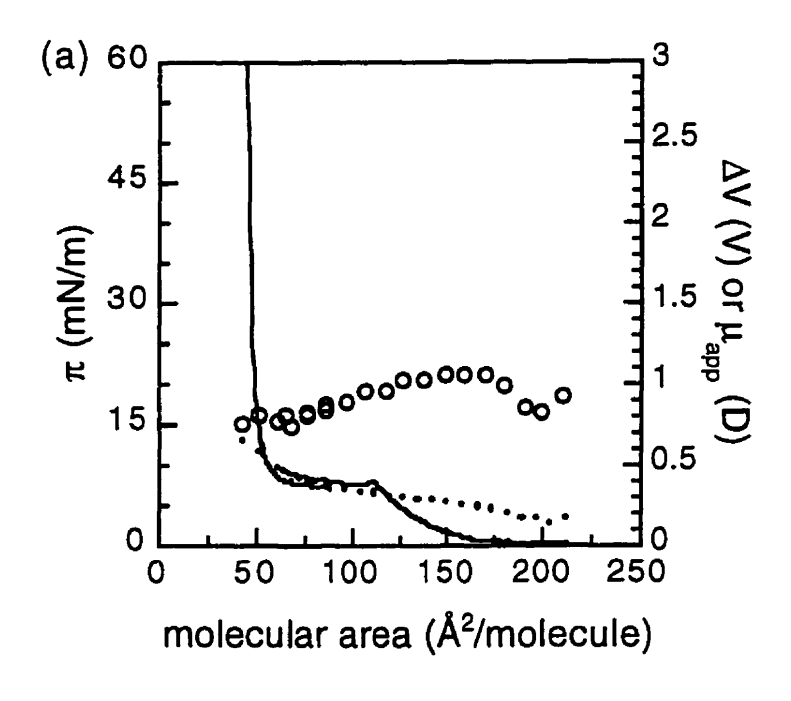
Figure 4.6. Isotherms of (a)1C<sub>18</sub>,2(7SO<sub>2</sub>)C<sub>17</sub>-PC and (b)1C<sub>18</sub>,2(11SO<sub>2</sub>)C<sub>17</sub>-PC monolayers at an air/water interface at 25°C. Surface pressure (———) and surface potential (• • • • • •) were recorded simultaneously. Surface dipole values (0000) were calculated from the measured surface potential using Equation 4.1.

# 4.35. The influence of temperature on the conformations of lipids in the expanded film and on the type of phase transition observed

What effect does increasing the temperature have on the nature of the phase transition of functionalised phospholipids? Figures 4.7(a) and (b) show the isotherms of bis(7SO<sub>2</sub>)C<sub>17</sub>-PC measured at 25°C and 33°C respectively. The surface dipole moment is constant during the phase transition at 25°C but decreases during the phase transition at 33°C. The decrease in the surface dipole moment indicates a reorientation of the sulfone group whereas at the lower temperature (25 °C) the constant surface dipole supports a constant dipole orientation. The  $\Delta\mu_{app}$  values (Table 4.1. 0.4 D at 25 °C and 1.8 D at 33°C) show that at the higher temperature the lipid exhibits behaviour typical of a bipolar lipid such as bis(11SO<sub>2</sub>)C<sub>17</sub>-PC and undergoes a reorientation during the plateau.

The high surface dipole moment observed at 33°C is consistent with the adoption of a horizontal conformation in the gas-expanded state (Figure 4.5(h)). Higher temperatures may favor the horizontal conformation by disrupting the van der Waals forces which otherwise stabilize the condensed domains of vertically oriented lipids (Figure 4.8(c)).

The nature of the phase transition is thus shown to be temperature dependent. The phase transitions changes because the expanded state phases in question differ. The vertical conformation is adopted at lower temperatures so that upon compression one observes an order-disorder phase transition. The horizontal conformation, which comprises the gascondensed phase, is accessible to functionalised lipids at the higher temperatures and compression yields a reorientational phase transition.



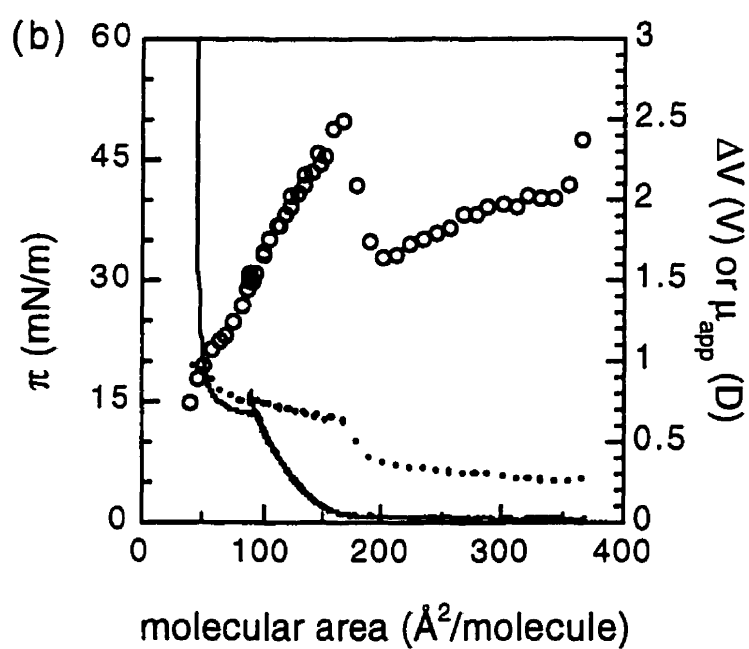


Figure 4.7. Isotherms of bis(7SO<sub>2</sub>)C<sub>17</sub>-PC monolayers at an air/water interface at (a) 25°C and (b) 33°C. Surface pressure (———) and surface potential (••••) were recorded simultaneously. Surface dipole values (0000)were calculated from the measured surface potential using Equation 4.1.

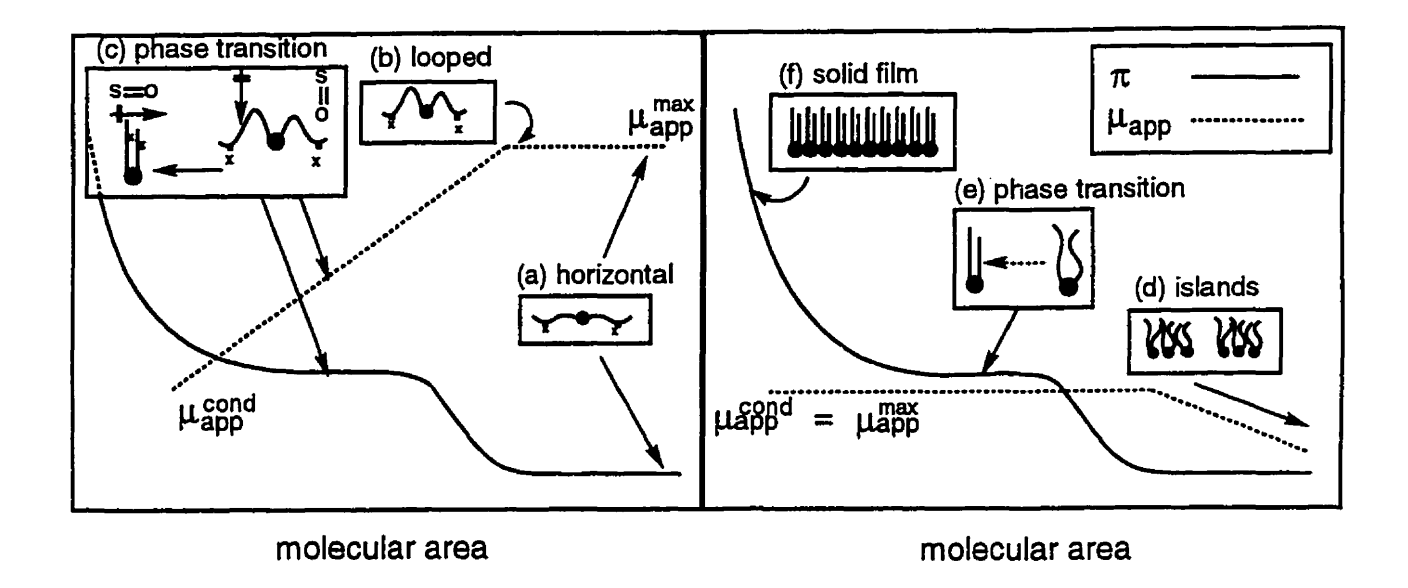


Figure 4.8. Proposed model to account for the differences between the surface dipole isotherms of functionalised and unfunctionalised phospholipids.

- (a) Lipid conformation proposed to be favored in the expanded state for functionalised lipids. The accessibility of the conformation is increased with position of the functional group and with temperature.
- (b) Looped conformation of functionalised lipids corresponding to the gas-condensed state.
- (c) Changes in conformation which occur during the monolayer phase transition region (plateau of  $\pi$ -A isotherm) for lipids functionalised at higher positions and for monolayer isotherms run at higher temperatures.
- (d) Islands of condensed domains are favored in the expanded state for unfunctionalised phospholipids and for functionalised lipids at low subphase temperatures.
- (e) Changes in conformation which occur during the phase transition of unfunctionalised phospholipids and of functionalised lipids at lower temperatures.
- (f) Representation of the fully compressed monolayer as a solid film.

## 4.4. Conclusions

- (1) Lipids functionalised with polar groups at positions near the midpoint of the chain or higher ( $n \ge 9$ ) adopt a horizontal conformation in the expanded film and the monolayer phase transition involves a reorientation of the acyl chain upon compression.
- (2) Unfunctionalised lipids or lipids functionalised near the headgroup ( $n \le 7$ ) adopt a vertical conformation in the expanded film and exist in islands of condensed domains. The monolayer phase transition corresponds to an order-disorder phase transition.
- (3) The type of monolayer phase transition experienced can be influenced also by the experimental temperature. The reorientational phase transition is favored at higher temperatures.

Although  $\pi$ -A isotherms of phospholipids of phospholipids may appear to be very similar the processes which they are describing can actually be extremely different as summarized in Figure 4.8. The surface dipole experiment provides a means of revealing these differences for phospholipids bearing polar groups by simultaneously reporting on chain conformation. The limitations in the use of the monolayer isotherm as a means of extracting meaningful structural information in the absence of such complementary measurements is thus highlighted.

# 4.5. References

- (1) Heitner, T., Berthiaume, G., Lennox, R. B. Langmuir 1998, submitted.
- (2) Poulis, J.A., Boonman, A. A. H., Gieles, P., Masses, C. H. Langmuir 1987, 3, 725-729.
- (3) Gaines, G.L. Insouble Monolayers at Liquid-Gas Interfaces; Interscience Publishers: New York, 1966.
- (4) Davies, J.T., Rideal, E. K. *Interfacial Phenomenon*; Academic Press: New York, 1961.
- (5) Demchak, R.J., Fort, T. J. Coll. Interface Sci. 1974, 46, 191-202.
- (6) Taylor, D.M., de Oliveira, O. N., Morgan, H. J. Coll. Interface Sci. 1990, 139, 508-518.
- (7) Petrov, J.G., Polymeropoulos, E. E., Mohwald, H. J. Phys. Chem. 1996, 100, 9860-9869.
- (8) Oliveira, O.N., Taylor, D. M., Lewis, T. J., Salvagno, S., Stirling, C. J. M. J. Chem. Soc., Faraday Trans. 1989, 85, 1009-1018.
- (9) Katsaras Biochem. Cell Biol. 1995, 73, 209-218.
- (10) Dluhy, R.A., Cornell, D.G. J. Phys. Chem. 1985, 89, 3195-3197.
- (11) Dluhy, R.A. J. Phys. Chem. 1986, 90, 1373-1379.
- (12) Dluhy, R.A., Wright, N.A., Griffiths, P.R. Appl. Spectrosc. 1988, 42, 138-141.
- (13) Mendelsohn, R., Davies, M. A., Brauner, J. W., Schuster, H. F., Dlumy, R. A. 1989, Biochemistry, 8934-8939.
- (14) Blaudez, D., Turlet, J.-M., Dufourcq, J., Bard, D., Buffeteau, T., Desbat, B. J. Chem. Soc., Faraday Trans. 1996, 92, 525-530.
- (15) Blaudez, D., Buffeteau, T., Cornut, J.C., Desbat, B., Escafre, N., Pezolet, M., Turlet, J.M. Appl. Spectrosc. 1993, 47, 869-874.
- (16) Blaudez, D., Buffeteau, T., Cornut, J.C., Desbat, B., Escafre, N., Pezolet, M., Turlet, J.M. Thin Solid Films 1994, 242, 146-150.
- (17) Cornut, I., Desbat, B., Turlet, J.M., Dufourcq, J. Biophys. J. 1996, 70, 305-312.
- (18) Vogel, V., Mobius, D. Thin Solid Films 1985, 132, 205-219.
- (19) Georges, C., Lewis, J. T., Llewellyn, J. P., Salvago, S., Taylor, D. M., Stirling, J. M., Vogel, V. J. Chem. Soc. Faraday Trans. 1988, 84, 1531-1542.
- (20) Dote, J.L., Barger, W.R., Behroozi, F., Chang, E.L.; Lo, S.L., Montague, C.E., Nagumo, M. *Langmuir* **1990**, *6*, 1017-1023.

#### Chapter 4

- (21) Menger, F.M., Richardson, S. D., Wood, M. G., Sherrod, M. J. *Langmuir* 1989, 5, 833-838.
- (22) Cadenhead, D.A., Muller-Landeau, F., Kellner, B. M. J. *Phase transitions in one and two-component films at the air/water interface*; Cadenhead, D.A., Muller-Landeau, F., Kellner, B. M. J., Ed.; North Holland: New York, 1980, pp 73-81.
- (23) Birdi, K.S. Lipid and Biopolymer Monolayers at Liquid Interfaces; 1 ed.; Plenum Press: New York, 1989.
- (24) Albrecht, O., Gruler, H., Sackmann, E. J. Physique 1978, 39, 301-313.
- (25) Fainerman, V.B., Vollhardt, D., Melzer, V. J. Phys. Chem. 1996, 100, 15478-15482.
- (26) Israelachvili, J. Langmuir 1994, 10, 3774-3781.
- (27) Ruckenstein, E., Li, B. Langmuir 1995, 11, 3510-3515.
- (28) Ruckenstein, E., Li, B. Langmuir 1996, 12, 2308-2315.
- (29) Heitner, T., Berthiaume, G., Tanenbaum, D., Lennox, R. B. Biophys. J. 1998, submitted.
- (30) Marsh, D. CRC Handbook of Lipid Bilayers; CRC Press: Boston, 1990.
- (31) Mantsch, H.H., McElhaney, R. N. Chem. Phys. Lipids 1991, 57, 213-226.
- (32) Levin, I. Vibrational spectroscopy of membrane assemblies; Levin, I., Ed.; Wiley Heyden: New York, 1984; Vol. 11, pp 1-48.

## Chapter 5

# The interaction of protein tyrosine phosphatase SHP-1 with phospholipids: A monolayer and fluorescence resonance energy transfer study

(co-authors: M. J. Pregel, A.C. Storer and R.B.Lennox)

#### Abstract

The Langmuir film-balance technique (LFB) was used to investigate the interaction of the protein tyrosine phosphatase SHP-1 with monolayer films of phospholipids at the air/water interface. The interaction of SHP-1 with liposomes was also monitored by fluorescence resonance energy transfer (FRET) experiments in parallel studies. The two techniques offer complementary information; penetration into the monolayer was monitored by the film-balance technique whereas surface association was measured using the fluorescence transfer experiments. A two-step model is proposed to describe the interaction of SHP-1 with membranes where weak association mediated by electrostatic interactions with the lipid headgroup is followed by penetration of the protein into the membrane or monolayer. The fluorescence experiments show that SHP-1 associates rapidly with liposomes with a preference for anionic phospholipids. LFB experiments show that the phosphatase insertion is a very slow (non-diffusion) limited process which is first order in associated (SHP-1-lipid) complex. Association rates were found to be greater at anionic phospholipid monolayers compared to zwitterionic lipid monolayers, but ultimately the extent of penetration was found to be headgroup independent. Increasing lipid surface density results in greater penetration rate constants, kobs, while at the same time limits the amount of protein which can be accommodated in the monolayer. High surface densities inhibit penetration by presenting a greater barrier but the rate at which the limited penetration is reached increases perhaps due to increase surface charge density at the interface. This demonstrates that despite the affinity of the protein for the lipid interface, the lipid presents a barrier to penetration. This is discussed in terms of discrepancies found between kinetics obtained for SHP-1 penetration into lipid monolayers in the constant area mode and in the surface expansion mode.

# 5.1. Introduction

Protein tyrosine phosphatases (PTPases) associate with cell-surface receptors involved in cell signaling processes which control the growth process. These receptors, called protein kinases, are activated through autophosphorylation and control processes such as cell growth, proliferation, differentiation and locomotion in addition to the proliferation of abnormal cancer cells. Protein phosphatases reverse the action of protein kinases by hydrolyzing phosphotyrosyl residues, resulting in deactivation of protein kinases and inhibition of the cell proliferation processes. This dephosphorylation, controlled by PTPases, has been considered as a modulator of tyrosine kinase receptor signaling, PTPases are thus of considerable pharmaceutical interest given their important role in the kinase signaling pathway.

Protein tyrosine phosphatases are a family of enzymes related by their function in the transfer of phosphate groups from phosphorylated receptor-bound kinases. SHP-1 (also known as HCP, SH-PTP1, and PTP1C) is a cytosolic PTPase associated with the EGF (epidermal growth factor) receptor. It is a non-transmembrane tyrosine phosphatase involved in signaling processes which regulate erythropoiesis,<sup>2</sup> T- and B-cell response,<sup>3,4</sup> and the function of natural killer cells.<sup>5</sup>

In vitro studies have demonstrated that SHP-1 phosphatase activity is influenced by bilayer membranes (liposomes) and that the nature of the effect varies with the phospholipid headgroup. Liposomes composed of anionic phospholipids increased SHP-1 activity by > 1000-fold towards some protein substrates such as myelin basic protein but reduced it towards another protein, phosphopeptide, and low-molecular-weight substrates. The effect was ascribed to binding of both the enzyme and some substrates to liposomes leading to co-localization at the membrane.

There are several indications that the anionic lipid, phosphatidic acid (PA), might be a physiological modulator of SHP-1 activity.<sup>6</sup> PA was found to enhance receptor

dephosphorylation in intact cell membranes whereas other lipids, including acidic lipids, have no such effect. It was concluded that treatment with PA enhances SHP-1 negative control of the EGF receptor. This enhancement is apparently due to the promotion of SHP-1 association with autophosphorylated EGF receptor by PA. One outstanding question concerns the possibility of that specific interactions between SHP-1 and PA lead to this promotion process. This question motivated us to directly investigate the kinetics of SHP-1 association with lipid membranes and addresses the possibility that protein-membrane association occurs in the absence of any specific receptor sites.

The interaction of proteins with lipid interfaces has been studied by a number of methods, including <sup>2</sup>H-NMR and <sup>31</sup>P-NMR, <sup>7</sup> fluorescence polarization<sup>8</sup> and fluorescence energy transfer, <sup>9,10</sup> differential scanning calorimetry, <sup>11</sup> light scattering techniques, <sup>12</sup> ellipsometry, <sup>13</sup> electron microscopy, <sup>14</sup> and surface plasmon resonance (SPR) spectroscopy, <sup>15</sup> and the lipid monolayer technique. <sup>14,16-23</sup>

In the monolayer, or Langmuir film balance (LFB) experiment, phospholipid molecules are spread at the air-water interface and are compressed to well-defined surface density values. Lipid monolayers under controlled area or surface pressure serve as a model system for studying lipid-protein interactions at the membrane level. 16,23-26 Both surface pressure and (average) molecular area are variable in experiments using three dimensional dispersions of lipids such as liposomes or whole cells. The LFB experiment permits the study of lipid/protein systems in a controlled manner by monitoring one variable while the other stays fixed. 27 The monolayer film technique has been used in the analysis of the specificity of the interactions between cardiotoxins and phospholipids, 28 snake venom proteins and membranes, 28 and substance P (SP) penetration of lipid monolayers. 19,21,29-31 Molecular details, otherwise inaccessible, are readily available using this technique. For example in the SP system, Scatchard analysis of the penetration reveals biphasic behaviour and has established that the binding of SP to negatively charged surfaces is governed by surface electrostatics. 29 The interaction of serum components

such as high density lipoproteins (HDL) and bovine serum albumin (BSA) with biological interfaces is important and is also readily measured by the LFB. For example, the interaction of BSA with phospholipid monolayers is the foundation of much of our understanding of protein-lipid interactions<sup>27,32,33</sup> and continues to be of interest.<sup>34</sup> The kinetics and mechanism of adsorption of protein to lipid monolayers are infrequently addressed in the literature, but when experimentally possible such an analysis provides new insights into the association process.<sup>35,36</sup>

The spreading of surface active molecules at the air-water interface results in the 'dilution' of the water molecules at the interface and a consequent lowering of the surface tension,  $\gamma_0$ , where  $\gamma_0 = \gamma_{air/buffer}$ . The surface pressure ( $\pi$ ) is defined as  $\pi = \gamma_f - \gamma_0$  where  $\gamma_f$  is the surface tension of the spread monolayer. This "dilution" reduces the strong attractive forces between water molecules from which the large surface tension value of water originates (72 mN/m at 25°C). The extent of surface tension reduction is directly related to the surface concentration of the surfactants forming the monolayer. The versatility of the LFB experiment allows one to study how the surface pressure, the subphase concentration, and the chemical composition of the lipid monolayer individually affect the adsorption of a proteins through changes in surface properties. The SHP-1 adsorption kinetics presented here were measured in both the constant surface area and surface expansion modes. Differences between the kinetics obtained uncovers a fundamental difference in the processes occurring which, to our knowledge, have not been addressed.

In parallel experiments, fluorescence resonance energy transfer (FRET) was used to characterize the interaction of SHP-1 with small unilammelar vesicles (liposomes) composed of egg-phosphatidic acid (PA), egg-phosphatidylcholine (PC) and the fluorescent dye dansyl-DHPE (N-(5-dimethylamino-naphthalene-1-sulfonyl)-1,2-dihexadecanoyl-sn-glycero-3-phospho-ethanolamine triethylammonium salt).<sup>37</sup> Energy transfer from the protein to the probe is dependent upon the proximity of the protein to the

probe<sup>10</sup> and thus is a sensitive marker of protein (i.e. SHP-1) association with the membrane.

This study focuses on the adsorption of SHP-1 onto lipid monolayers. It is found to be controlled by several factors. Of greatest significance and relevance to the PTPase issue is the dependence of the penetration kinetics of SHP-1 upon the ionic character of the lipid headgroup. The influence of lipid surface density is also investigated and is shown to affect the extent of penetration of SHP-1. The extent of penetration, measured as a change in surface pressure ( $\Delta \pi$ ), decreases non-linearly with increasing initial surface pressure ( $\pi$ ) unlike other systems which show a linear relationship.  $^{16,26,38,39}$  A well defined maximum  $\pi$  value is observed above which protein penetration is no longer observable. The separate kinetic regimes accessed through the FRET and LFB experiments have permitted the assignment of a two-step kinetic model for the adsorption process in the constant surface area mode.

#### 5.2. Materials and Methods

#### 5.21. Fluorescence Transfer Experiments

Vesicles composed of egg-PA (Sigma, St. Louis) and egg-PC (Avanti Polar Lipids, Alabaster, AL) containing dansyl-labeled phospholipid (dansyl DHPE, Molecular Probes, Eugene, OR) were titrated with PTPase (SHP-1 70 kD). An increase in fluorescence intensity due to resonance energy transfer from the protein to the labeled phospholipid is a means of monitoring the formation of a protein-lipid complex.

Vesicles were prepared as follows. Chloroform solutions of egg-PA and dansyl DHPE were added to a glass vial, the CHCl<sub>3</sub> was removed under vacuum, and the residual lipid was hydrated with 5 mL of filtered, degassed buffer. The lipids were suspended by stirring, then bath sonicated in ice water for 20 min, resulting in an opalescent solution. This was allowed to stand (on ice in the dark) for at least one hour before use. The resulting SUV working solution contains 134  $\mu$ g/mL egg-PA or egg-PC and 9.4  $\mu$ M dansyl DHPE. For fluorescence transfer experiments, the buffer was 50 mM HEPES/NaOH, pH 7.4, I = 0.15 M (NaCl). In both cases, the SUV working solution was diluted with the corresponding buffer.

Fluorescence experiments were performed on a SPEX Fluorolog 1681 ().22m spectrometer with excitation at 280 nm, emission at 520 nm, and slits set at 1 mm. Final concentrations of 10µg/mL egg-PA or egg-PC and 0.7 µM dansyl DHPE were used.

#### 5.22. Monolayer Experiments

### (a) Materials

Lipid solutions were prepared in HPLC grade chloroform (BDH) to a final concentration of ~2 mg/mL. Egg-phosphatidic acid and egg-phosphatidylserine were purchased from Sigma and egg-phosphatidylcholine (PC), phosphatidylethanolamine (PE), and phosphatidylglycerol (PG) were purchased from Avanti. Buffers used for the subphase were prepared containing 20 mM HEPES (Sigma), 142 mM NaCl, 1 mM EDTA

(Sigma) and 1 mM dithiothreitol (DTT) (Sigma). Water was purified using a Millipore Milli-Q water purification system. Protein was purified and concentrations were determined using previously described methods<sup>40</sup>. Enzyme samples were stored under N<sub>2</sub> (4 °C) and were treated with DTT (1 mM) 6-24 hours prior to use.

#### (b) Methods

Lipid monolayers were spread from an organic solution in a dropwise fashion onto a buffered subphase (250 mL). 25 μL of stock lipid solution, deposited in small drops (≤ 0.5 μl) were incrementally deposited on the surface by touching the liquid surface with the tip of a Hamilton syringe. In each experiment ~10 μg of lipid was deposited and allowed to stand for 20 min. Monolayers were adjusted to the desired surface pressure with the aid of the movable barrier. The subphase was stirred continuously with a magnetic stir bar. Prior to protein injection the stability of the monolayer was monitored for 10-15 minutes. During this period no change in surface pressure or barrier movement was observed. The desired amount of protein solution was injected under the subphase to yield the final concentrations listed. Immediately after protein injection kinetic data acquisition was manually initiated and data collected through computer control using the KSV software.

The subphase temperature was maintained at 25 °C for all experiments using a circulating bath and surface pressure was measured using a Wilhelmy plate (platinum plate, roughened by scouring with emery paper) suspended from a torsion balance by a thread and 2" platinum wire. A constant lateral surface pressure was maintained by the use of a computer-controlled feedback system (KSV software) which controlled the position of the barrier.

#### (i) Constant Surface Area Method

The surface pressure was adjusted to the appropriate initial surface pressure  $(\pi_i)$  with the aid of the moveable barrier. The lipid monolayer was held at  $\pi_i$  until a constant barrier position was maintained. Barrier control was then terminated and the barrier position was held constant so that surface area remained constant during the experiment. Protein was injected into a stirred subphase after at least 15 minutes of monolayer stability was confirmed by the absence of change in the surface pressure,  $\pi_i$ .

Concentration dependence. The concentration dependence of SHP-1 binding to egg-PA monolayers was determined by the constant surface area mode at initial surface pressures of 20 mN/m and SHP-1 subphase concentrations of 0.9 nM, 1.8 nM, 3.6 nM, 7.1 nM and 17.1 nM.

Lipid Specificity. An initial surface pressure of 20 mN/m and a SHP-1 subphase concentration of 3.6 nM was used in each case.

Penetration capacity: effect of initial surface pressure ( $\pi_i$ ). To demonstrate the influence of the initial surface pressure on the association kinetics of SHP-1 the initial surface pressure of the egg-PA monolayer was varied (15 mN, 20 mN, 25 mN, 30 mN) while the subphase concentration of SHP-1 was held constant at 3.6 nM.

Surface activity of SHP-1 at the air/water interface before and after denaturation.

The increase in surface pressure at a clean air/water interface ( $\pi_i$ =0 mN/m) was determined at an SHP-1 subphase concentration of 11 nM. In order to assess the relevance of tertiary protein structure in the surface activity the increase in surface pressure at a clean air/water interface was measured for a 200 µg sample of SHP-1 which had been subjected to denaturing conditions (heating (80°C, 60 s) and sonication (30 s).

#### (ii) Surface Expansion Method

After evaporation of the spreading solvent, lipid monolayers were compressed to 20 mN/m and maintained throughout the experiment at that  $\pi$  using the movable barrier.

An expansion of the surface area is therefore an indication of changes in the monolayer. When proteins are involved the surface area expansion is assumed to be directly proportional to the amount of protein incorporated into the membrane.

Concentration dependence. The concentration dependence of SHP-1 association with egg-phosphatidic acid (egg-PA) monolayers was measured at subphase concentrations of 0.88 nM, 1.92 nM and 2.68 nM.

Lipid Specificity. Changing the headgroup of the lipid used in forming the monolayer allowed us to study lipid specificity in the SHP-1 association process. All experiments were conducted using a PTPase subphase concentration of 3.5 nM.

#### (c) Data Analysis

Values of surface concentration ( $\Gamma$ ) were calculated in both the surface expansion method and the constant surface area methods. The surface expansion technique allows for the direct calculation of the surface concentration ( $\Gamma$ ), provided the size of the penetrating species is known. Since the film area is directly proportional to the number of molecules incorporated into the monolayer the surface area corresponding to the cross-sectional area occupied by the protein in the monolayer can be estimated by assuming a spherical shape for the protein in solution. From light scattering measurements the radius of the protein in such a conformation was estimated to be 40 Å. The crossectional area is thus estimated as 5024 Å<sup>2</sup>. Using this value for A,  $\Gamma$  can be calculated for the surface expansion method using Equation 5.1, where

$$\Gamma = \frac{\text{barrier movement (mm) x width of barrier (mm) x (10}^{7} \text{Å/mm})^{2}}{(5024 \text{ Å}^{2} \text{ x N}_{0} \text{ x trough area (cm}^{2}))}$$
(5.1)

( $\Gamma$  is the surface concentration of adsorbed species in mol/cm<sup>2</sup>. The dimensions of the lipid monolayer are 100 mm by 150 mm (area = 150 cm<sup>2</sup>), N<sub>0</sub> = 6.02 x 10<sup>23</sup>.) The relationship between surface area increase and protein surface concentration has been discussed previously.<sup>29</sup>

In the absence of any barrier to penetration, protein adsorption can be described by

$$\Gamma = 2C_h(Dt/\pi)^{1/2} \tag{5.2}$$

where  $C_b$  is the bulk concentration of the adsorbing species and D is its diffusion coefficient. If the process is irreversible then this equation is expected to hold only for the initial stages of the process. A2,43 An expression which takes into account the desorption of the protein from the interface, which becomes important at later stages in the penetration kinetics, has also been derived. A model which takes into account both diffusional factors and interactive processes is evaluated for the SHP-1 system. The experimental data was fitted to equation 5.2, which predicts a linear relationship between  $t^{1/2}$  and  $\Gamma$  if the kinetics are diffusion controlled, to evaluate the extent to which diffusion through the bulk phase can account for the observed adsorption kinetics of the protein.

In the constant area mode, the area occupied by the lipid changes (decreases) as the protein inserts into the monolayer. If the change in area per lipid is multiplied over the entire monolayer, the total area change is proportional to the amount of protein inserting. The constant area mode experiment involves monitoring changes in  $\pi$ , so this area change must be derived from the surface pressure change. With a known amount of lipid at the surface  $(L_t)$ , the area change  $(\Delta A_{total})$ , for a given increase in surface pressure  $\Delta \pi$ , was determined by dividing  $\Delta \pi$  by the rate of area change, v, and multiplying this by L<sub>t</sub>.  $\Delta A_{total}$  was converted into a surface concentration as per the surface expansion method.<sup>29</sup> The rate of area change with surface pressure (v) was interpolated from the monolayer isotherm of egg-PA between the surface pressures of 20 and 35 mN/m by taking the slope of the isotherm between these two surface pressures (Appendix II, Figure AII.1). These  $\pi$  values were chosen since the experiments described in the present study involve surface pressure changes within this range. The value (v), which is analogous to the dilational modulus of the monolayer (E), was found to be 0.88 mN·molecule/(m·Å<sup>2</sup>). This approach to determine the surface concentration in the absence of direct surface concentration determination has been previously described. 39,46

#### 5.3. Results

#### 5.31. Fluorescence Resonance Energy Transfer Experiments (FRET)

The interaction between SHP-1 and egg-PA and egg-PC vesicles which contain dansyl fluorescent probes was evaluated at varying bulk concentrations of SHP-1 (Figure 5.1). The time required to reach steady-state levels is too short (~seconds) for the kinetics to be accurately analyzed. The steady-state concentration dependence can, however, be analyzed. A least-squares fit of the adsorption isotherm (Figure 5.1.) to a Langmuir adsorption isotherm (Equation 5.3), yields a K<sub>D</sub>assoc of 20 nM for egg-PA vesicles and a K<sub>D</sub>assoc of 4 nM for egg-PC vesicles where

$$%F = (F_{\text{max}}/Q)[SHP-1]/K_D+[SHP-1])$$
 (5.3)

%F is the ratio of fluorescence signal obtained after addition of protein (F) to the initial fluorescence ( $F_0$ ) due to dansyl-DHPE. The  $F_{max}/Q$  values obtained are  $77\pm4$  nM<sup>-1</sup> and  $46\pm5$  nM<sup>-1</sup> for egg-PA and egg-PC respectively. Q is the quantum efficiency of the fluorescence signal. Although it is unknown, it can be assumed that Q for the two systems studied is the same and thus a comparison between values is valid. The preference of SHP-1 for the anionic lipid vesicles is supported by these results. The FRET experiments are highly sensitive to variations in sample preparation however. Different protein preparations and liposome solutions will yield different results. Since care was taken to prepare liposome samples consistently and the same protein sample was used for both lipids studied, comparison of these results is believed to be valid.

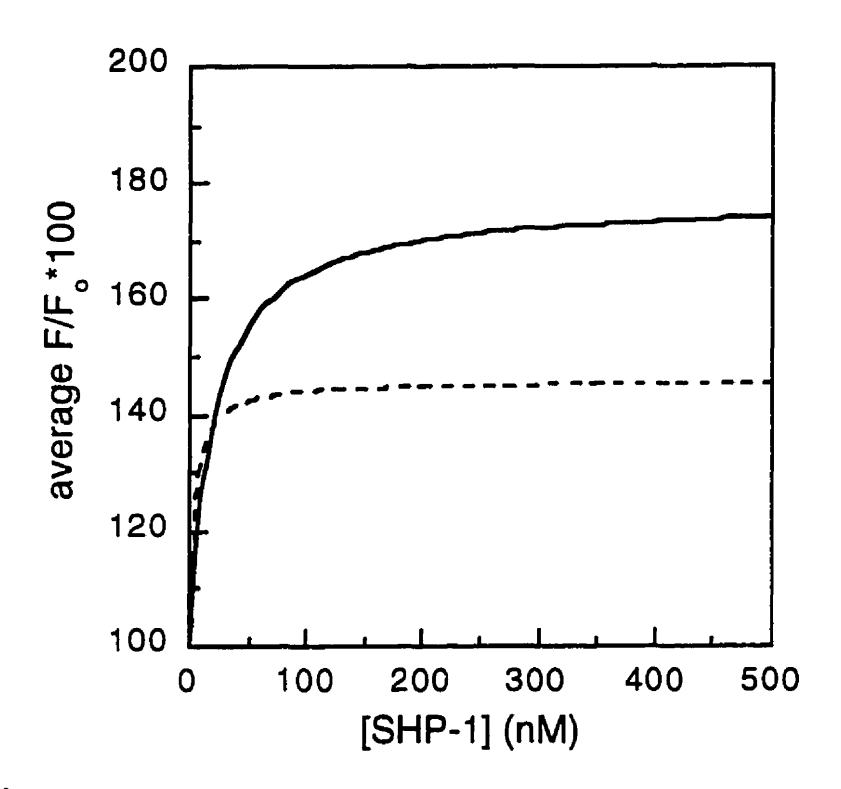


Figure 5.1. Fluorescence transfer between tryptophan residues and dansyl-DHPE lipid probe at egg-PA (\_\_\_\_\_\_) and egg-PC (\_\_\_\_\_\_) vesicles containing 1% lipid probe.

#### 5.32. Monolayer Experiments

The response measured in the LFB technique<sup>a</sup> requires hydrophobic interactions between protein and lipid and therefore can be attributed solely to penetrating protein. It has been shown that proteins which are known to associate electrostatically to lipid interfaces (such as phospholipase A<sub>2</sub>),<sup>47-49</sup> do not produce any change in the surface pressure at constant area. Demel also showed that electrostatic association of proteins to lipid monolayers does not produce a change in the surface pressure.<sup>50</sup> Thus, it is accepted that the increase in surface pressure (or the expansion of the film at constant ) which results from the addition of protein to the aqueous subphase, in either the constant surface

<sup>&</sup>lt;sup>a</sup> Response measured in the LFB experiment is surface pressure increase in the constant surface area mode and barrier movement in the constant surface area mode.

area or surface expansion techniques, results from the penetration of protein into the monolayer assembled at the air/water interface. 25,32

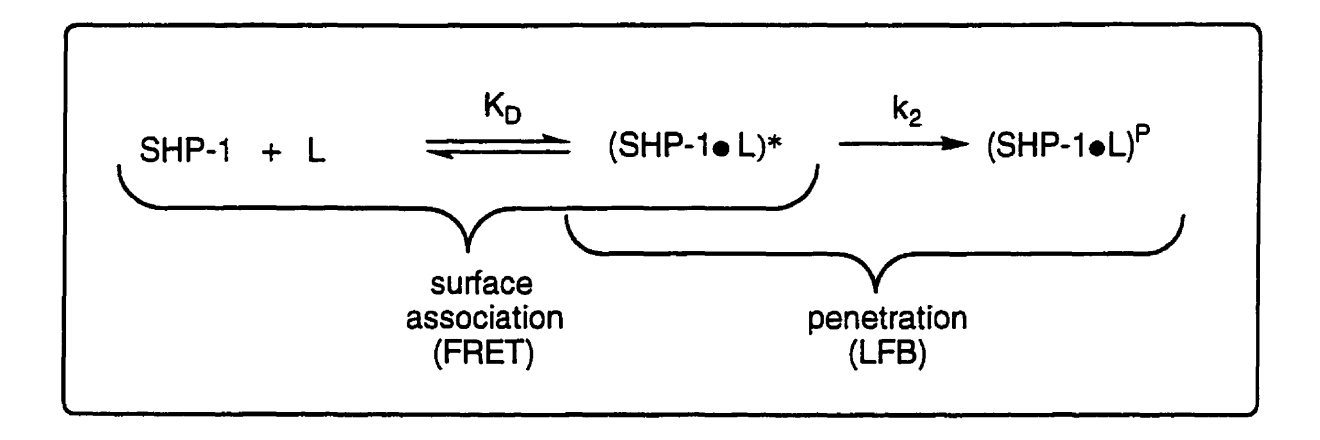


Figure 5.2. Proposed model depicting the interaction mechanism of SHP-1 with lipid assemblies where (SHP-1·L)\* is the loosely associated surface complex, (SHP-1·L)P is the penetration complex and [L] is the lipid surface concentration.

#### (i) Penetration Kinetics Obtained in the Constant Surface Area Mode

Penetration kinetics obtained at varying subphase concentration of SHP-1

The adsorption of SHP-1 to a lipid monolayer can be described by the scheme shown above in Figure 5.2, where:

$$\begin{split} \frac{d[(SHP-1\cdot L)^{P}]}{dt} &= k_{2} \left[ (SHP-1\cdot L)^{*} \right] \\ &= K_{D}^{assoc} = \underbrace{[(SHP-1\cdot L)^{*}]}_{[SHP-1][L]} \\ &= [(SHP-1.L)^{*}] = K_{D} \left[ (SHP-1) \right] [L] \\ \\ \frac{d[SHP-1\cdot L]^{P}}{dt} &= k_{2} K_{D} \left[ (SHP-1) \right] [L] = k_{obs} \cdot [L] \end{split}$$

The rate constant for penetration ( $k_{obs}$ ) is obtained from a first-order least-squares fit of the curves  $\pi$ -t curves (Figure 5.3 (a), Table 5.1). In the constant surface area experiment where lipid surface density is held constant,  $k_{obs} = k_2 K_D$  [SHP-1] and a plot of  $k_{obs}$  vs [SHP-1] yields a line of slope 2.4 x 10<sup>-4</sup> s<sup>-1</sup> nM<sup>-1</sup> which is equal to  $k_2$  K<sub>D</sub>.

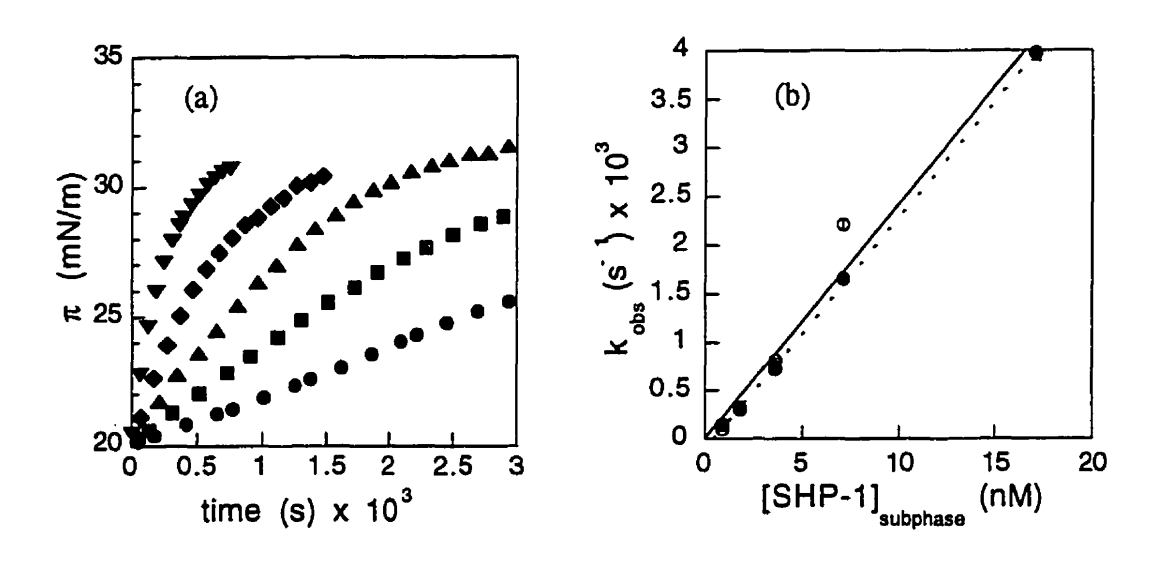


Figure 5.3. (a) representative results of surface pressure  $(\pi)$  as a function of the final bulk substrate concentration of SHP-1 with stirring at an egg-PA / buffer interface spread to an initial film pressure of 20 mN/m . 0.9 nM  $(\bullet)$ , 1.8 nM( $\blacksquare$ ), 3.6 nM  $(\triangle)$ , 7.1 nM  $(\diamondsuit)$ , 17.8 nM  $(\blacktriangledown)$ . (b) observed rate constants obtained from a first order fit of the data shown in (a)

Table 5.1. Observed rate constants (k<sub>obs</sub>) obtained from a first-order least squares iterative fit of the data to an infinity value where,

 $\pi_t = \pi_i + \Delta \pi (1 - e^{-Kobs})^a$ 

70 - 70 - 70 - 70 - 70 - 70 - 70 - 70 -						
[SHP-1] (nM)	k <sub>Obs</sub> (s <sup>-1</sup> x 10 <sup>3</sup> )	$\pi_{ss}^b$ (± 4 mN/m)	Rc			
0.9	0.09	39	0.99909			
0.9	0.14	37	0.99976			
1.8	0.32	35	0.99956			
1.8	0.30	36	0.99983			
3.6	0.81	33	0.99951			
3.6	0.72	33	0.99910			
7.1	2.21	31	0.99970			
7.1	1.66	32	0.99952			
17.1	3.98	32	0.99959			

<sup>&</sup>lt;sup>a</sup>  $\pi_t$ -surface pressure at time, t.  $\pi_i$ -initial surface pressure,  $\Delta \pi = \pi_{ss} - \pi_i$ , t - time.

As a control, the surface activity of a thermally denatured SHP-1 sample was investigated. Surface pressure changes were undetected at both an egg-PA monolayer and at an air/buffer interface for the denatured protein. This highlights the importance of the tertiary protein structure in the surface activity of a protein and penetration of the protein at interfaces.

### Dependence of the penetration kinetics upon the monolayer lipid composition

The charge of the lipid headgroup influences the rate of penetration of SHP-1 into the monolayer. Lipids possessing a negatively-charged headgroup demonstrate enhanced rates of penetration as compared to zwitterionic lipids (Table 5.2). Negatively charged lipids (egg-PA, egg-PG, and egg-PS) experience similar rates of SHP-1 penetration, while at the same subphase protein concentration zwitterionic lipids (egg-PC and egg-PE) experience measurably lower rates of penetration (Fig. 5.4 (a)). These results support an electrostatically-facilitated association/penetration mechanism. The  $\pi_{SS}$  values appear to be

b values are reported as an average of two experiments

c correlation coefficient derived from the least squares fit of penetration kinetics to a first order process

# Chapter 5

independent of the lipid headgroup charge, as within experimental error, these values are equivalent (Table 5.2 ). The headgroup charge therefore does not affect the extent of penetration but solely affects the rate at which the steady-state value is reached. In this experiment both lipid surface density and [SHP] are held constant such that ,  $k_{\text{Obs}} = k_2$   $K_D$ .

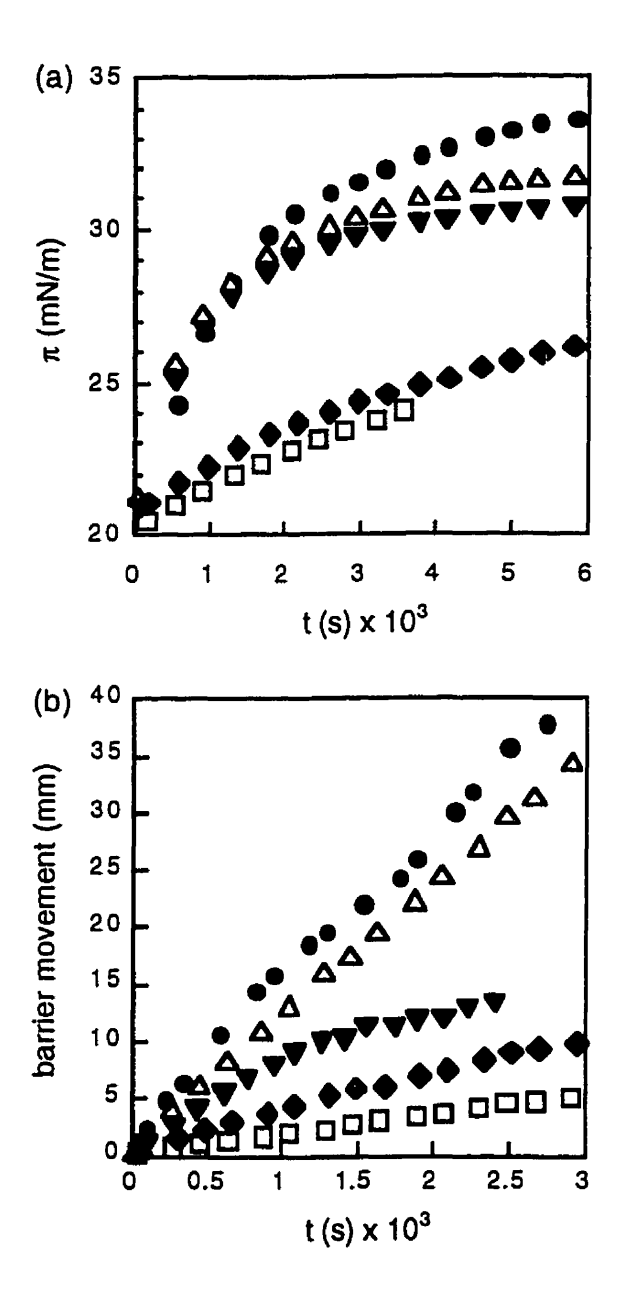


Figure 5.4.(a) Representative kinetics obtained in the constant surface area mode of SHP-1 (3.58 nM bulk concentration) at the lipid/buffer interface where monolayers were spread to an initial surface pressure  $(\pi_i)$  of 20 mN/m.(b) kinetics obtained in the surface expansion mode at 20 mN/m 35°C and [SHP-1]<sub>subphase</sub> of 3.44 nM. egg-PA ( • ), egg-PG (  $\Delta$  ), egg-PS (  $\nabla$  ), egg-PE ( • ) and egg-PC (  $\square$  ).

Table 5.2. Dependence of observed rate of penetration on the lipid headgroup chemical structure at [SHP-1]<sub>subphase</sub> (3.44 nM)

headgro up	k <sub>obs</sub> (s <sup>-1</sup> x 10 <sup>3</sup> ) <sup>a</sup>	$\pi_{\rm ss}$ (± 4 mN/m) <sup>2</sup>	R
PA	0.62	34	0.9965
PG	0.86	32	0.9942
PS	0.92	31	0.9962
PE	0.22	28	0.9989
PC PC	0.17	30	0.9993

<sup>&</sup>lt;sup>a</sup> obtained from a first order least-squares iterative fit of the kinetics to an infinity value (see Table 5.1).

It is necessary to use lipid preparations possessing a mixture of acyl chains (such as egg-PA) for this study instead of pure lipids such as dipalmitoylphosphatidic acid (DPPA) so that the results do not reflect differences in lipid phases such as packing and domain boundary effects. Pure lipids such as DPPA possess well-defined phase transitions and their monolayer isotherms reflect the thermodynamic state of the lipid at the given temperature. At a given temperature and surface pressure, pure lipids with widely-different phase transition temperatures usually have very different molecular areas and packing densities. Egg-PA, on the other hand, consists of lipids with the phosphatidic acid headgroup and a mixture of chain lengths and degrees of unsaturation. The presence of acyl chain heterogeneity imparts a fluidity to the monolayer such that all monolayers, regardless of the specific headgroup composition exhibit expanded isotherms at the temperature of interest. The differences between isotherms of such lipids are small, so differences in lipid packing and the effect of domain formation are negligible.

The effect of surface packing upon the penetration kinetics of SHP-1 into egg-PA monolayers

Both the rate constant ( $k_{obs}$ ) and the extent of penetration ( $\Delta \pi$ ) of SHP-1 into egg-PA monolayers are dependent upon the initial lipid surface packing  $(\pi_i)$  or lipid surface density (ρ). ρ values were taken from the isotherm of egg-PA (Appendix II, Figure AII.1) as 1/A at the appropriate surface pressure. The steady-state level ( $\pi_{ss}$ ) exhibits lipid surface packing independence within experimental error (Figure 5.5 (a), Table 5.3).  $\pi_{ss}$  was assigned the value 33 mN/m as the average saturation value obtained from a first-order least-squares fit of the data (Table 5.3). The  $\Delta\pi$  values decrease with increasing initial film pressure, as previously observed for other proteins penetration studies. 16,17,51 In contrast to literature reports this occurs in a non-linear fashion (Figure 5.5 (b)). An optimum initial surface pressure ( $\pi_{\text{optimum}}$ ) is speculated from the non-linear nature of the relationship as being the condition at which protein association and penetration processes are balanced. Extrapolation to  $\Delta \pi = 0$  yields the threshold level above which penetration cannot take place  $(\pi_{max})$ . This value is approximately 32 mN/m. This cut-off value is of interest since others<sup>36,50</sup> have estimated the surface pressure of erythrocyte membranes to be between 30 and 35 mN/m. In this experiment the lipid surface concentration, [L], is varied while [SHP-1] concentrations are constant, therefore  $k_{obs} = k_2 K_D [L]$ .  $k_{obs}$  values increase slightly with increasing surface density (Table 5.3), as predicted by this relationship, indicating that although the extent of penetration becomes limited, the rate at which a steady-state level is reached is enhanced by greater lipid packing.

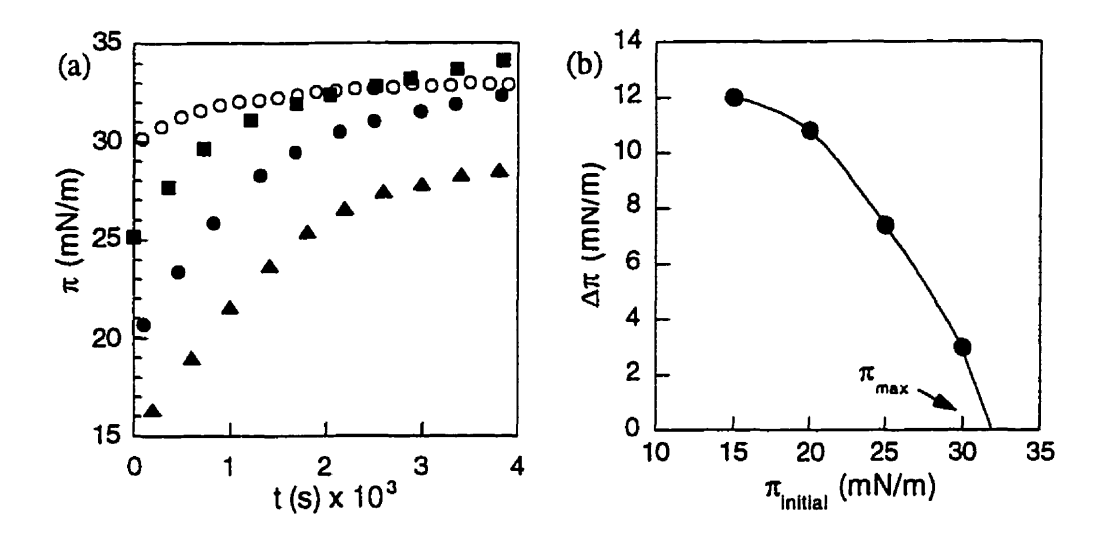


Figure 5.5.(a) interaction of SHP-1 (3.6 nM bulk concentration) at the egg-PA/buffer interface where films were spread to initial surface pressures of 15 mN/m ( $\triangle$ ), 20 mN/m ( $\bigcirc$ ), 25 mN/m ( $\bigcirc$ ) and 30 mN/m ( $\bigcirc$ ) (b) effect of initial surface pressure on the extent of protein penetration into films of egg-PA at the lipid/buffer interface.  $\triangle \pi$  values were taken from curves shown in (a).

Table 5.3. Penetration rate constants and saturation levels ( $\pi_{ss}$ ) of SHP-1 into egg-PA monolayers at different initial surface pressures

π <sub>i</sub> expt (mN/m)	π <sub>i</sub> fit (mN/m) <sup>a</sup>	ρ (molecules/Å <sup>2</sup> )	k <sub>obs</sub> (s <sup>-1</sup> x 10 <sup>3</sup> ) <sup>2</sup>	π <sub>SS</sub> (± 4 mN/m) <sup>b</sup>	Δπ (mN/m) <sup>a</sup>
15	14	0.011	0.7	30	16
20	20	0.012	0.8	33	13
25	25	0.013	0.9	34	9
30	30	0.014	1.1	32	3

a obtained from a first-order iterative least-squares fit of the kinetics to an infinity value (see Table 5.2.)

 $b \pi_{ss} = \pi_i^{fit} + \Delta \pi$ 

#### Chapter 5

## (ii) Penetration kinetics obtained in the surface expansion mode

The penetration kinetics obtained by the surface expansion mode yield results complementary to those obtained via the constant surface area mode. The dependence of the kinetics on subphase protein concentration is shown in Figure 5.6. Unlike the data obtained via the constant surface area mode the surface expansion method does not yield data which can be fitted to a first order process. These results uncover a fundamental difference between the kinetics obtained by the two modes of measurement. To our knowledge such a difference has not been previously addressed in the literature. A direct comparison of the penetration kinetics obtained in the two modes (at 0.9 nM and 0.88 nM SHP-1 respectively) is shown in Figure 5.7. The response has been translated into units of surface concentration ( $\Gamma$ ) to permit comparison. The comparison is believed to be valid since the assumption of surface area occupied by the protein is the same in both measurement modes. A greater  $\Gamma$  value is reached in the constant surface area mode than in the surface expansion mode at any given time. Qualitatively the surface expansion data yield the same conclusions concerning the influence of electrostatic attraction on the penetration kinetics. For example, higher rates of film expansion are observed at anionic lipid monolayers than at zwitterionic monolayers (Figure 5.4 (b)).

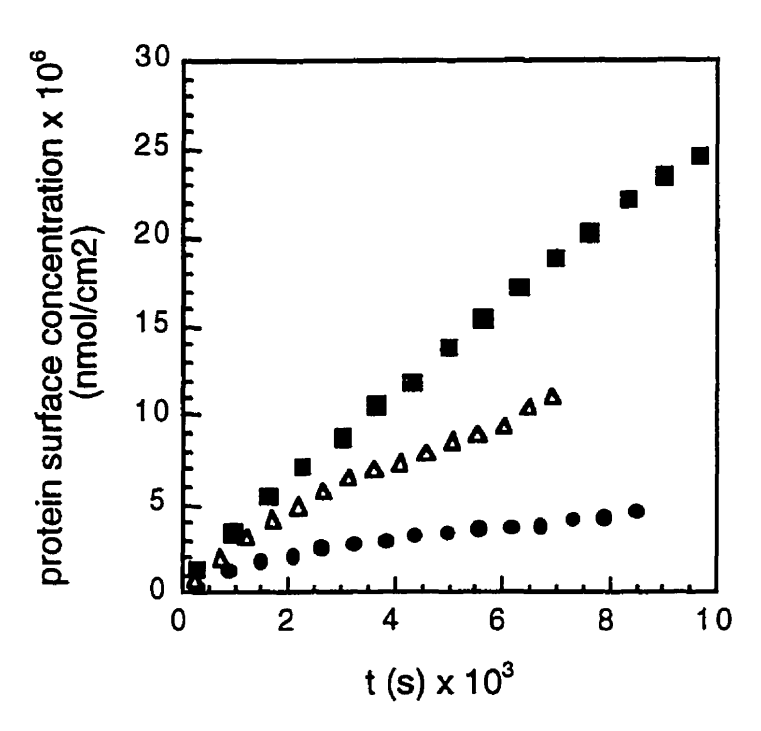


Figure 5.6. Penetration kinetics of SHP-1 into egg-PA monolayers at 20 mN/m, 25°C in the surface expansion mode at subphase concentrations of 0.88 nM ( $\blacksquare$ ), 1.92 nM ( $\Delta$ ), 2.68 nM ( $\blacksquare$ ).

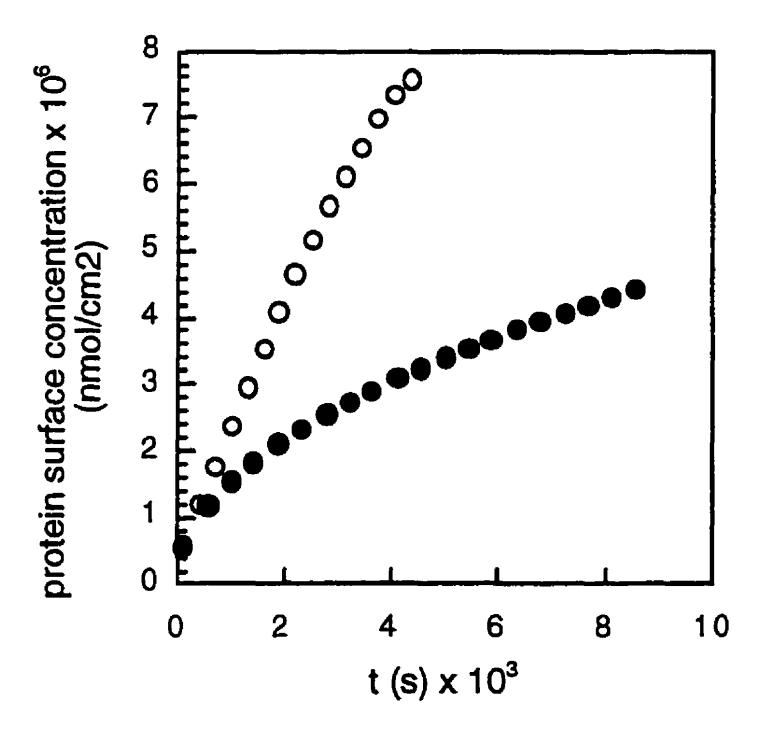


Figure 5.7. Comparison of SHP-1 penetration kinetics obtained in the constant surface area mode (O) with that obtained in the surface expansion mode  $(\bullet)$  at a protein subphase concentration of 0.88 nM.

# (iii) Evaluation of the role of diffusion in the penetration kinetics of SHP-1 at lipid monolayers

Casting the response of the LFB technique into units of  $\Gamma$  also permits the evaluation of the contribution of diffusion to the overall kinetics using Equation 5.2 (Figure 5.8 (a) and (b)). The dependence of the surface concentration,  $\Gamma$ , upon  $t^{1/2}$  is non-linear indicating that at no point along the adsorption isotherm is the process being controlled by diffusion. In addition, the level of protein penetration at a given time is several orders of magnitude lower than predicted by equation 5.2.

In the calculation of surface concentration, it is assumed that the surface pressure increase caused by the protein interaction with the monolayer is identical to a surface pressure increase caused if an equivalent number of lipid molecules occupy the same surface area as the protein. This proportionality is based on a model in which the surface tension measured by the Wilhelmy plate is exclusively due to the lateral compression of the lipid monolayer caused by protein insertion. We also assume that the protein surface area is constant, and that no adsorption of protein to the Wilhelmy plate occurs. The former assumption is necessary in estimating the surface coverage of the protein. The latter may not hold for later stages of the adsorption kinetics.

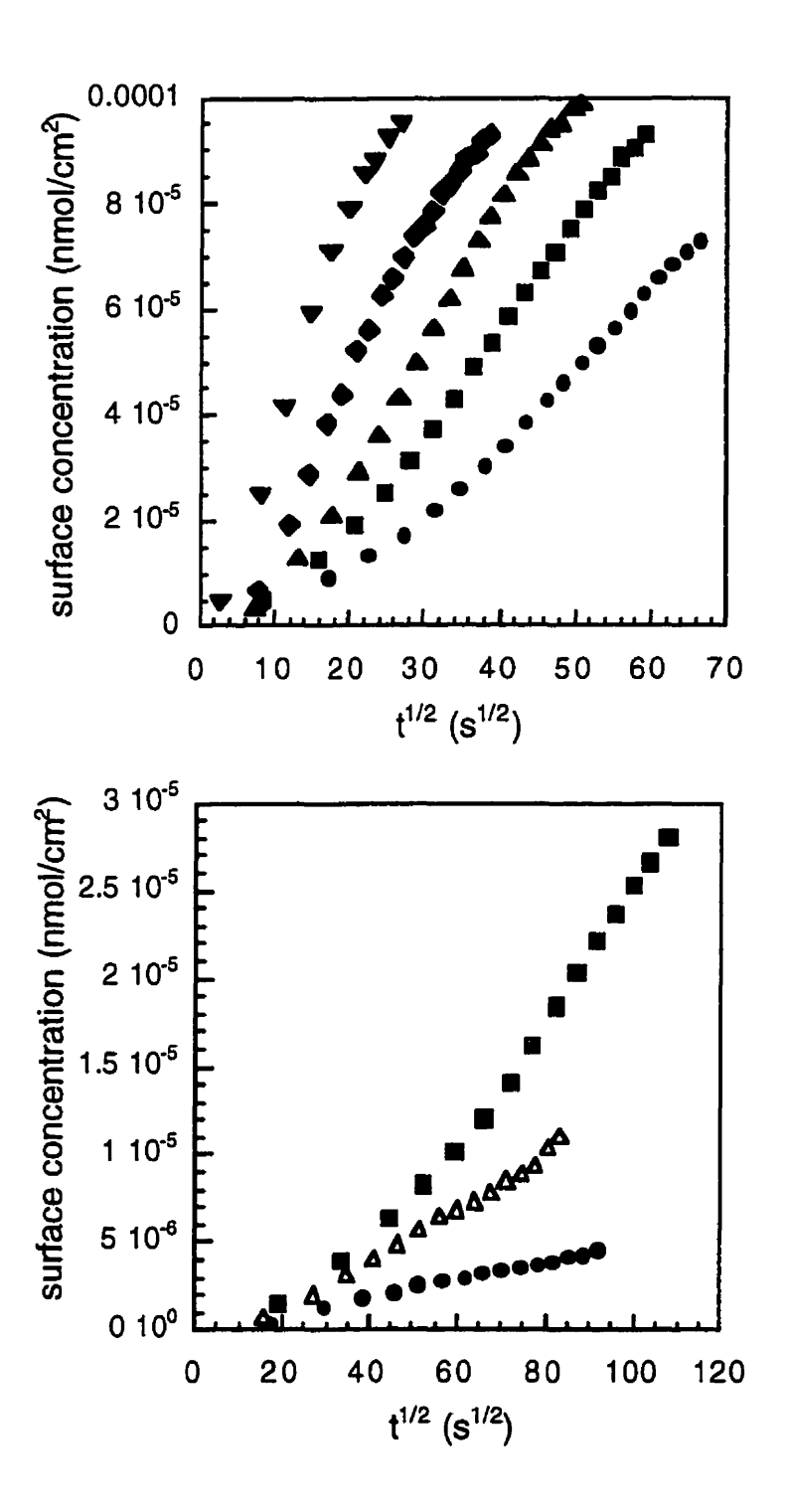


Figure 5.8. Assessment of the role of diffusion in penetration kinetics obtained in (a) the constant surface area mode: 0.9 nM ( $\bullet$ ), 1.8 nM ( $\blacksquare$ ), 3.6 nM ( $\triangle$ ), 7.1 nM ( $\bullet$ ), 17.8 nM ( $\blacktriangledown$ ) and (b) the surface expansion mode: 0.88 nM ( $\triangle$ ), 1.92 nM ( $\bullet$ ), 2.68 nM ( $\blacksquare$ ). Kinetics are taken from Figures 2(a) and 5 respectively. Surface concentrations were calculated assuming a protein radius of 40 Å.<sup>41</sup>

# 5.4. Discussion

# 5.41. Fluorescence Transfer Experiments

Fluorescence transfer between protein tryptophan residues and the dansyl group is confirmed by the detection of emission at 520 nm following addition of SHP-1 to egg-PA and at egg-PC vesicles containing the fluorescent probe dansyl-DHPE (Figure 5.1). The interaction of protein with the lipid vesicles is thus clearly demonstrated. Two important results are obtained from the fluorescence experiments. Firstly, although fluorescence transfer from both surface-associated protein and inserted protein can occur, the time scale of the fluorescence experiment (seconds) can account only for surface association. The attainment of steady state penetration levels requires much longer times (hours) as shown by the LFB technique. Information concerning the association and the penetration of SHP-1 at lipid monolayers can therefore be distinguished using FRET experiments and the monolayer film-balance techniques respectively (Figure 5.3). The type of information which can be extracted from the two techniques differs for the SHP-1/egg-PA system. The steady state fluorescence levels fit a Langmuir isotherm and dissociation constants (K<sub>D</sub>) can be determined (Figure 5.9 (a)). The difference in fluorescence resonance energy transfer between the egg-PA and the egg-PC vesicles confirms the preference of SHP-1 for an anionic interface, where  $K_D(egg-PA) = 5K_D(egg-PC)$ . The dissociation constants are 20  $s^{-1}$   $nM^{-1}$  (egg-PA) and 4  $s^{-1}nM^{-1}$  (egg-PC). The  $K_D$  obtained by this treatment is a measurement of the ratio of free to bound protein.

#### 5.42. Monolayer experiments

#### (a) Analysis of penetration kinetics

The treatment most often found for protein penetration kinetics using the LFB technique is qualitative and it is uncommon to find reports of kinetic data which fit a detailed model. The penetration process has been accounted for by diffusion at its early

stages and by reversible diffusion throughout the observed time frame.<sup>44</sup> A relationship to describe the diffusion of a substance to an interface is used to evaluate the contribution of diffusion in the overall kinetics (Equation 5.2). If such a relationship is applicable then the process in question is said to be diffusion controlled and must involve an irreversible process which possesses no other significant barrier to penetration<sup>52</sup>. These models have been shown to account for penetration kinetics in systems where lipid surface densities were much lower than those used in the present study (*i.e.* lipid films at a very expanded surface state), <sup>16,39,42,43</sup> but do not describe the SHP-1 penetration kinetics presented here.

Other models have also been considered for the analysis of penetration kinetics. The Langmuir isotherm describes the equilibrium adsorption of protein to an air/water interface, but fails to account for the penetration in the presence of an insoluble monolayer where cohesive and repulsive interactions are involved. A Langmuir model involves protein interaction with vacant sites between the lipid molecules at the air/water interface. In this model the lipid reduces the area available for adsorption. The Gibb's adsorption isotherm has also been applied to protein penetration kinetics, 53,54 but does not adequately describe the penetration in most cases due to the requirement of reversible adsorption.

Diffusion does not account for protein adsorption at any stage of the monolayer kinetic profile (Figure 5.8). The non-linearity of the kinetic fits shown in Figure 5.8(a) indicates that Equation 5.2 cannot adequately describe the mechanism of SHP-1 penetration into phospholipid monolayers. It should be emphasized that the true surface concentration data, required for a rigorous analysis of diffusion, is unavailable. The reasonable assumption that there exists a proportionality between surface pressure and surface concentration has been used in this analysis

Monolayer penetration studies are useful for the observation of the interaction of protein with lipid, but the penetration kinetics are difficult to resolve. The penetration occurs on a time scale (minutes) which permits a kinetic analysis and is found to be

consistent with a first-order process. A least squares analysis of the kinetics reveals a constant steady-state level independent of the SHP-1 subphase concentration (Table 5.1). The adsorption isotherm is therefore inaccessible for the penetration kinetics since [SHP-1]<sub>subphase</sub> is in the concentration regime well above the K<sub>D</sub> of penetration (Figure 5.9(b)). This behaviour is rationalized by a low K<sub>D</sub> which is consistent with irreversible protein adsorption.

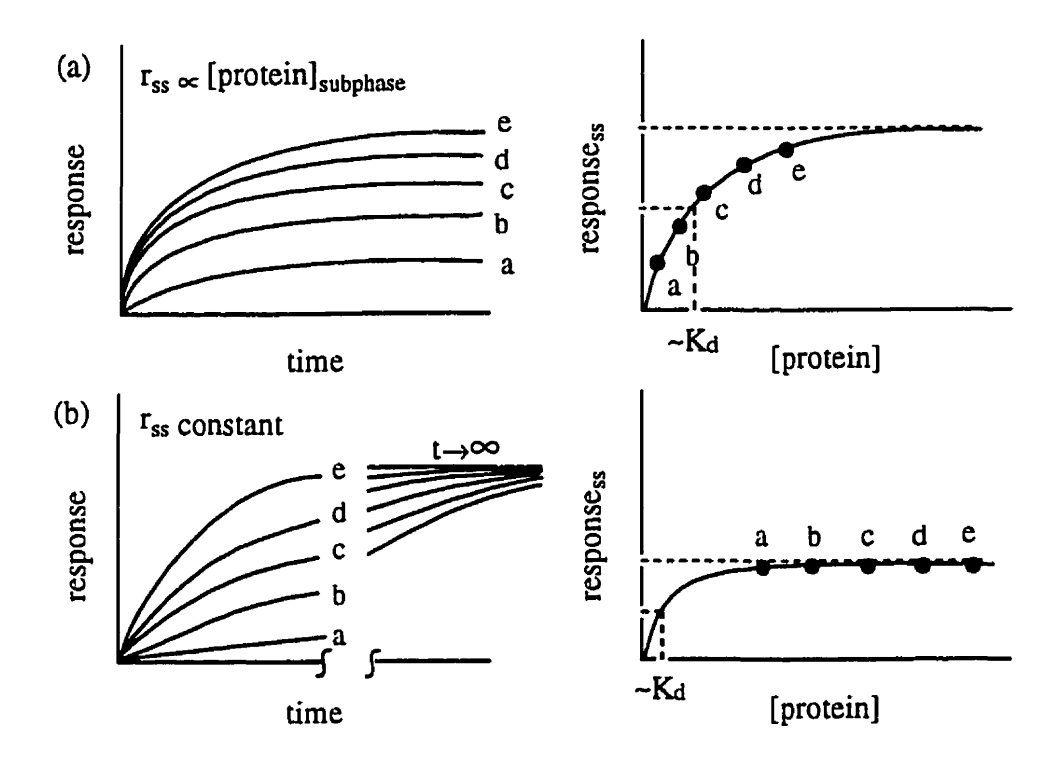


Figure 5.9. Schematic representation of adsorption kinetics and the corresponding adsorption isotherm for (a) [protein]<sub>subphase</sub>  $\approx$  K<sub>d</sub> and (b) [protein]<sub>subphase</sub>  $\approx$  K<sub>d</sub>. SHP-1 penetration kinetics observed by the LFB technique in the constant surface area mode are represented by situation (b). a, b, c, d and e correspond to arbitrary protein subphase concentrations in increasing order. The response corresponds to  $\pi$  in the LFB experiments and to F/F<sub>0</sub>x100 in the FRET experiment.

Recently, Sundaram presented a model which describes the penetration of a lipid monolayer by a surface-active protein taking into account diffusion, penetration and desorption.<sup>45</sup> The dynamics of non-specific adsorption of a surface active protein to a pre-

existing layer of another amphiphile has been studied theoretically and compared with experimental data. This model describes a diffusion-controlled process combined with Frumkin-like non-ideal interactions. The time to reach a certain extent of penetration was calculated and compared to experimental values. At low protein subphase concentration and low lipid surface density the model collapses to a diffusion controlled process. Mixed kinetic/diffusion processes occur at elevated bulk protein concentration and at elevated lipid surface density when either the protein subphase concentration or lipid surface density is increased. The time scale for diffusion is reduced because the width of the diffusion layer (h) tends to zero as the protein concentration increases.

The time scales calculated for the penetration studies reported in the literature  $^{45}$  are much greater than those reported here. The origin of our (relatively) rapid rates can be found in the differences in experimental conditions used in the studies. The type of protein used, the type of lipid used, and most importantly the initial lipid surface concentration used for the penetration kinetics differ in the two cases. The experimental data used to verify the validity of the literature model was collected at a surface concentration ( $\pi_i = 3$ -4 mN/m, 250 Å<sup>2</sup>/molecule) far lower than those used in the present study ( $\pi_i = 20$  mN/m, 85 Å<sup>2</sup>/molecule). In addition, a pure DPPC monolayer, which is likely to exhibit phase heterogeneity at 25°C<sup>55</sup>, was used. Such a monolayer is probably not ideal for penetration studies since domain boundary effects can readily affect adsorption kinetics. The present study uses a heterogeneous lipid preparation (egg-PA) to avoid the influence of domain boundary effects. The lipid surface concentrations used here are also more relevant to those found in biological systems.

Sundaram's kinetic/diffusion model<sup>45</sup> predicts that the rate of adsorption compared to diffusion increases upon decrease of the diffusion layer thickness. This is achievable by an increase in protein subphase concentration and by increasing the lipid surface density. Therefore both the concentration regime and the lipid surface density account for the difference in time scales of the two experiments. The time required to reach 90% of  $\pi_{SS}$  for

a lysozyme/lipid system is 270 min at [lysozyme]<sub>subphase</sub> = 95 nM and lipid surface density  $x_1 = 0.44$ . On the other hand the time to reach 90% of  $\pi_{ss}$  in the SHP-1/egg-PA system is 8 min at  $x_1 = 0.9$ . At a similar lipid surface density ( $x_1 \approx 0.9$ ) the predicted time to reach 90% of  $\pi_{ss}$  for the lysozyme system is 7 min, consistent with the results presented here. The time required to reach equilibrium is expected to be shortened at greater lipid surface concentrations if cohesive lipid-protein interactions are involved. The concurrence between the SHP-1/egg-PA data and the model suggests that Frumkin-like protein-lipid interactions are important.

# (b) Headgroup Specificity

Phospholipid headgroup charge clearly controls the rate of penetration as is evident from both the constant surface area and the surface expansion LFB experiments. Greater rates of penetration are observed for anionic lipids compared to zwitterionic lipids (Table 5.2). The preferred association of proteins with negatively charged lipids has been a frequently reported. 19,25,26,29,56,57

The concurrence of the  $\pi_{SS}$  values between lipid classes (Table 5.2) supports a penetration process controlled by the hydrophobic interaction between the lipid acyl chains and hydrophobic side chains of the protein. Although the rate at which steady-state levels are reached is affected by the electrostatics of the monolayer, the final steady-state association levels in the different monolayers are the same. The independence of  $\pi_{SS}$  upon headgroup structure confirms that k is headgroup independent. If [SHP-1.lipid]\* (surface associated protein-lipid complex) were known k could be determined from the relationship  $k_{Obs}=k[SHP-1.lipid]$ \*. The enhanced rate of penetration at anionic lipid monolayers may result from an increased local concentration of the protein in the diffusion layer caused by electrostatic attraction between the protein and the monolayer. This statement is supported by the fluorescence transfer experiments which demonstrate a greater affinity of SHP-1 for anionic lipid vesicles. Assuming that k is independent of surface charge, the decreased  $k_{Obs}$ 

observed at zwitterionic monolayers can be rationalized by a decrease in [SHP-1·lipid]\*. Factoring out the surface concentration would yield a constant k. This behaviour supports a penetration mechanism in which electrostatics drive the initial protein-surface association required for penetration to ultimately occur. The fact that SHP-1 penetrates zwitterionic monolayers establishes that hydrophobic interactions are substantial in both the presence or absence of favorable surface electrostatics (Figure 5.4).

#### (c) Influence of Phospholipid Packing Density on Penetration of SHP-1

The x intercept of the  $\Delta\pi$  vs  $\pi_i$  curve (Figure 5.5 (b)) yields a  $\pi_{max}$  value (32 mN/m) which is equal to the average  $\pi_{ss}$  value obtained from the first order fit of the penetration kinetics (32 mN/m) (Table 5.3).  $\pi_{ss}$  is therefore shown to be an limiting value above which film penetration cannot occur.

The observed rate constant  $(k_{obs})$  is proportional to the lipid surface density  $(\rho)$  (Table 5.3). It is unclear if this density dependence is attributable to an increase in concentration of the association complex  $((SHP-1.lipid)^*)$  arising from electrostatics alone (increased surface charge density) or if enhanced hydrophobic interactions between lipid and protein residues are also involved. This issue could be resolved by measurement of the kinetics over a wider range of surface densities or by a parallel study using a zwitterionic lipid monolayer in place of egg-PA.

# (d) Source of differences observed for the penetration kinetics obtained in the constant surface area mode and the surface expansion mode

Comparison of penetration kinetics measured in the surface expansion mode and in the constant surface mode reveal an underlying difference between the two techniques. Firstly, kinetics obtained by the constant surface area mode obey first-order kinetics while those obtained by the surface expansion technique do not. These discrepancies show that some fundamental difference in the adsorption processes involved in the two modes of study must be considered.

Secondly, the time required to reach saturation is shown to be less in the constant area mode than in the surface expansion mode (Figure 5.7). This difference is due to the nature of the surface expansion experiment. As we have seen, the penetration rate (k<sub>obs</sub>) is proportional to the lipid surface density. In the constant area mode, the lipid surface density is fixed. In the surface expansion mode lipid surface density decreases as the experiment progresses and the equilibrium position is continually being adjusted. If the penetration kinetics depend upon the free space (as in a diffusional or Langmuir model) then the extent of protein penetration at any given time would be expected to be greater in the surface expansion mode than in the constant surface area mode, due to the increase in available space as the barrier moves to expand the surface area. However, lower extents of penetration<sup>c</sup> observed in the surface expansion mode support the dependence of k<sub>obs</sub> on the surface density as discussed earlier and further demonstrate the inapplicability of Langmuir and diffusional models to the kinetics. The difference between the constant surface area mode and the surface expansion mode shows that lipid surface density needs to be considered in the analysis of penetration kinetics.

#### 5.5. Conclusions

The kinetics of penetration have been shown to be dictated by a diffusive association of protein to the interface coupled to a second, insertion step, in which hydrophobic interactions are formed. Protein penetration into the monolayer is not simply a reflection of the protein occupying "empty" sites at the interface, but comparison of results to a literature model has shown that a cohesive interaction between protein and lipid occurs. The first step is a surface association mediated by electrostatic interactions and the second is the monolayer penetration which involves interactions between protein residues and the hydrophobic core of the monolayer (Figure 5.9).

The association constant of electrostatic association was obtained by fitting the fluorescence data to a Langmuir isotherm and the binding constant (KDassociation) was determined. A higher binding constant obtained for anionic lipid vesicles compared to zwitterionic lipid vesicles reveals a greater SHP-1 affinity for anionic interfaces. The monolayer penetration kinetics are first order in [SHP-1·lipid]\*. Although observed rate constants (kobs) are [SHP-1.lipid]\* dependent, when the subphase concentration is factored out (Figure 5.2.(b)), a rate constant describing penetration (k') was found (2.4 x  $10^{-4}~\text{s}^{-1}\text{nM}^{-1})$  which contains the factor ( $K_D^{penetration}$  · [lipid])).  $k_{obs}$  also exhibits a headgroup charge dependence for a given [SHP-1]<sub>subphase</sub> and surface density (p). This can be rationalized by [SHP-1.lipid]\* being determined by the value of KDassociation. Qualitatively, a low  $K_D^{penetration}$  which is revealed by the independence of the  $\pi_{ss}$  [SHP-1]<sub>subphase</sub> (Figure 5.8) supports a description of irreversible protein penetration in the lipid monolayer. The absence of interfacial activity of the denatured protein in the presence of lipid demonstrates the importance of SHP-1 tertiary structure for its interfacial activity and suggests that the effects of SHP-1 arise from its insertion into the monolayer rather than its denaturation (unfolding).

The interaction of SHP-1 with lipid vesicles or monolayers illustrates its capacity to associate with the phospholipid matrix in the absence of a ligand or anchor such as the

EGF receptor embedded in the matrix. It offers the possibility that the membrane phospholipid composition has a role other than a structural one in the dephosphorylation mechanism. We therefore speculate that the enhancement in SHP-1 enzymatic activity by various acidic lipids in vitro may be the result of an increase in the local concentration of the lipid at the receptor site fostered by the charged lipid bilayer assemblies. This may occur instead of, or in conjunction with, the PA-facilitated conformational change. A scheme in which an electrostatically facilitated penetration increases the concentration of the protein at the interface where dephosphorylation takes place, is supported and a positive role of PA in the association has been confirmed.

Finally we note that although penetration kinetics have traditionally been studied in either the constant surface area mode or the surface expansion mode, results obtained by both methods for the same system are rarely reported. We have found that the kinetics obtained in the constant surface area mode differ markedly from those obtained in the surface expansion mode and emphasize that caution must be exercised in comparing kinetics derived from the two experiments.

#### 5.6. References

- (1) Brautigan, D.L. Biochim. Biophys. Acta 1992, 1114, 63-77.
- (2) Klingmuller, U., Lorenze, U., Cantley, L., Neel, B., Lodish, H. Cell 1995, 80, 729-738.
- (3) Olcese, L., Lang, P., Velt, F., Cambiaggi, A., Marguet, D., Blery, M., Hippen, K., Biasoni, R., Moretta, L., Cambier, J., Vivier, E. J. Immunol. 1996, 156, 4531-4534.
- (4) Plas, D., Johnson, R., Pingel, J., Matthews, R., Dalton, M., Roy, G., Chan, A., Thomas, M. Science 1996, 272, 1173-1176.
- (5) Zhao, Z., Shen, S.H., Fischer, E.H. Proc. Nat. Acad. Sci. 1993, 90, 4251-4255.
- (6) Bohmer, F.-D., Tomic, S., Greiser, U., Lammers, R., Kharitonekov, A., Imyanitov, E., Ullrich, A J. Biol. Chem. 1995, 270, 21277-212384.
- (7) Watts, A., Sixl, F., Brophy, P.J. Biochemistry 1984, 23, 2032-2039.
- (8) Lehtonen, J.Y.A., Rytomaa, M., Kinnunen, P.K.J. *Biophys. J.* **1996**, *70*, 2185-2194.
- (9) Smrcka, A.V., Romoser, V., Ball, R. J. Biol. Chem. 1996, 271, 25071.
- (10) Brand, L., Wu, P. Anal. Bioch. 1994, 218, 1-13.
- (11) Sackmann, E., Sui, S. Biochemistry 1988, 27, 7463-7469.
- (12) Nelsestuen, G.L., Bazzi, M.D., Youakim, M.A. *Biochemistry* 1992, 31, 1125-1134.
- (13) Hermens, W.T., Kop, J.M.M.; Cuypers, P.A., Lindhout, T., Hemker H.C. J. Biol. Chem. 1984, 259, 13993-13998.
- (14) Newman, R.H., Whitehead, P., Lally, J., Coffer, A., Freemont, P. Biochim. Biophys. Acta 1996, 1281, 111-116.
- (15) Salamon, Z., Meyer, T.E., Tollin, G. Biophys. J. 1995, 68, 648-654.
- (16) Camejo, G., Colacicco, G., Rapport, M. J. Lipid Res. 1968, 9, 562-569.
- (17) Colacicco, G. J. Colloid. Interface Sci. 1969, 29, 345-364.
- (18) Fritz, M., Zimmerman, R.M., Barmann, M., Gaub, H.E. *Biophys. J.* 1993, 65, 1878-1885.
- (19) Duplaa, H., Convert, O., Sautereau, A., Tocanne, J., Chassaing, G. Biochim. Biophys. Acta 1992, 1107, 12-22.
- (20) Lakhdar-Ghazal, F., Vigroux, A., Willson, M., Tocanne, J., Perie, J., Fayes, J. Biochem. Pharmacol. 1991, 42, 2099-2105.
- (21) Seelig, A. Biochemistry 1992, 31, 2897-2904.

- (22) Seelig, A., Hanakam, F., Gerisch, G., Lotz, S., Alt, T. *Biochemistry* 1996, 35, 11036-11044.
- (23) Weinberg, R.B., Ibdah, J.A., Philips, M.C. J. Biol. Chem. 1992, 267, 8977-8983.
- (24) Leenhouts, J.M., Torok, Z., Demel, R.A., de Gier, J., de Kruijff, B. *Mol. Membr. Biol.* 1994, 11, 159-164.
- (25) Demel, R.A., London, Y., Guerts van Kessel, W.S.M., Vossenberg, F.G.A., van Deenen, L.L.M. Biochim. Biophys. Acta 1973, 311, 507-519.
- (26) Demel, R.A., Peelen, T., Siezen, R.J., deKruijff, B., Kuipers, O. European J. Biochem. 1996, 235, 267-274.
- (27) Verger, R., Pattus, F. Chem. Phys. Lipids 1982, 30, 189-227.
- (28) Bougis, P., Rochat, H., Pieroni, G., Verger, R. *Biochemistry* 1981, 20, 4915-4920.
- (29) Seelig, A., Macdonald, P.M. Biochemistry 1989, 28, 2490-2496.
- (30) Seelig, A. Biochim. Biophys. Acta 1990, 1030, 111-118.
- (31) Seelig, A., Holzemann, G., Greiner, H.E., Harting, J., Barnickel, G. Regulatory Peptides 1993, 46, 453-454.
- (32) Quinn, P., Dawson, R.M.C. Biochem. J. 1970, 119, 21-25.
- (33) Chattoraj, D.K., Birdi, K.S. Adsorption and the Gibbs Surface Excess; Plenum Press: New York, 1984.
- (34) Cho, D., Narsimhan, G., Franses, E.I. Langmuir 1997, 13, 4710-4715.
- (35) Gaines, G.L. Insouble Monolayers at Liquid-Gas Interfaces; Interscience Publishers: New York, 1966.
- (36) Seelig, A. Biochim. Biophys. Acta 1987, 899, 196-204.
- (37) Ghiggino, K., Lee, A.G., Meech, S.R., O'Connor, D.V., Philips, D. *Biochemistry* 1981, 20, 5381-5389.
- (38) Mayer, L.D., Pusey, M.L., Griep, M.A., Nelsestuen, G.L. *Biochemistry* 1983, 22, 6226-6232.
- (39) Phillips, M.C., Evans, T.A., Hauser, H. Adv. Chem. Series 1975, 144, 217-230.
- (40) Pregel, M.J., Shen, S.-H., Storer, A.C. Protein Eng. 1995, 8, 1309-1316.
- (41) Schrag, J. NRC-BRI, personal communication 1997.
- (42) MacRitchie, F., Alexander, A.E. J. Colloid Sci. 1963, 18, 453-457.
- (43) Graham, D.E., Phillips, M.C. J. Colloid Interface Sci. 1979, 70, 403-414.
- (44) Ward, A.F.H., Tordai, L. J. Chem. Phys. 1964, 14, 453-465.
- (45) Sundaram, S., Stebe, K.J. Langmuir 1997, 13, 1729-1736.

#### Chapter 5

- (46) Benjamins, J., Feijter, J.A., Evans, M.T.A., Phillips, M.C. *Disc. Faraday Soc.* **1975**, *59*, 218-229.
- (47) Verger, R., Mieras, M.C.E., de Haas, G.H. J. Biol. Chemistry 1973, 248, 4023-4034.
- (48) Verger, R., de Haas, G.H. Chem. Phys. Lipids 1973, 10, 127-136.
- (49) Verheij, H.M., Egmond, M.R., de Haas, G.H. Biochemistry 1981, 20, 94-99.
- (50) Demel, R.A. Biochim. Biophys. Acta 1975, 406, 97-107.
- (51) Verger, R., Gargouri, Y., Moreau, H., Pieroni, G. European J. Biochem. 1989, 180, 367-371.
- (52) Graham, D.E., Phillips, M.C. J. Colloid Interface Sci. 1979, 70, 415-426.
- (53) Fowkes, F.M. J. Phys. Chem. 1962, 66, 1863-1866.
- (54) Fowkes, F.M. J. Phys. Chem. 1964, 65.
- (55) Klopper, K.J., Vanderlick, T.K. J. Colloid Interface Sci. 1996, 182, 220-229.
- (56) Breukink, E., Demel, R.A, de Korte-Kool, G., de Kruijff, B. Biochemistry 1992, 31, 1119-11.
- (57) McLaughlin, S., Kim, J., Mosior, M., Chung, L., Wu, H. *Biophys. J.* 1991, 60, 135-148.

# Chapter 6

#### 6.1. Conclusions

The physical properties of a number of phospholipid analogs possessing polar groups in the acyl chain region have been investigated. The main gel  $(L_{\beta})$  to liquid-crystalline  $(L_{\alpha})$  phase transition temperature (DSC-determined  $T_m$ ) of these phospholipids are generally lower than that of parent molecule DSPC with the exception of bis(nSO<sub>2</sub>)C<sub>17</sub>-PC lipids. The depression in the  $T_m$  is related to the position of the polar groups along the chain. Bis(nSO<sub>2</sub>)C<sub>17</sub>-PC lipids exhibit elevated  $T_m$ 's with respect to DSPC and the elevation in the  $T_m$  is also dependent upon the position of the functional group. These lipids were also shown to phase separate from DSPC over a wide range of compositions, while lipids functionalised in only one chain mix over a wide range of compositions.

Monolayer studies of both  $1C_{18}$ , $2(nSO_2)C_{17}$ -PC and bis $(nSO_2)C_{17}$ -PC reveal an  $SO_2$  position-dependent phase transition mechanism. The mechanism was revealed by the relationship between the monolayer critical temperature  $(T_c)$  and the  $T_m$ . Monolayers of lipids which were unfunctionalised or functionalised at positions close to the headgroup exhibit a critical temperature  $(T_c)$  equal to the  $T_m$  of the lipid. The phase transition of these lipids was therefore attributed to an order-disorder process. Unlike phospholipids which undergo a conventional order/disorder transition the  $T_c$ 's of lipids functionalised near the midpoint of the acyl chain do not correlate with the  $T_m$ . The mechanism of their monolayer phase transition involves a reorientation of the molecule at the air/water interface from a horizontal position to a vertical position. The reorientational mechanism is related to the bipolar nature of the lipid. Lipids functionalised near the headgroup therefore do not display bipolar behaviour.

Normalization of monolayer isotherms is performed by measuring isotherms on a reduced temperature scale with respect to their  $T_c$ . This permits the direct comparison of the films and provides for the extraction of relevant structural information. Isotherms of the

#### Chapter 6-Conclusions

diacyl phospholipids DMPC, DPPC and DSPC superimpose upon normalization. This shows that the lipids are iso-structural. Normalized isotherms of unfunctionalised lipids do not superimpose showing that these lipids are not iso-structural. The phenomenon is not fully understood but the difference is believed to be due to a gradual shift in the transition mechanism as the bipolarity of the lipid change as the substituent is placed further and further down the chain. The polar functional group destabilises the condensed lipids film resulting in higher reduced transition pressures and a reduction in the critical temperature of the orientational phase transition.

The phase transition of monolayers was also investigated by surface potential studies. A decrease in the surface dipole during the monolayer phase transition was observed for lipids functionalised at higher positions and for which  $T_m \neq T_c$ . This decrease is consistent with the expulsion of the polar moiety from the air/water interface. The surface dipole moment remains constant for lipids which are functionalised near the headgroup and which show a correlation between  $T_m$  and  $T_c$ . This supports the order-disorder phase transition mechanism for these lipids. The comparison of  $T_c$  with  $T_m$  is established as a diagnostic of the phase transition in these cases.

The association and penetration kinetics of protein tyrosine phosphatase (SHP-1) were studied by fluorescence resonance energy transfer spectroscopy (FRET) and by the Langmuir film-balance technique (LFB) in both the constant surface area and surface expansion modes. The surface-association of SHP-1 is accessible by FRET. The association is shown to fit a Langmuir isotherm. The association constant of SHP-1 at an anionic lipid interface is five times higher than at a zwitterionic lipid interface. Penetration kinetics were measured by the monolayer techniques. The penetration is first order in the surface-associated complex [SHP-1-lipid]\*. The kinetics of penetration are not consistent with a diffusion-controlled process nor do they fit a Langmuir isotherm. This inconsistency shows that the inclusion of the protein within the monolayer cannot be attributed to the occupation of vacant sites (unoccupied by lipid) at the interface. In addition, the

## Chapter 6-Conclusions

comparison of our data with a literature model reveals a consistency which supports the interaction of the protein with the lipid in a lipid-activated film penetration. The first-order penetration rate constant was greater for anionic lipid monolayers compared to zwitterionic lipid monolayers, but the extent of penetration was shown to be the same throughout. This shows that it is the hydrophobic interaction between protein and lipid which ultimately controls the penetration process.

# 6.2. Contributions to Original Knowledge

- (1) We systematically investigated the dependence of the main phase transition temperature upon lipid structure of a series of acyl chain-functionalised phospholipids. The unusual phase transition behaviour of a novel phospholipid analog was observed. Bis( $nSO_2$ )C<sub>17</sub>-PC lipids exhibit enhanced thermal stability with respect to DSPC as shown in their elevated  $T_m$  values.
- (2) The phase separation of bis(11SO<sub>2</sub>)C<sub>17</sub>-PC over the entire range of compositions was revealed.
- (3) We developed a strategy for the analysis of phospholipid monolayer isotherms which involves their normalization with respect to  $T_c$ . An exposed an unconventional monolayer phase transition mechanism in monolayers of bipolar and tripolar phospholipids was observed.
- (4) The use of the monolayer as a model for the lipid bilayer is shown to have limitations since lipids possessing polar groups in the acyl chains may access conformations which are not present in lipid bilayers.
- (5) The complimentarity of FRET and LFB techniques for the study of the association and penetration of artificial membranes respectively was highlighted.
- (6) A difference between penetration kinetics obtained in the constant surface area and surface expansion modes was observed.
- (7) An association constant and a penetration rate constant for SHP-1 at lipid monolayers were determined. These studies showed that the penetration of SHP-1 was mediated by electrostatics of the interface but controlled by the hydrophobic interaction between protein and lipid. Once the surface concentration of the associated SHP-1·lipid complex was factored out, the observed rate penetration constants are predicted to be independent of surface charge density.

## 6.3. Directions for Future Work

## 6.31. The characterization of functionalised lipids

- (1) Study of the temperature dependence of the monolayer phase transition of functionalised fatty acids employing the strategy proposed in this thesis would further expand our understanding of the monolayer behaviour of bipolar lipids as well as test the general applicability of the normalization procedure to lipid monolayers.
- (2) The investigation of the effect of the polar group upon chain order dynamics by Raman spectroscopy may help to directly evaluate the role of dipole-dipole cross-linking to the properties of lipids functionalised with polar groups. The use of the functionalised fatty acids for the assignment of the sulfone and sulfoxy stretching frequencies prior to analysis of lipid spectra may help to deconvolute the spectra. The phosphate stretching frequencies occur in the same region as the sulfone and sulfoxy groups which complicates the analysis of phospholipids bearing SO or SO<sub>2</sub> groups in their acyl chains.
- (3) Thermal studies have revealed the greater stability of bis( $nSO_2$ )C<sub>17</sub>-PC lipids and shown that they phase separate upon mixing with DSPC. To further investigate the stability of these types of lipids their metabolic stability and permeability needs to be determined. Metabolic stability may be partially evaluated by the resistance to hydrolysis by phospholipase A<sub>2</sub> (PLA<sub>2</sub>). The entrapment of fluorescent dye is commonly used for the assessment of liposome permeability.

#### 6.32. The role of lipids in the function of SHP-1

- (1) The use of the LFB in conjunction with surface potential studies may allow the study of the association kinetics by LFB since the surface potential experiment will be mainly sensitive to charge neutralization by the protein at the anionic lipid interface.
- (2) The measurement of protein surface concentrations upon penetration would allow a more thorough analysis of association and penetration kinetics and permit the calculation of the size of the protein fragment which inserts into the monolayer to be determined

- (3) The extension of the investigation of the effect of the initial surface pressure upon the extent of penetration to lower surface pressures may reveal the existence of a maxima which would be associated with an optimal lipid surface density for penetration.
- (4) The kinetics of truncated protein (Figure 6.1) can be compared to the penetration of native, full length protein, SHP-1, to determine which sections of the protein are involved in the association and penetration at lipid interfaces

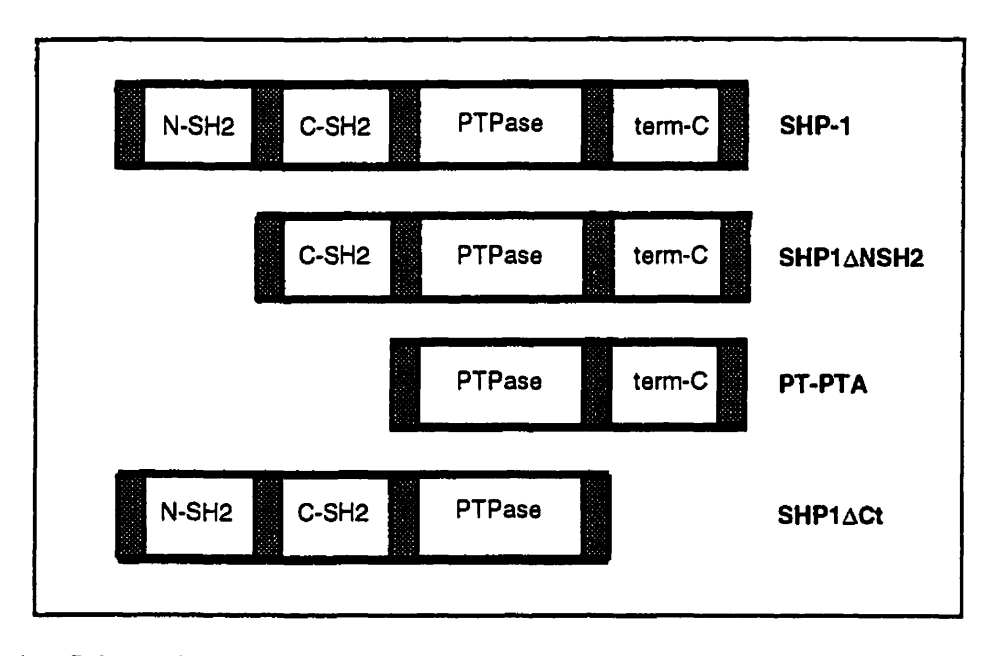


Figure 6.1. Schematic representation of SHP-1 truncated protein analogs obtained by tryptic an peptic digests of the full-length enzyme.

- (5) The inclusion of a substrate in the lipid monolayer may be useful to study the effect of lipid composition and surface density upon the rate of dephosphorylation by SHP-1.
- (6) The penetration of SHP-1 into lipid vesicles within a similar time scale as found from the monolayer experiments can be determined by ESR spectroscopy employing a spin probe containing the nitroxyl group within the hydrophobic region. Such studies may have more biological relevance since the bilayer is a more realistic model of the cell membrane than is the monolayer.

# Appendix I.

Table AI.1. Measured features of the monolayer phase transition taken from the temperature dependence of the phase transition

T (°C)	$\pi_t \pm 0.3$	A <sub>t</sub> 0.5	$A_{t}$ - $A_{s}$ 0.5		
	(mN/m)	(Å <sup>2</sup> /molecule)	(Å <sup>2</sup> /molecule)		
DMPC					
7.6	20	66	19		
12.7	30	57	13.5		
14.3	34	55	10.6		
DPPC					
Dire					
17	1	84	33		
20	5	80	26.5		
25	13	67	15		
32	24	61.5	11		
DSPC					
30.9	0	-	-		
33.2	1.5	-	-		
34.3	2.5	76	32		
36.2	4.2	73.5	29.5		
39.3	9.3	65	21		

T (°C)	t 0.3	A <sub>t</sub> 0.5	$A_{t}-A_{s}$ 0.5	
	(mN/m)	(Å <sup>2</sup> /molecule)	(Å <sup>2</sup> /molecule)	
1C <sub>18</sub> ,2(5SO <sub>2</sub> )C <sub>17</sub> -PC				
10.7	3.5	100.5	50.5	
16.4	10	86	36	
18.1	11.3	82.7	34	
21.5	16.5	79	30	
27.0	23.5	70	20	
1C <sub>18</sub> ,2(7SO <sub>2</sub> )C <sub>17</sub> -PC				
9.5	11.5	102	52	
16.7	18	88	38	
20.5	23	87	33	
24.0	31	76	26	
28.0	43	66	16	
1C <sub>18</sub> ,2(9SO <sub>2</sub> )C <sub>17</sub> -PC				
11	13.0	115	65	
16.7	16.5	106	56	
18.7	18.0	104	54	
25.0	23.0	93	43	
32.0	37.0	82	32	
1C <sub>18</sub> ,2(11SO <sub>2</sub> )C <sub>17</sub> -PC				
10.7	7	133	83	
15	12.5	128	78	
16.5	13.5	127	77	
21.7	16	125	75	
27.3	19	122	77	
35.5	27	100	50	

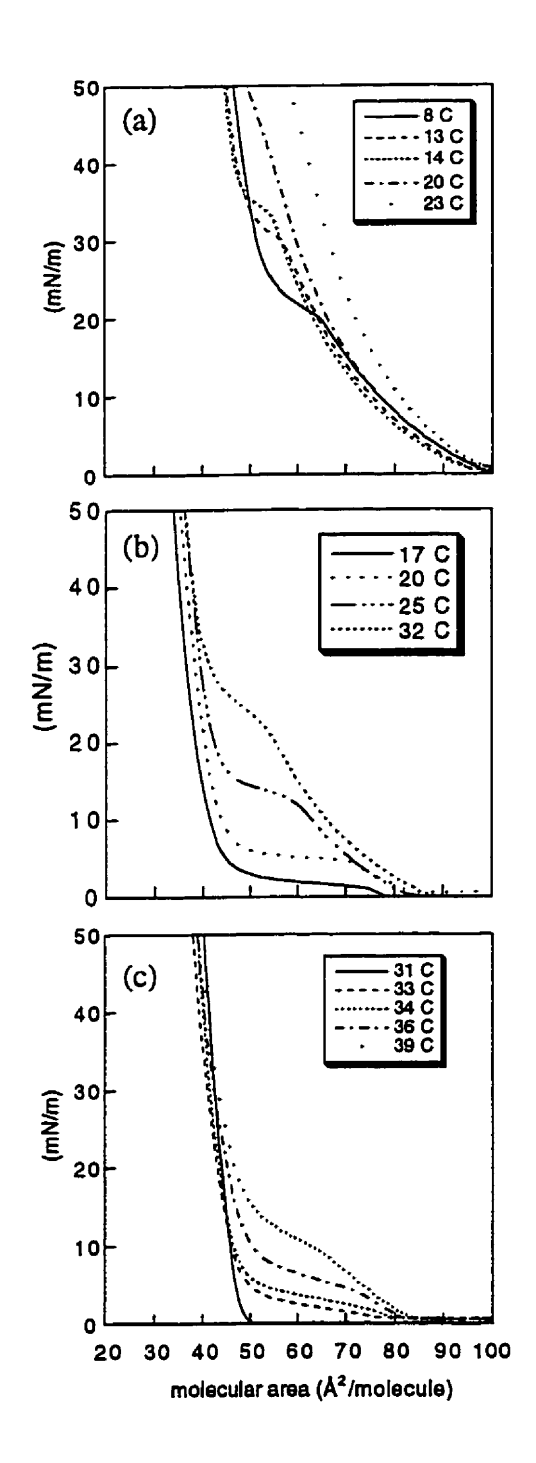


Figure AI.1. Temperature dependence of monolayer isotherms of (a) DMPC, (b) DPPC, and (c) DSPC aquired on a water subphase.

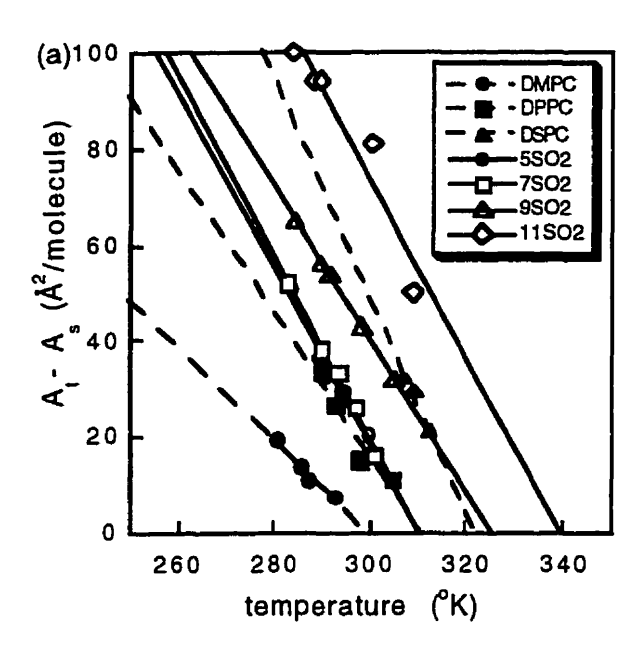


Figure AI.2. (a) At the critical point the transition area is zero and the critical temperature is determined from the x intercept of the graph of transition area  $(A_t - A_s)$ , vs  $T_{isotherm}$ .

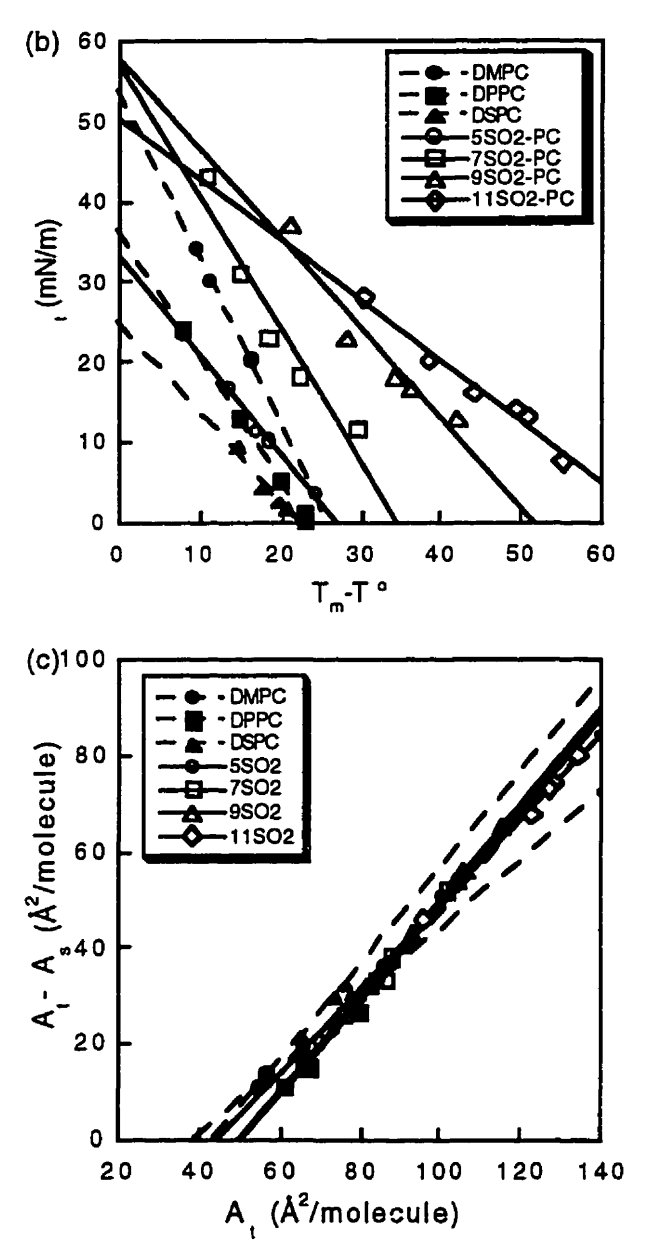


Figure AI.2. (b) At the critical point  $T_{isotherm} = T_c$  so the critical pressure is obtained from the y intercept of the graph. (c) The critical area is obtained from the x intercept of the graph.

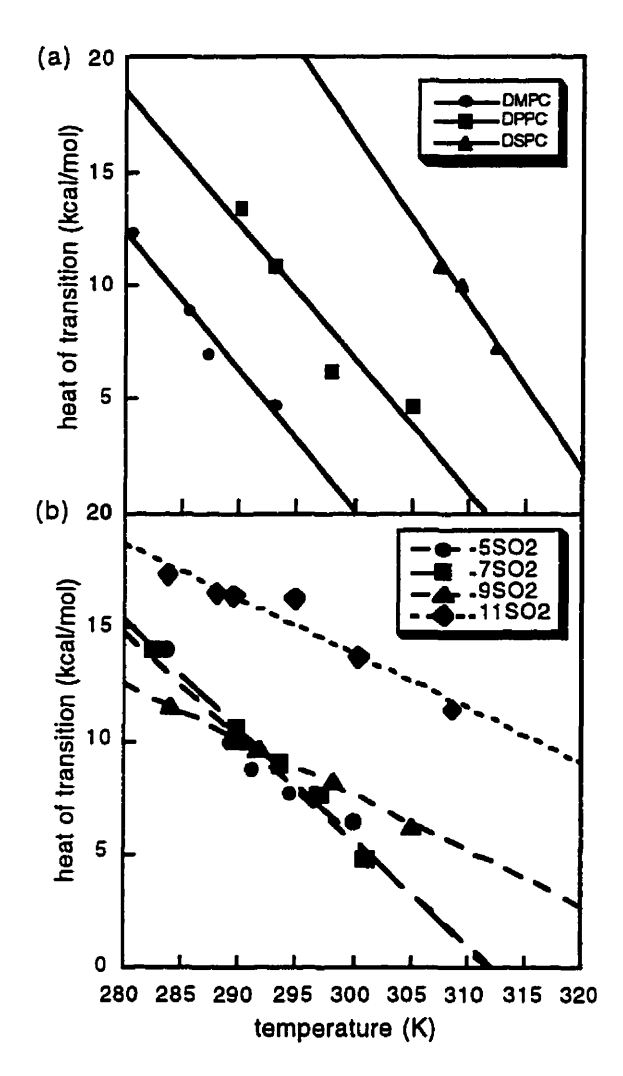


Figure AI.3. At the critical point the heat of the transition is zero. The critical temperature is obtained from the x intercept of the graph. (a) DMPC, DPPC, DSPC (b)  $1C_{18}$ , $2(nSO_2)C_{17}$ -PC.

# Appendix II

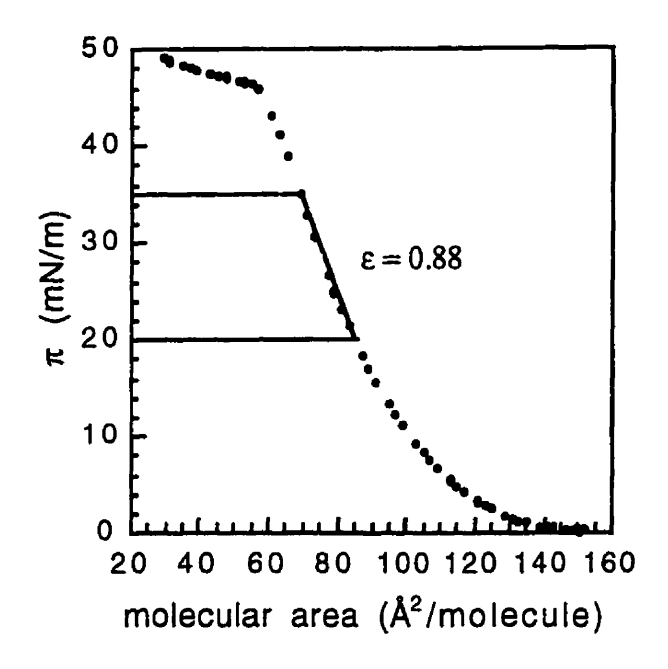


Figure AII.1. Isotherm of egg-PA measured at 25°C on a subphase of 20 mM HEPES, 142 mM NaCl, 1 mM DTT, 10 mM EDTA.